Beam Emittance
and
Beam Profile Monitors

by K. Wittenburg –DESY-

Transport lines and Linacs

Phosphor Screens
SEM Grids/Harps
OTR
Wire scanners (Linacs)

Emittance of single shots

Hadron accelerators

Wire scanners
Residual Gas Ionization (IPM)
Residual Gas Scintillation
Synchrotron light (Edge effect, wigglers)
Scrapers/current (destructive)

Emittance preservation

Electron accelerators

Synchrotron light
Wire Scanners
Scrapers/current (destructive)
Laser Wire Scanner

Aspect ratio/coupling

Idea of this course: Beam Profile monitors use quite a lot of different physical effects to measure the beam size. Many effects on the beam and on the monitor have to be studied before a decision for a type of monitor can be made. In this session we will

1) discuss emittance measurements (2 experiments)
2) some detailed examinations of at least one monitor to demonstrate the wide range of physics of the profile instruments.
3) A very short introduction to halo measurements (1 experiment)

Synchrotron Light Profile Monitor

- Introduction
- Resolution limits
- Small Emittance Measurements
- (Proton Synchrotron Radiation Diagnostics)

Synchrotron light profile monitor

In electron accelerators the effect of synchrotron radiation (SR) can be used for beam size measurements. In this course we will **focus on profile determination**, but SR can also be used for bunch length measurements with e.g. streak cameras with a resolution of < 1 ps. From classical electrodynamics the radiated power is given for a momentum change dp/dt and a particle with mass m_0 and charge e:

$$P_{SR} = \frac{e^2 c}{6\pi\varepsilon_0 (m_0 c^2)} \left[\frac{dp}{dt} \right]^2$$

For linear accelerators dp/dt = dW/dx. For typical values of dW/dx = 10 - 20 MeV/m the **SR is negligible**. In bending magnets an **acceleration perpendicular to the velocity** exists mainly in the dipole magnets (field B) with a bending radius $\rho = \beta\gamma m_0 c/(eB)$. The **total power** of N circulating particles with $\gamma = E/m_0c^2$ is than

$$P_{tot} = \frac{e^2 c \gamma^4}{6\pi\varepsilon_0 \rho^2} N$$

This expression is also valid for a ring having all magnets of the same strength and field-free sections in between.

The critical wavelength λ_c divides the Spectrum of SR in two parts of equal power:

$$\lambda_c = 4\pi\rho / 3\gamma^3$$

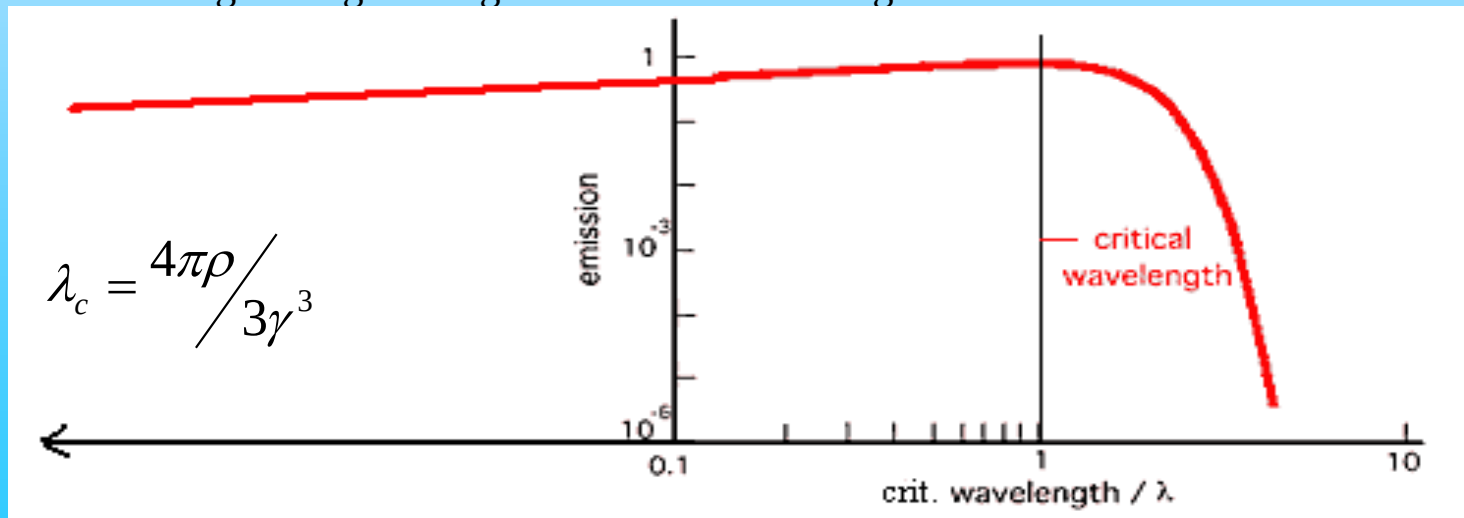

Opening angle Ψ of SR (1/2 of cone!) for $\lambda >> \lambda_c$(!!!):
with

$$\Psi = \frac{1}{\gamma}\left(\frac{\lambda}{\lambda_c}\right)^{1/3} = \left(\frac{3\lambda}{4\pi\rho}\right)^{1/3}$$

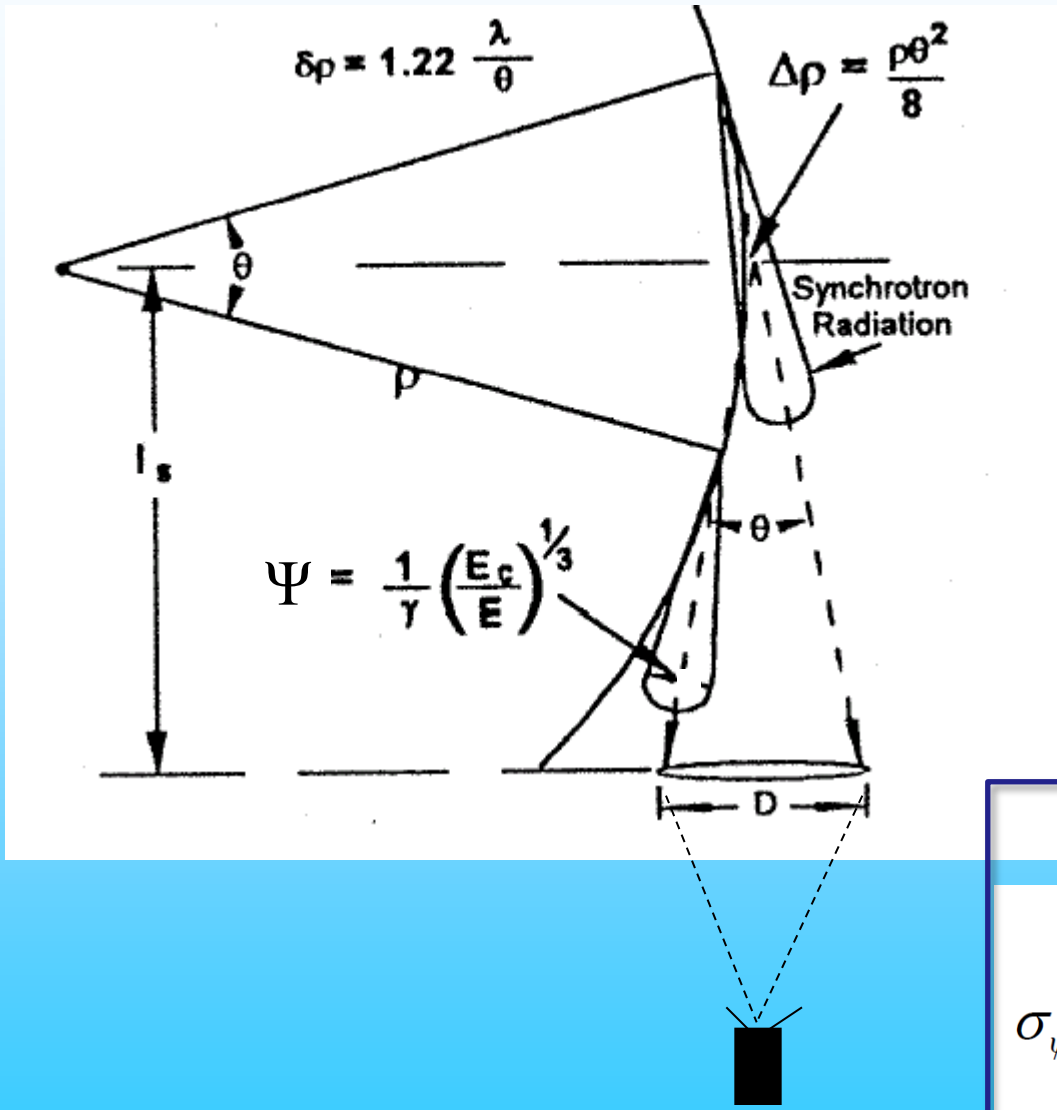

$\gamma = E/m_0c^2 = E\,[\mathrm{MeV}]/0.511$
$\gamma = 23483$ at 12 GeV and
$\gamma = 52838$ at 27 GeV
Path length s:
$s = \rho\theta$
ρ = Bending radius of Dipole

J. Flanagan (IPAC2011)

$$\sigma_\psi = \begin{cases} 1.07[3\lambda/(4\pi\rho)]^{1/3} & ; \quad \lambda >> \lambda_c \\ 0.64/\gamma & ; \quad \lambda \approx \lambda_c \\ 0.58[3\lambda\gamma/(4\pi\rho)]^{1/2} & ; \quad \lambda << \lambda_c \end{cases}$$

Example HERAe (46 mA circulating electrons at 27 GeV)

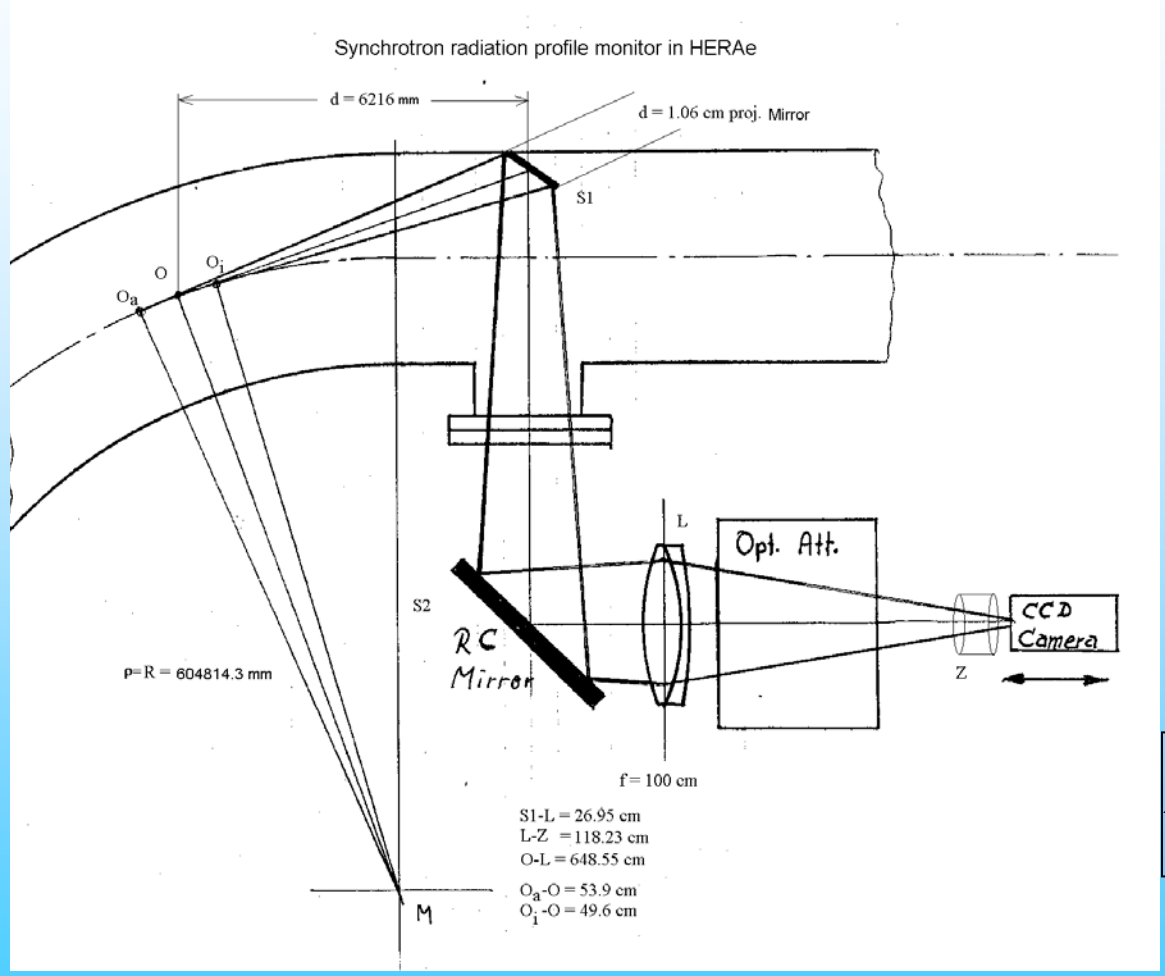

R = ρ = 604814.3 mm
G = O-L = 6485.5 mm
B = L-Z = 1182.3 mm
O-S1 = 6216 mm
L = O_a-O_i = 1035 mm
opening angle (horizontal): tanθ/2 = d/2/6216 => θ/2 = arc tan d/2/6216 = <u>0.85 mrad</u>
opening angle (vertikal):

$\Psi(\lambda) = 1/\gamma\ (\lambda/\lambda_c)^{1/3}$

$$\lambda_c = {4\pi\rho}/{3\gamma^3} = 0.017\,nm << \lambda \approx 500\,nm$$

<u>Exercise SR1 : Which problems with the setup can be expected?:</u>

Heating of mirror:

⇒total emitted Power per electron:

$$P = \frac{e^2 c \gamma^4}{6\pi\varepsilon_0 \rho^2}$$

total Power of 46 mA circulating electrons at 27 GeV (Number of electrons $N_e = 6 \cdot 10^{12}$)

$$\mathbf{P_{tot} = 6 \cdot 10^6\ W}$$

The mirror will get $P_{tot} * \Theta / (2\pi) =$ **1600 W** (Integral over all wavelength!!!)

Solutions?

=> mirror is moveable, mirror has to be cooled
Material with low Z is nearly not visible for short wavelength => Beryllium
Still 100 W on mirror in HERAe
not sufficient to prevent image distortion

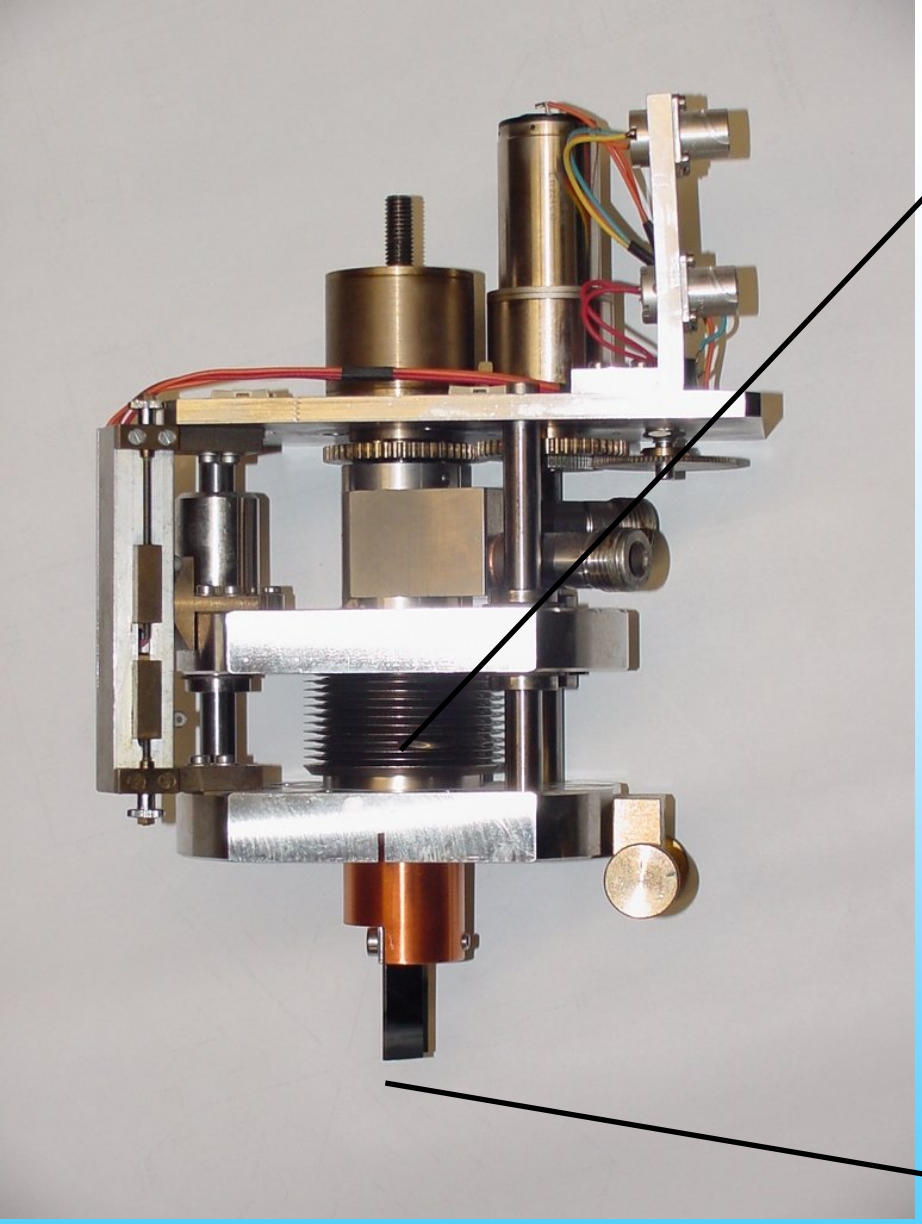

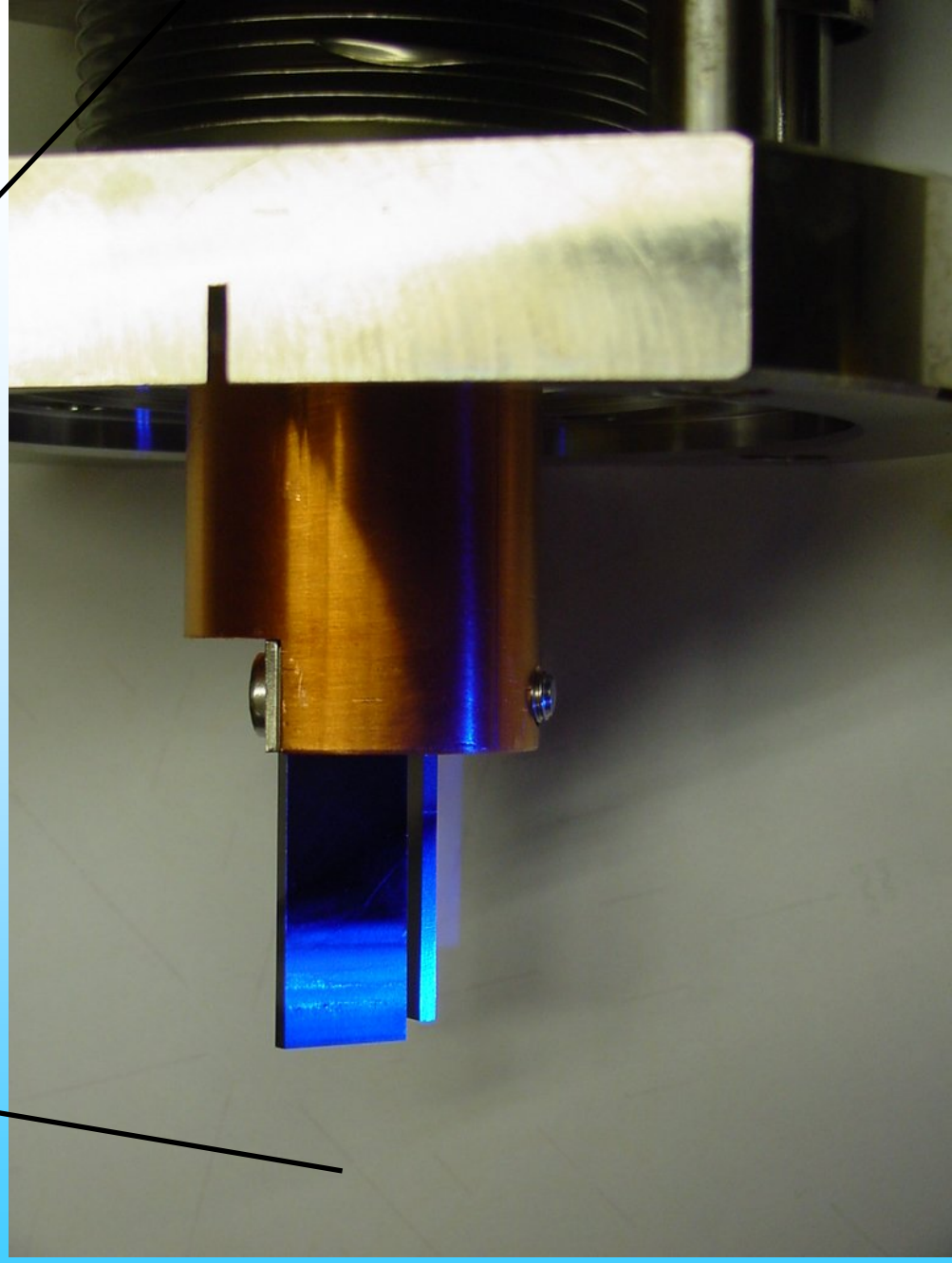

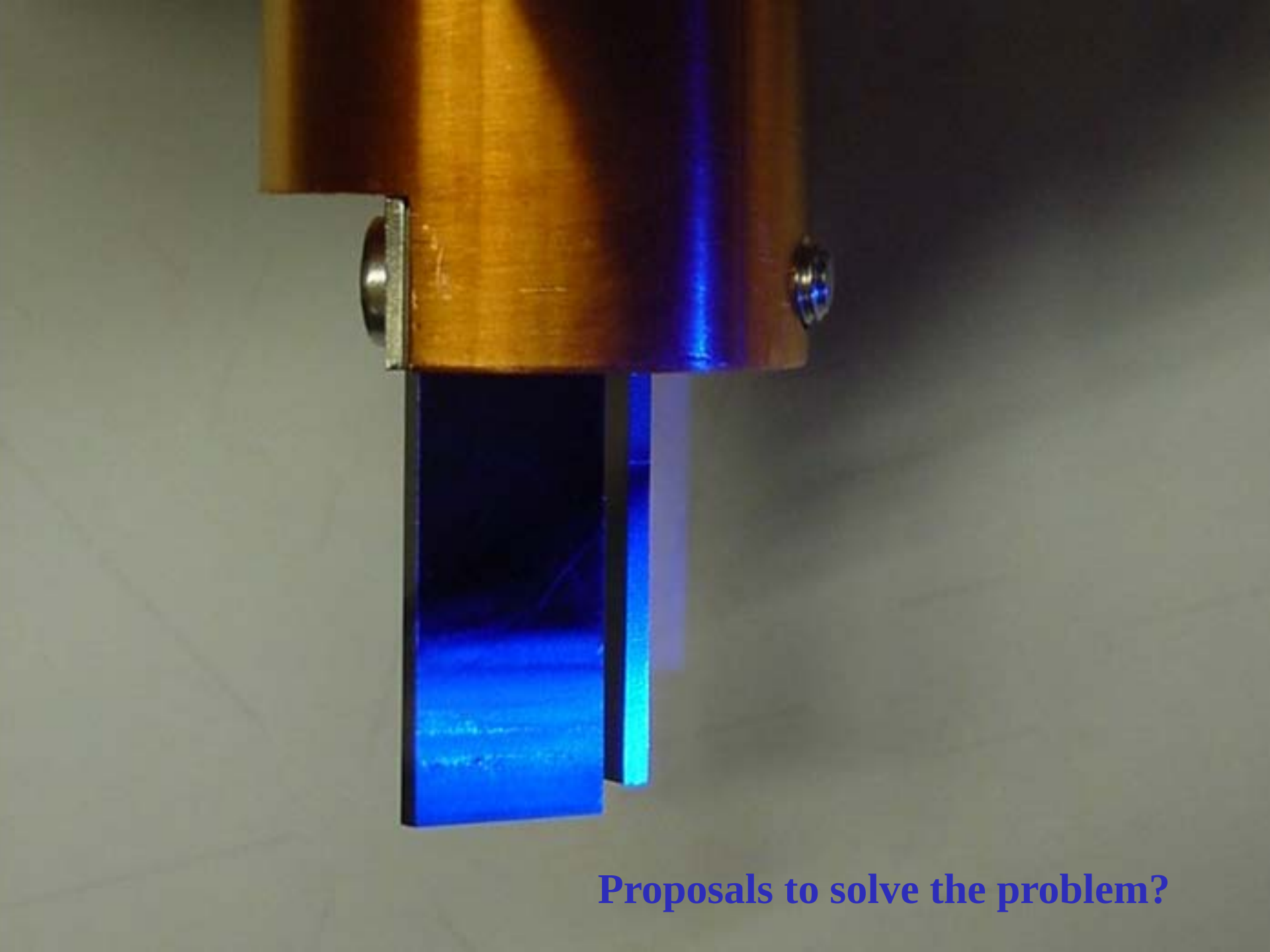

Proposals to solve the problem?

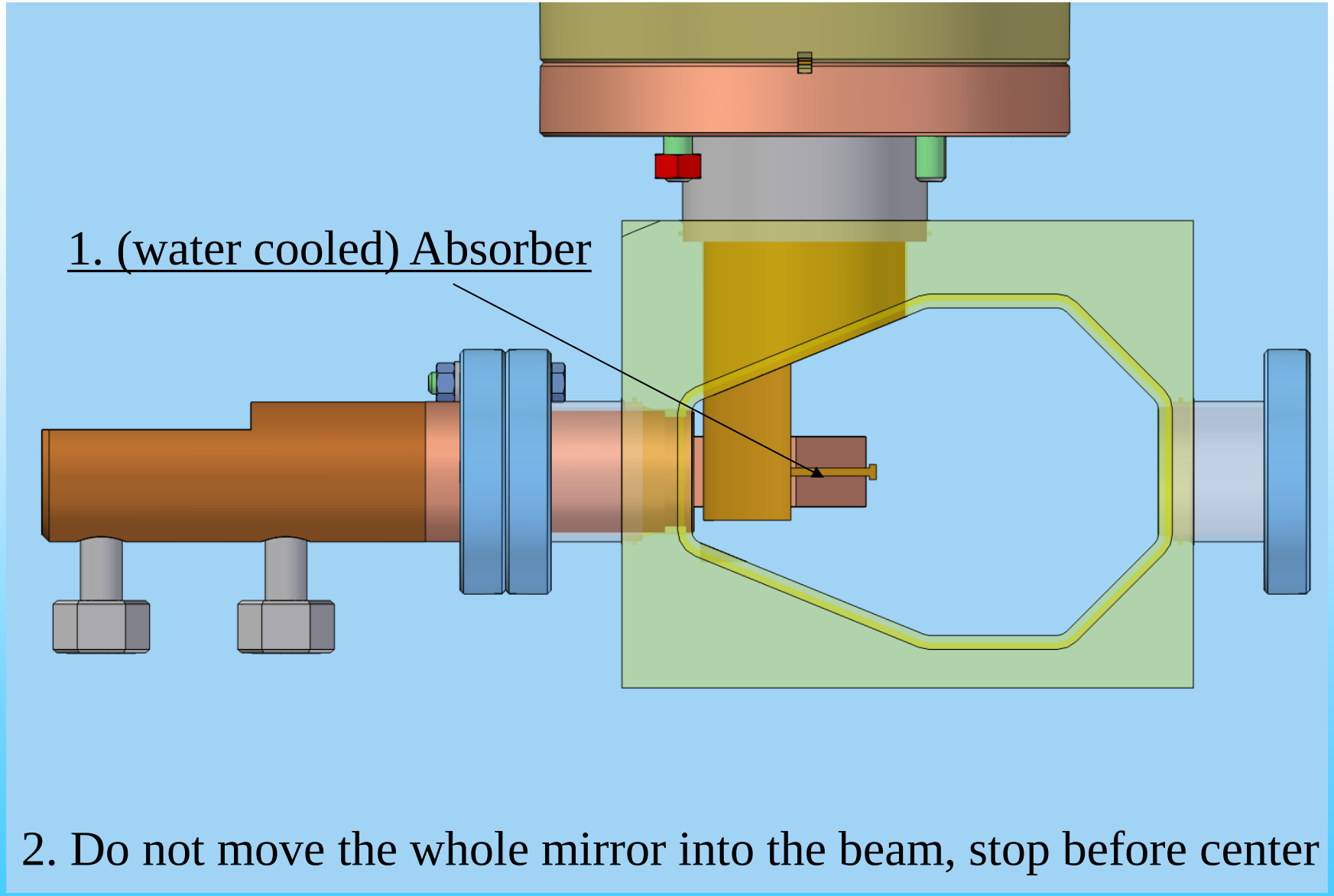

2. Do not move the whole mirror into the beam, stop before center

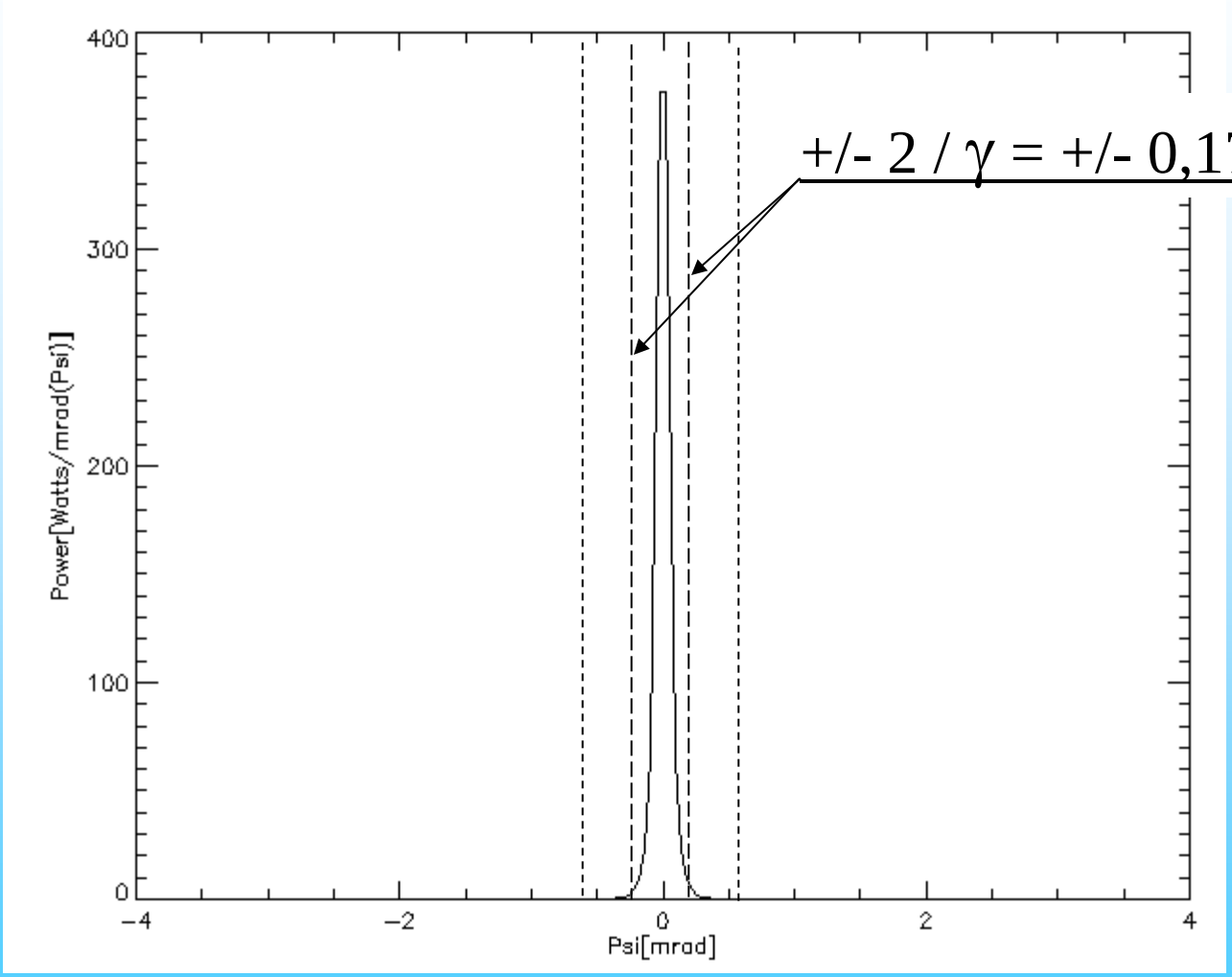

„Total“ power within +/- 0,6 mrad

Visible part

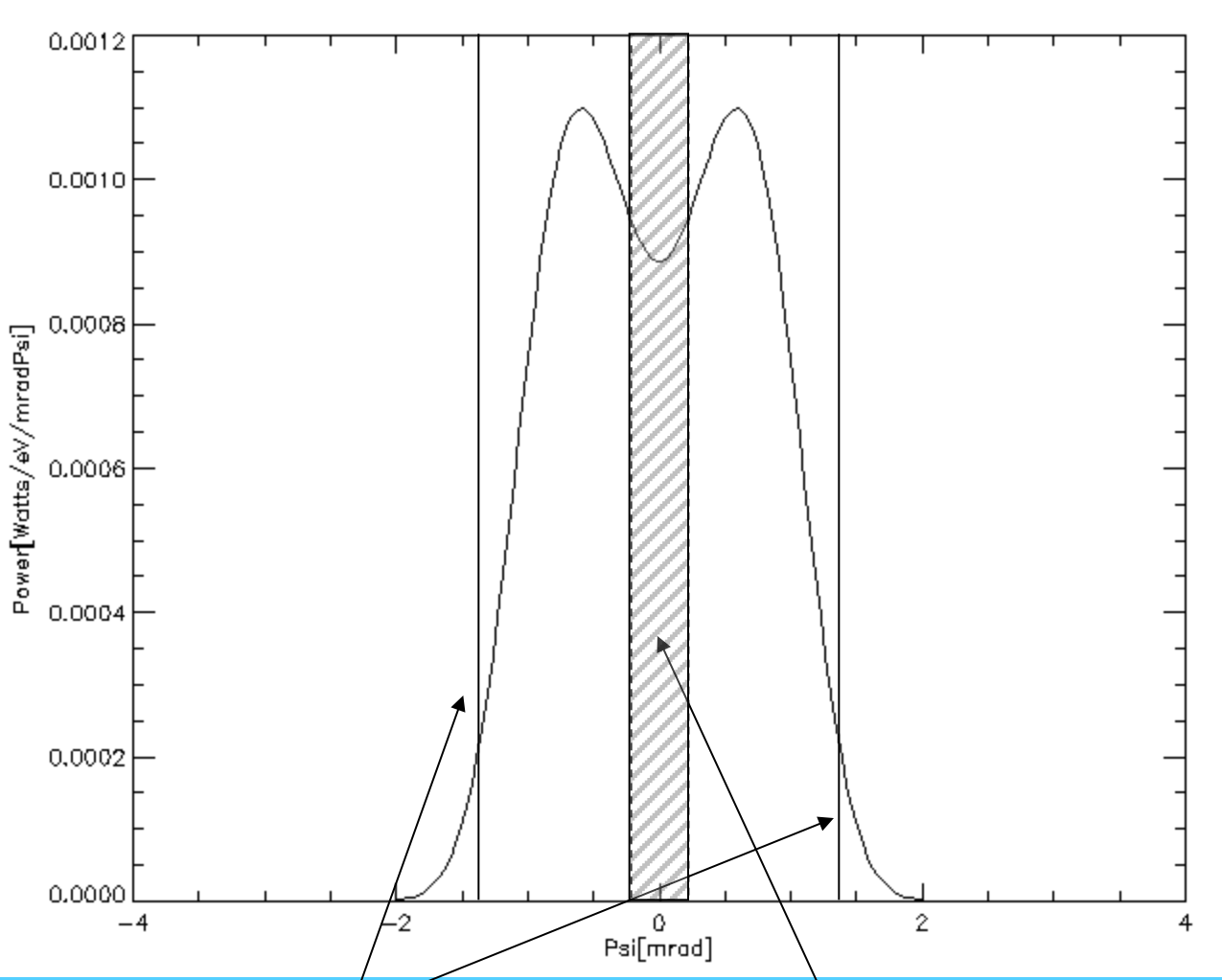

Mirrorsize

Fade out ± 2/ γ by Absorber

Exercise SR2: What limits the spatial resolution?

Diffraction, depth of field, arc, camera => physical
Alignment, lenses, mirrors, vibrations => technical

How to calibrate the optics?

Grid (yardstick) at point of emission, orbit bumps, …

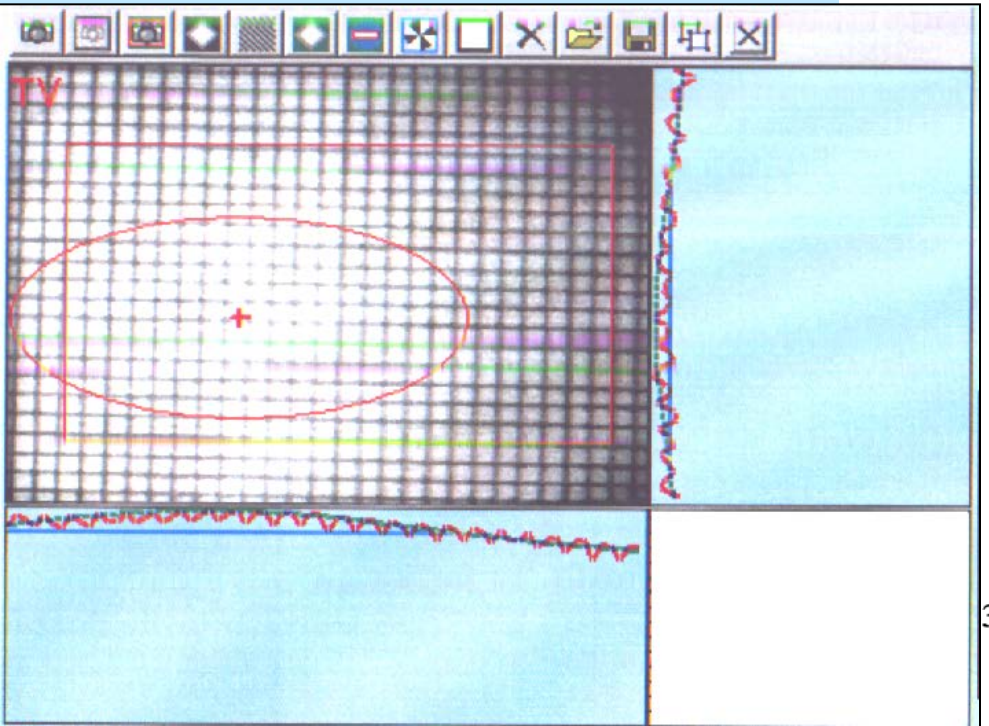

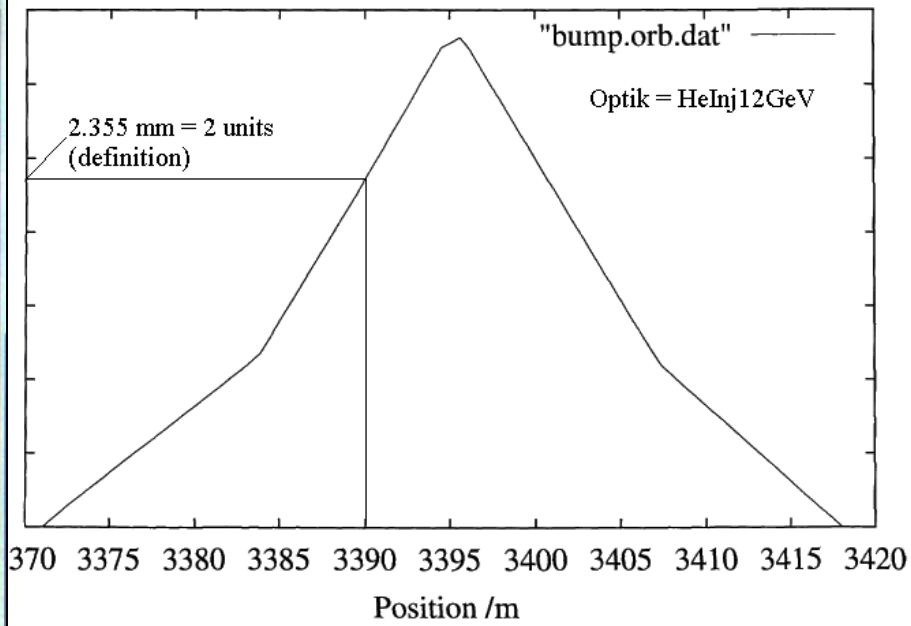

Diffraction:

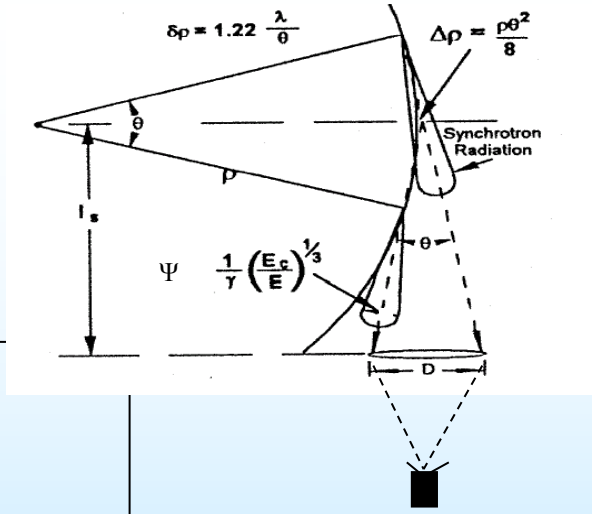

EQ 1:
Diffraction limit (for Object):
For normal slit:
$\sigma_{Diff} = 0.47 * \lambda/\theta/2$ (horizontal, mirror defines opening angle θ)
$\sigma_{Diff} \approx 0.47 * \lambda/\Psi$ (vertikal)

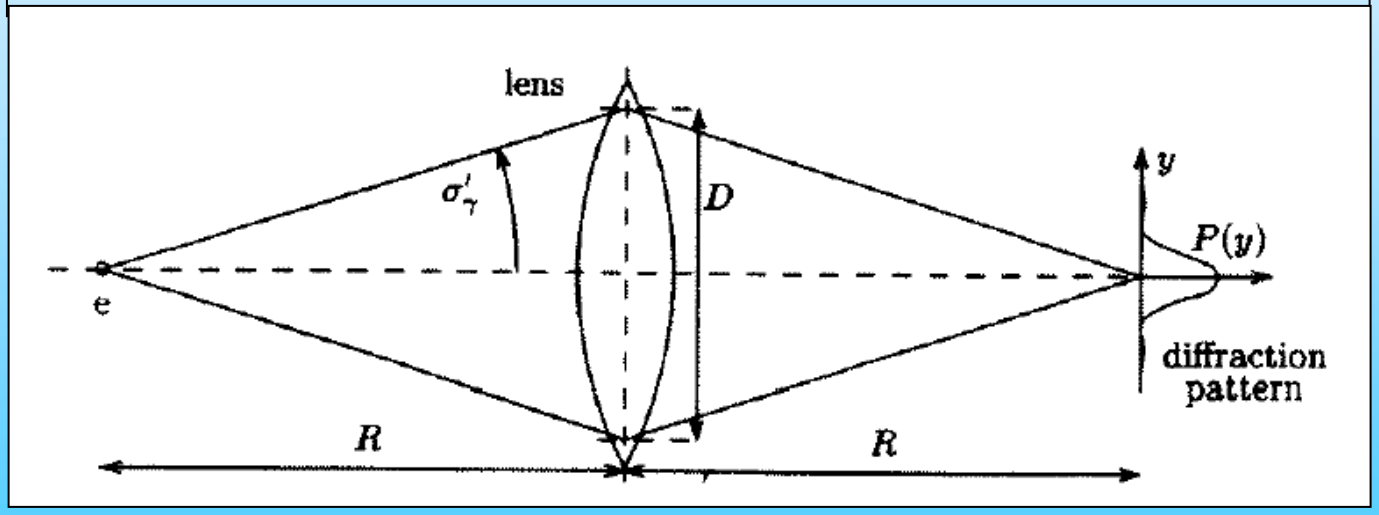

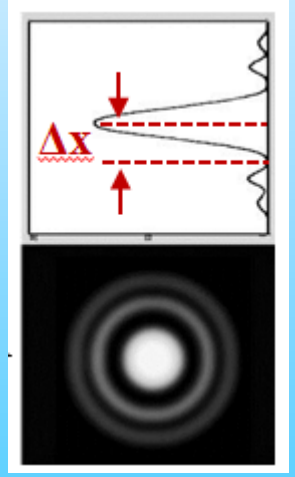

Depth of field:

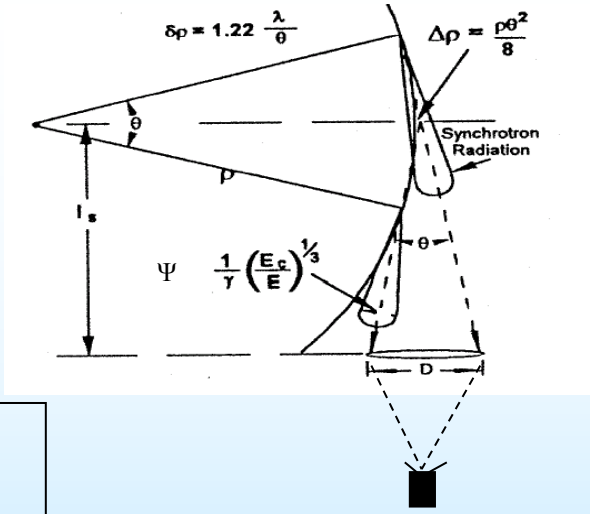

EQ 2:
depth of field:
Vertical: $\Delta_{depth} \approx L/2 * \Psi = \sigma_{depth}$
Horizontal: $\Delta_{depth} \approx L/2 * \theta/2 = \sigma_{depth}$ (mirror defines opening angle θ)
$L \approx \rho \tan\theta$ or $2\rho\,(\theta/2 + \Psi)$

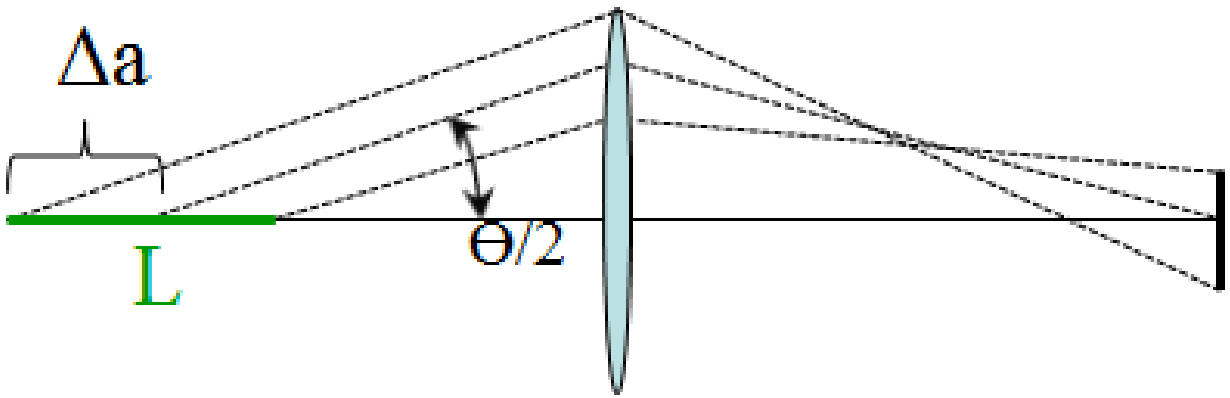

Arc:

EQ 3:
Arc (horizontal):
Observation of the beam in the horizontal plane is complicated by the fact that the light is emitted by all points along the arc. The horizontal width of the apparent source is related to the observation angle as:

$\Delta x_{arc} = \rho\, \theta^{2}/8 = \sigma_{arc}$ (mirror defines opening angle θ)

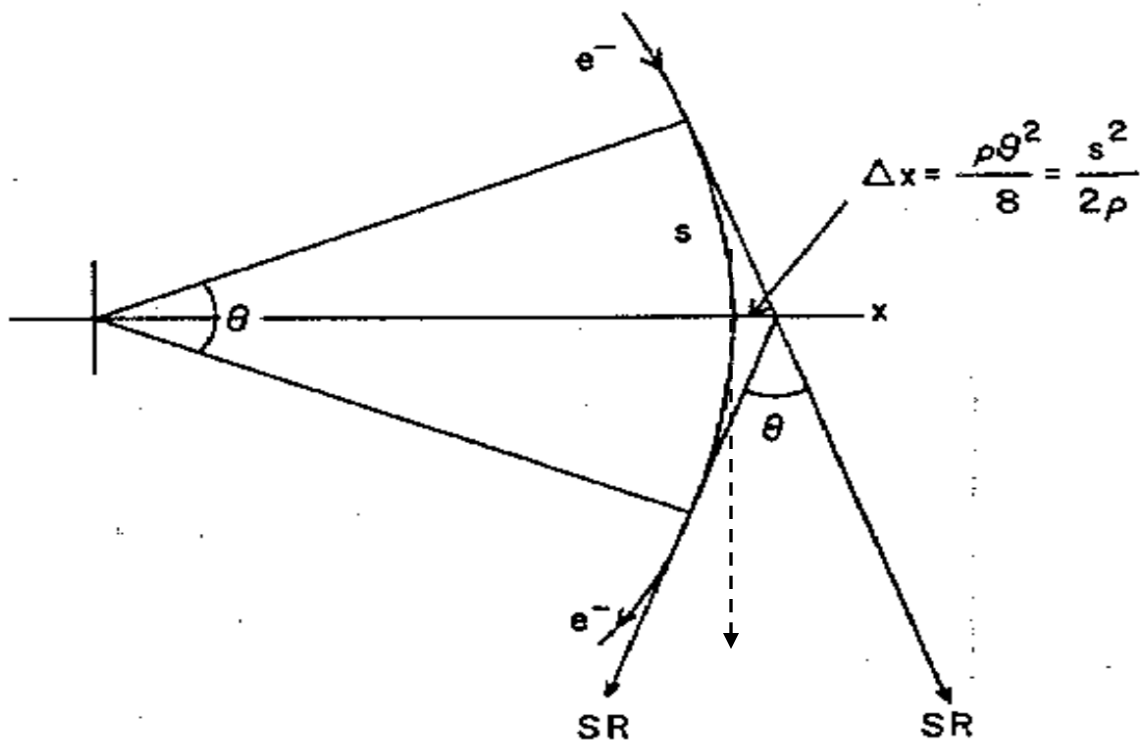

Camera (finite pixel size)

EQ 4:
Camera:
image gain = G/B = 5.485
typical resolution of camera CCD chip: $\sigma_{chip} = 6.7\ \mu m$
$\sigma_{camera} = \sigma_{chip} * G/B = 37\ \mu m$

Resolution:

<u>λ not monochromatic !</u>

$\sigma_{Diff} =$	$0.47 * \lambda/\theta$ (horizontal)	= <u>??? Depends on wavelength</u>
$\sigma_{Diff} =$	$0.47 * \lambda/\Psi$ (vertikal)	= <u>??? Depends on wavelength</u>
$\sigma_{depth} =$	$L/2 * \theta/2$	= <u>440 μm</u>
$\sigma_{arc} =$	$\rho\ \theta^2/8$	= <u>219 μm (horizontal)</u>
$\sigma_{camera} =$	$\sigma_{chip} * G/B$	= <u>37 μm</u>

typical spectral sensitivities from CCD Sensors:

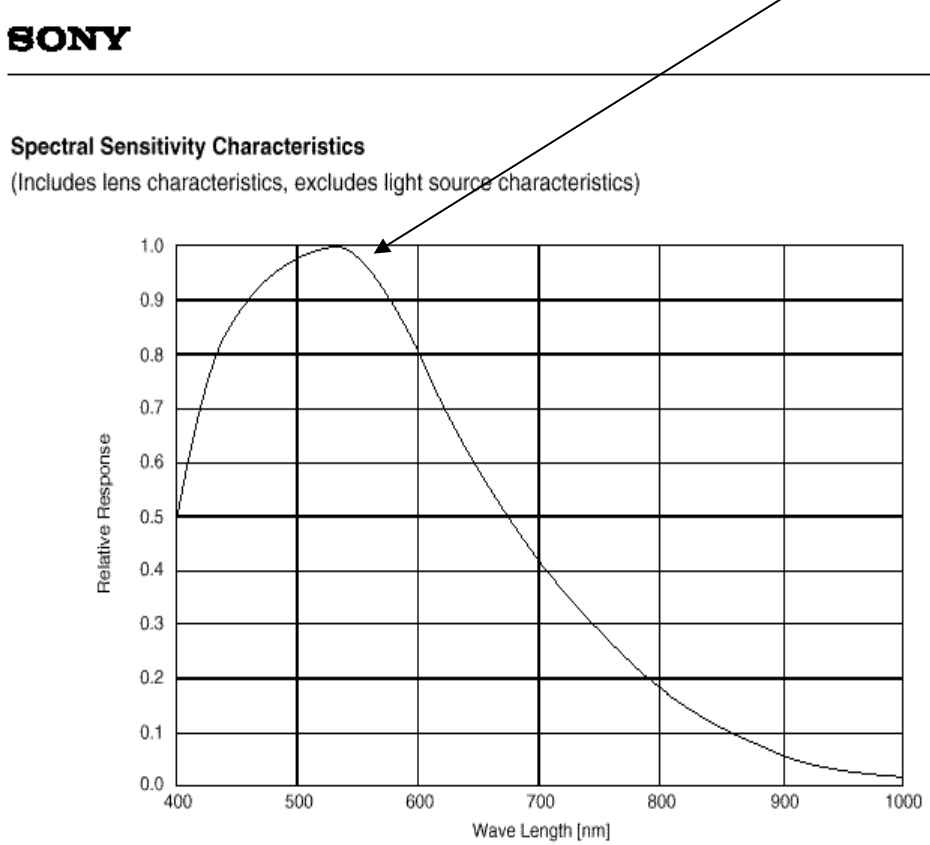

Use a filter (monochromatic light)

Assume: $\lambda = 550$ nm;

$(\gamma = E/m_0c^2)$

$\gamma_{12} = 2.35 * 10^4$ (E = 12 GeV)

$\gamma_{35} = 6.85 * 10^4$ (E = 35 GeV)

$\lambda_{c,12} = (4\pi\rho)/(3\gamma^3) = 0.195$ nm at 12 GeV

$\lambda_{c,35} = (4\pi\rho)/(3\gamma^3) = 0.008$ nm at 35 GeV

opening angle (horizontal): $\tan\theta/2 = d/2/6216 \Rightarrow$

$\theta/2 = \arctan d/2/6216 =$ 0.85 mrad

opening angle (vertikal):

$\Psi(\lambda) = 1/\gamma\ (\lambda/\lambda_c)^{1/3} = [(3\lambda)/(4\pi\rho)]^{1/3} = 0.6$ mrad

(mirror has to be larger than spot size on mirror) =>

σ_{diff} (horizontal) $= 0.47 * \lambda/\theta/2$	= 304 µm
σ_{diff} (vertical) $= 0.47 * \lambda/\Psi$	= 431 µm
$\sigma_{depth} = L/2 * \theta/2$	= 440 µm
σ_{arc} (horizontal) $= \rho\ \theta^2/8$	= 219 µm
$\sigma_{camera} = \sigma_{chip} * G/B$	= 37 µm

$\sigma_{cor} = (\sigma_{diff}{}^2 + \sigma_{depth}{}^2 + \sigma_{arc}{}^2 + \sigma_{camera}{}^2)^{1/2}$ = 579 µm ; (horizontal)

$\sigma_{cor} = (\sigma_{diff}{}^2 + \sigma_{depth}{}^2 + \sigma_{camera}{}^2)^{1/2}$ = 617 µm ; (vertical)

<u>Horizontal:</u>

$\sigma_{cor} = [(\rho\ \theta^2/8)^2 + (L/2 * \theta/2)^2 + (0.47 * \lambda/\theta/2)^2]^{1/2}$

with $L \approx \rho \tan\theta \approx \rho\ \theta$

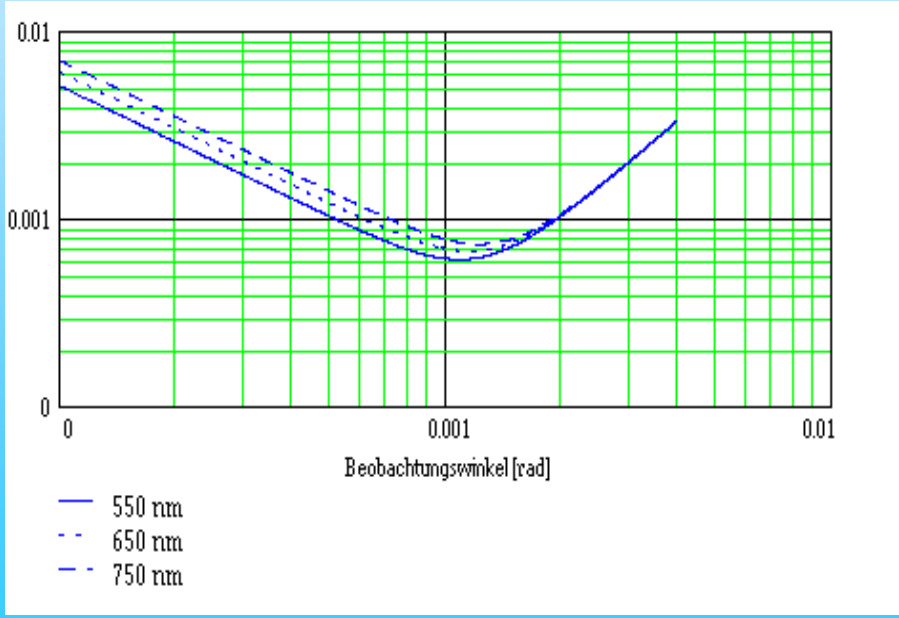

<u>Vertical:</u>

$\sigma_{cor} = [(L/2 * \Psi)^2 + (0.47 * \lambda/\Psi)^2]^{1/2}$ with

$L \approx \rho \tan\theta \approx \rho\ \theta$

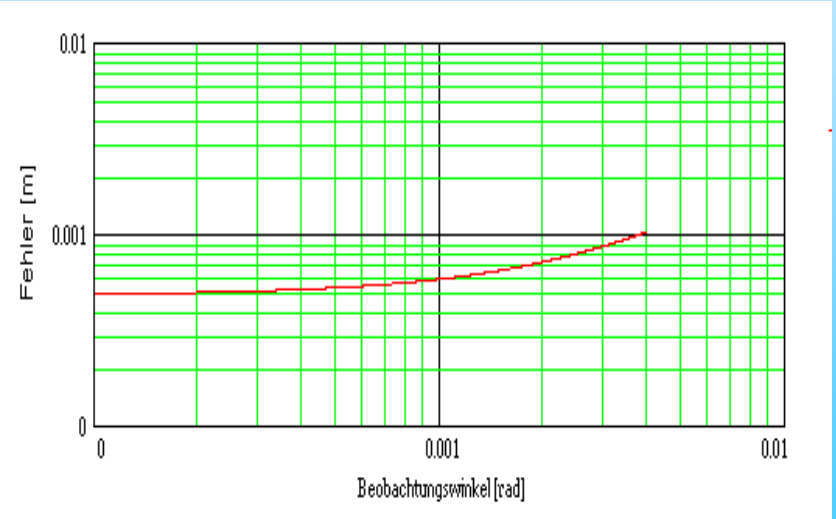

We measured sometimes a negative emittance??? (Not the whole truth so far)

1) Diffraction:

a) Ψ_{exact} is larger than the Gauss approximation (e.g. 0.79 → 1.08 mrad at Tristan)

b) For a gaussian beam the diffraction width is $\sigma_{diff} \approx 1/\pi * \lambda/\Psi$

(Ref: **ON OPTICAL RESOLUTION OF BEAM SIZE MEASUREMENTS BY MEANS OF SYNCHROTRON RADIATION**. By A. Ogata (KEK, Tsukuba). 1991. Published in Nucl.Instrum.Meth.A301:596-598,1991)

=> $\sigma_{diff} \approx 1/\pi * \lambda/\Psi_{exact}$ = <u>218 μm</u> (Ψ_{exact} = 0.8 mrad, λ = 550 nm) vertical

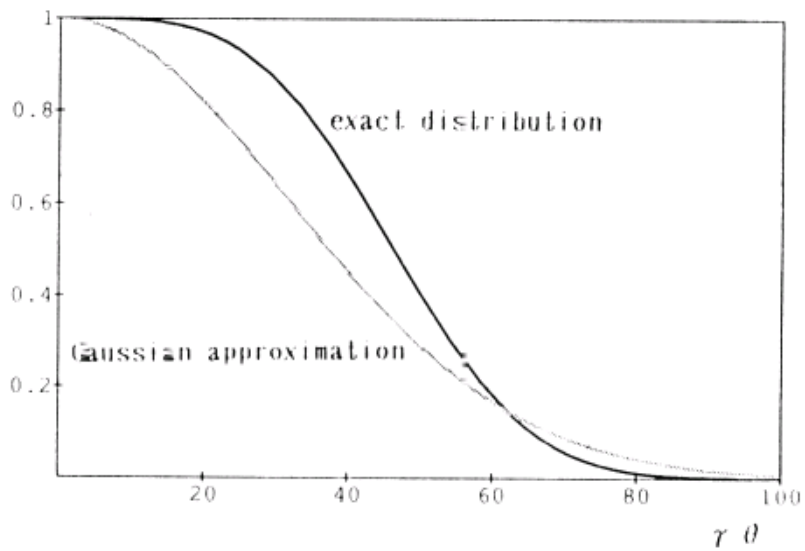

Fig. 1 Angular distribution of the 500 nm component of the synchrotron radiation from the TRISTAN MR bending magnet (246 m bending radius) operated at 30 GeV, and its Gaussian approx mation.

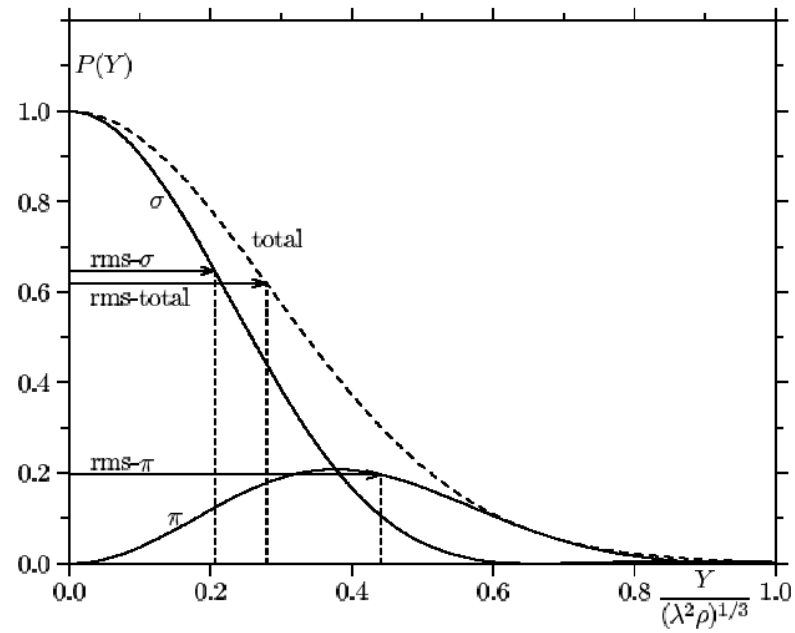

8: Fraunhofer diffraction for synchrotron radiation from long magnets

2) Depth of field:

The formula $R_{depth} = L/2 * \theta/2$ describes the radius of the distribution due to the depth of field effect. It is not gaussian and has long tails. The resolution of an image is probably much better than the formula above. A gaussian approximation with the same integral is shown in the figure below resulting in a width of $\sigma_{depth} = 61\ \mu m$.

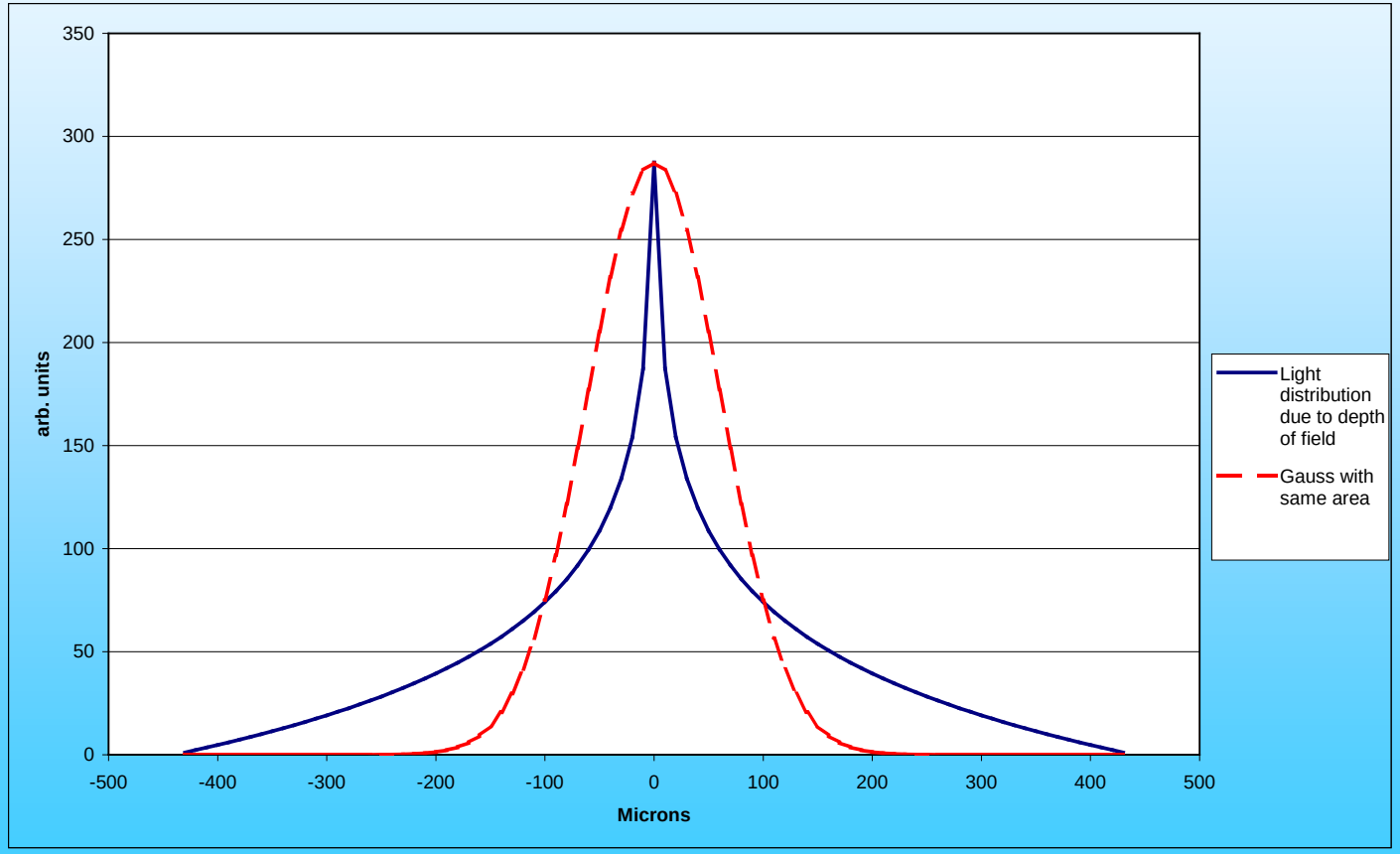

$\sigma_{diff} = 0.47 * \lambda/\theta/2$ = 304 μm (horizontal)

$\sigma_{diff} = 1/\pi * \lambda/\Psi$ = 218 μm (vertical)

$\sigma_{depth} = L/2 * \theta/2$ = 61 μm

$\sigma_{arc} = \rho\, \theta^{2}/8$ = 219 μm (horizontal)

$\sigma_{camera} = \sigma_{chip} * G/B$ = 37 μm

before:

(431 μm)

(440 μm)

$\sigma_{cor} = (\sigma_{diff}^{2} + \sigma_{depth}^{2} + \sigma_{arc}^{2} + \sigma_{camera}^{2})^{1/2}$

$\sigma_{cor} = (\sigma_{diff}^{2} + \sigma_{depth}^{2} + \sigma_{camera}^{2})^{1/2}$

= 381 μm ; (horizontal) (579 μm)

= 229 μm ; (vertical) (617 μm)

Beam width $\sigma_{beam} = (\sigma_{fit\_measured}^{2} - \sigma_{cor}^{2})^{1/2}$

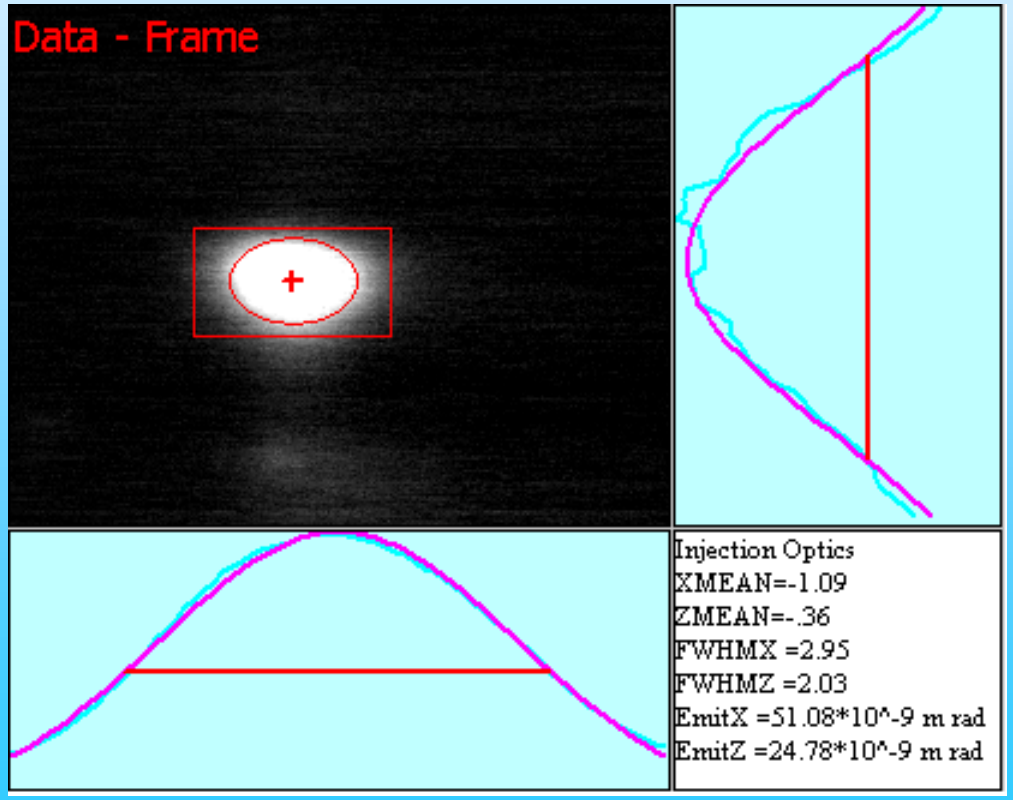

σ_{vert} = 860 μm

Exercise SR3: Discuss possible improvements of an SR-monitor:

- Monochromator at shorter wavelength (x-rays, need special optic)
- Use optimum readout angle
- Polarization - filter
- Use x-ray ($\lambda < 0.1$ nm)

More:

Interferometer

The principle of measurement of the profile of an object by means of **spatial coherency** was first proposed by H.Fizeau and is now known as the Van Cittert-Zernike theorem. It is well known that A.A. Michelson measured the angular dimension (extent) of a star with this method.

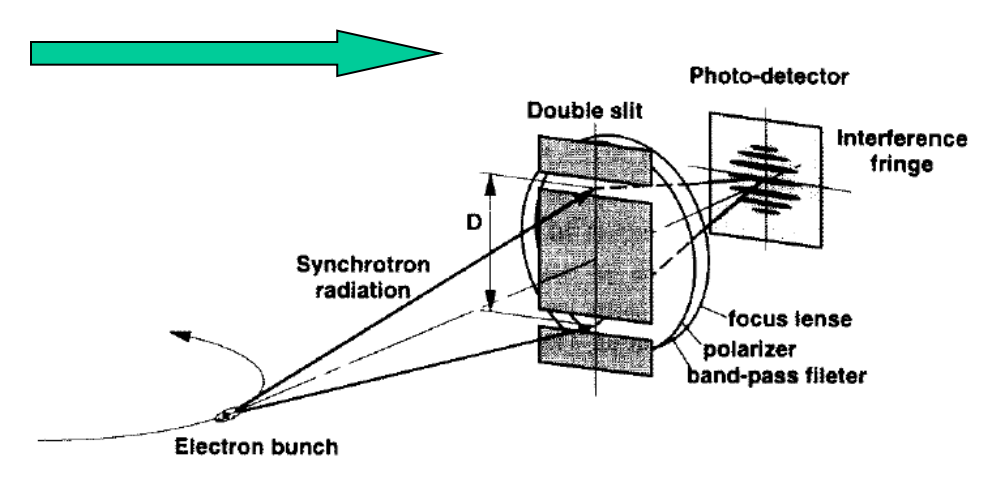

Referenzes

SPATIAL COHERENCY OF THE SYNCHROTRON RADIATION AT THE VISIBLE LIGHT REGION AND ITS APPLICATION FOR THE ELECTRON BEAM PROFILE MEASUREMENT.
By T. Mitsuhashi (KEK, Tsukuba). KEK-PREPRINT-97-56, May 1997. 4pp. Talk given at 17th IEEE Particle Accelerator Conference (PAC 97): Accelerator Science, Technology and Applications, Vancouver, Canada, 12-16 May 1997.

Intensity Interferometer and its application to Beam Diagnostics, Elfim Gluskin, ANL, publ. PAC 1991 San Francisco

MEASUREMENT OF SMALL TRANSVERSE BEAM SIZE USING INTERFEROMETRY
T. Mitsuhashi
High Energy Accelerator Research Organisation, Oho, Tsukuba, Ibaraki, 305-0801 Japan
DIPAC 2001 Proceedings - ESRF, Grenoble

X-ray Pinhole Camera

- „camera obscura“

  description of phenomenon already by Aristoteles (384-322 b.C.) in „Problemata“

- most common emittance monitor

  simple setup ⟷ limited resolution $\sigma_{res} \geq 10\,\mu m$

example: ESRF

P.Elleaume, C.Fortgang, C.Penel and E.Tarazona, J.Synchrotron Rad. 2 (1995) , 209

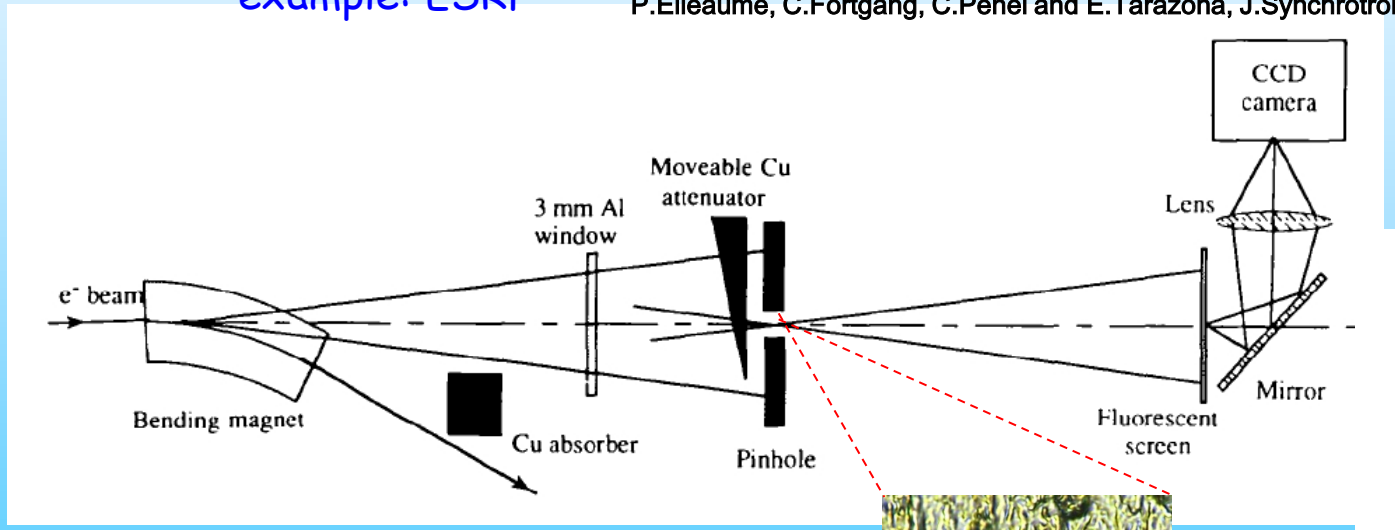

ID-25 X-ray pinhole camera:

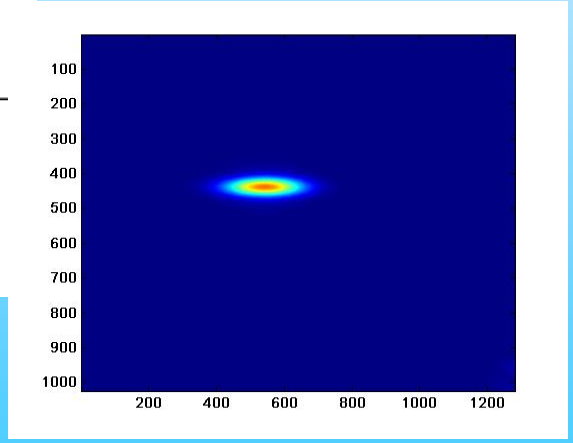

courtesy of K.Scheidt, ESRF

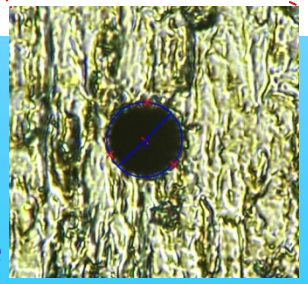

PETRA III pinhole camera:

Ø 18 µm hole in 500 µm thick W plate

Compound Refractive Lens

lens-maker formula: $1/f = 2(n-1) / R$

X-ray refraction index : $n = 1 - \delta + i\beta, \quad \delta \approx 10^{-6}$

- concave lens shape
- strong surface bending R

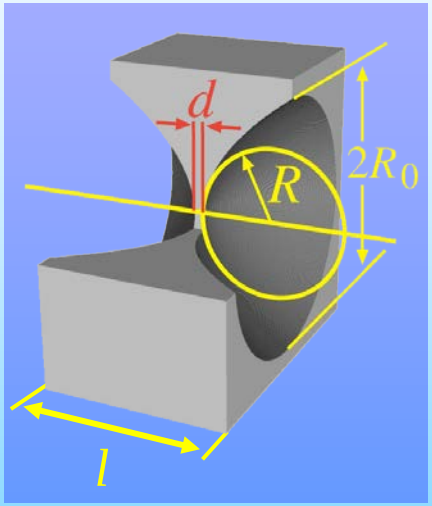

- small Z (Be, Al, …)
- small d

$$f = \frac{R}{2\delta N}$$

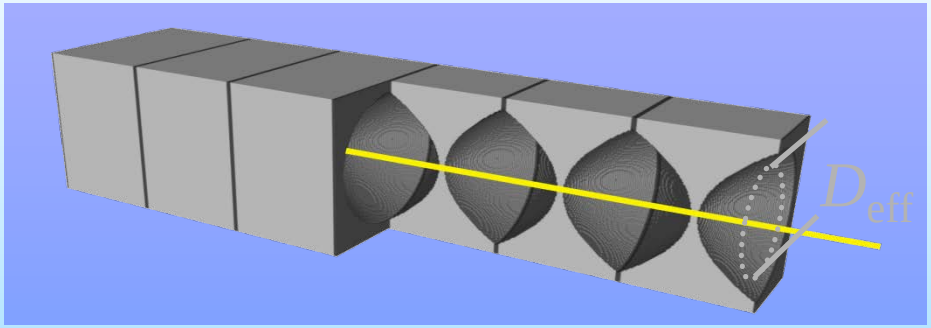

many lenses (N=10…300)

PETRA III @ 20 keV:

- R = 200 µm, R_0 = 500 µm, d = 10 µm, l = 1mm
- N = 31
- material: beryllium

$f = 3.8\,\mathrm{m}$

$\sigma_{res} \approx 0.6\,\mu\mathrm{m}$

CRL Monitor @ PETRA III (DESY)

- PETRA III diagnostics beamline

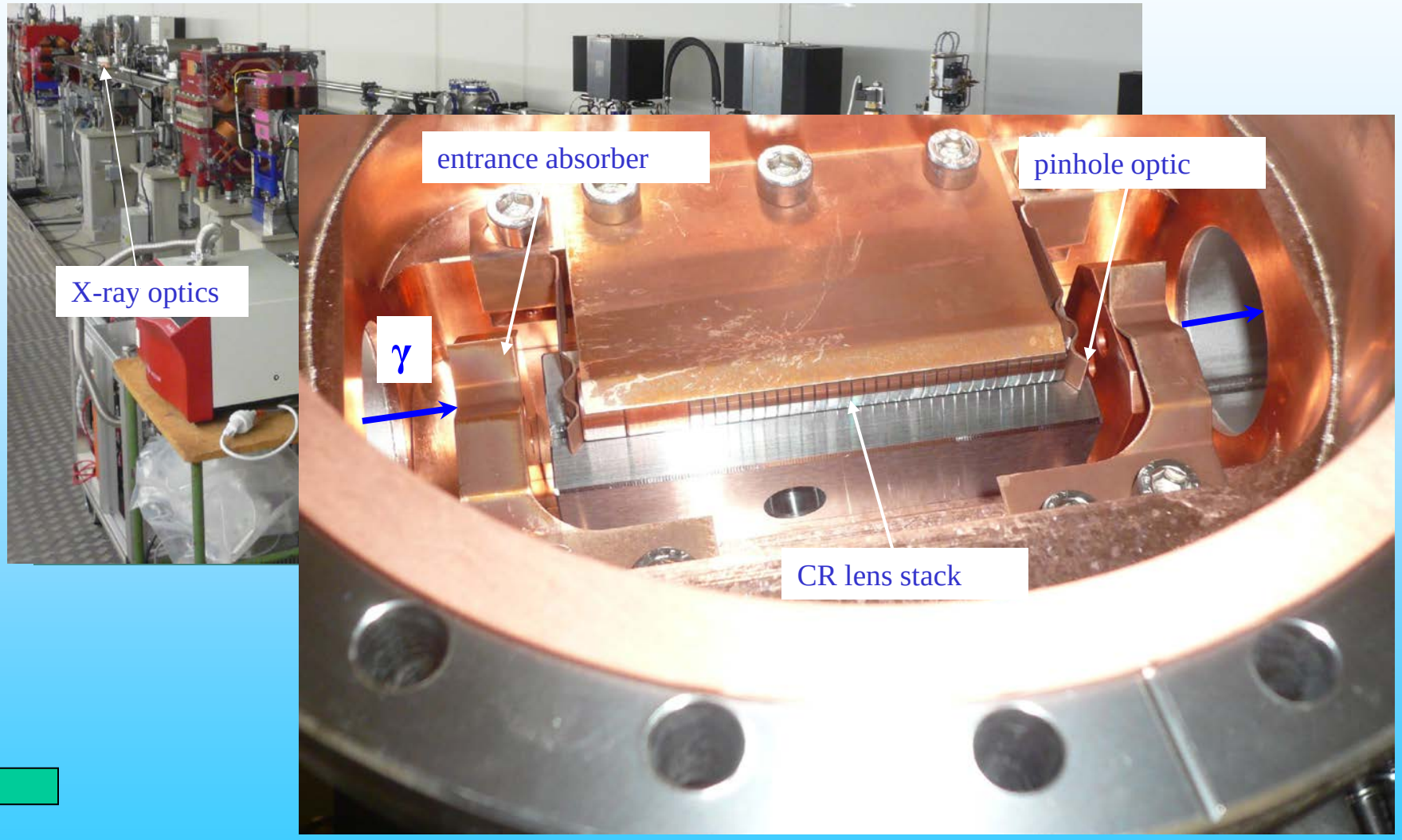

Resolution Improvements

2.) interferometric approach

T. Mitsuhashi , Proc. Joint US-CERN-Japan-Russia School of Particle Accelerators, Montreux, 11-20 May 1998 (World Scientific), pp. 399-427.

⟹ probing spatial coherence of synchrotron radiation

point source

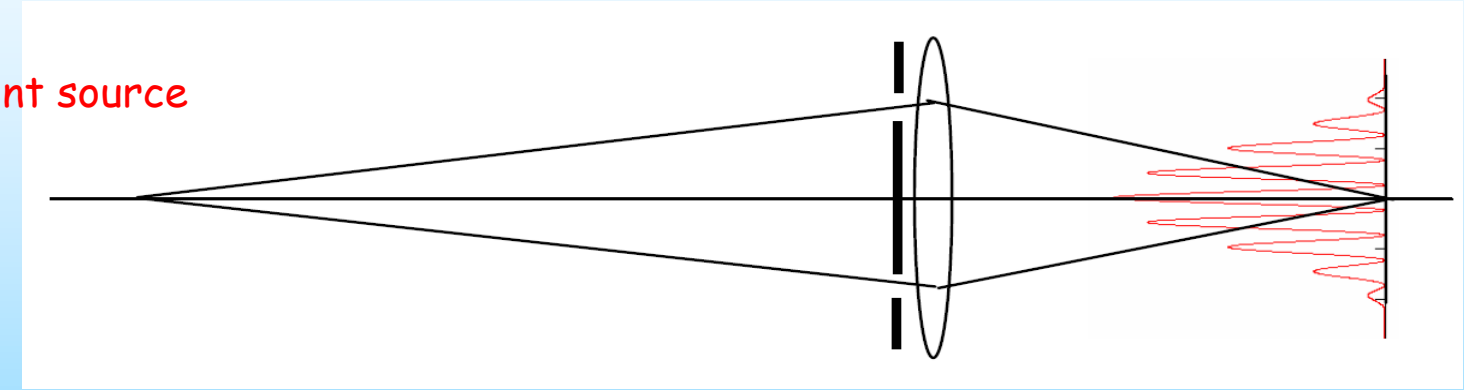

visibility:

$$V = \frac{I_{max} - I_{min}}{I_{max} + I_{min}}$$

$V = 1$

extended source

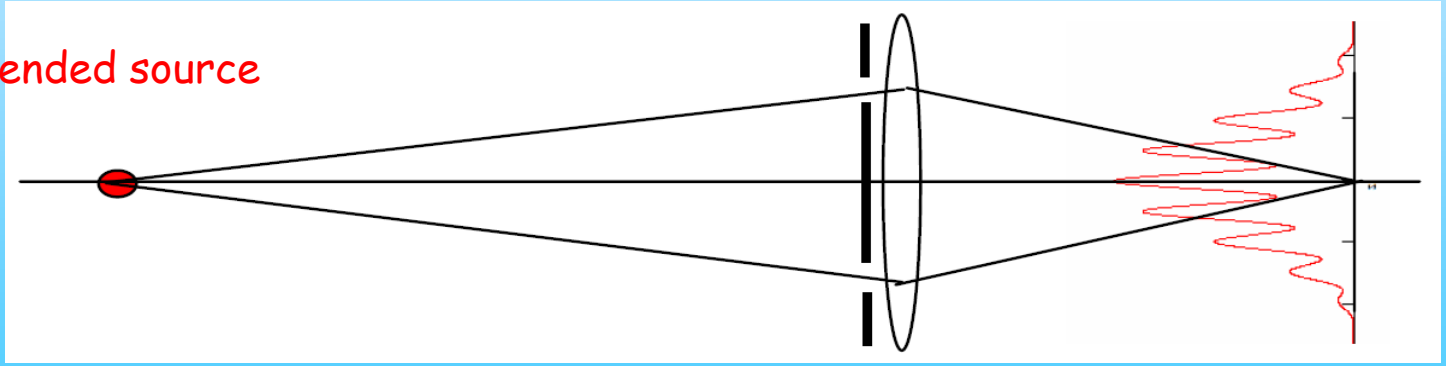

$V < 1$

- resolution limit: uncertainty principle $\Delta n \cdot \Delta\Phi \approx 1$

Δn: photon number

$\Delta\Phi$: photon phase

T. Mitsuhashi, Proc. BIW04, AIP Conf. Proc. 732, pp. 3-18

Interference: ATF (KEK)

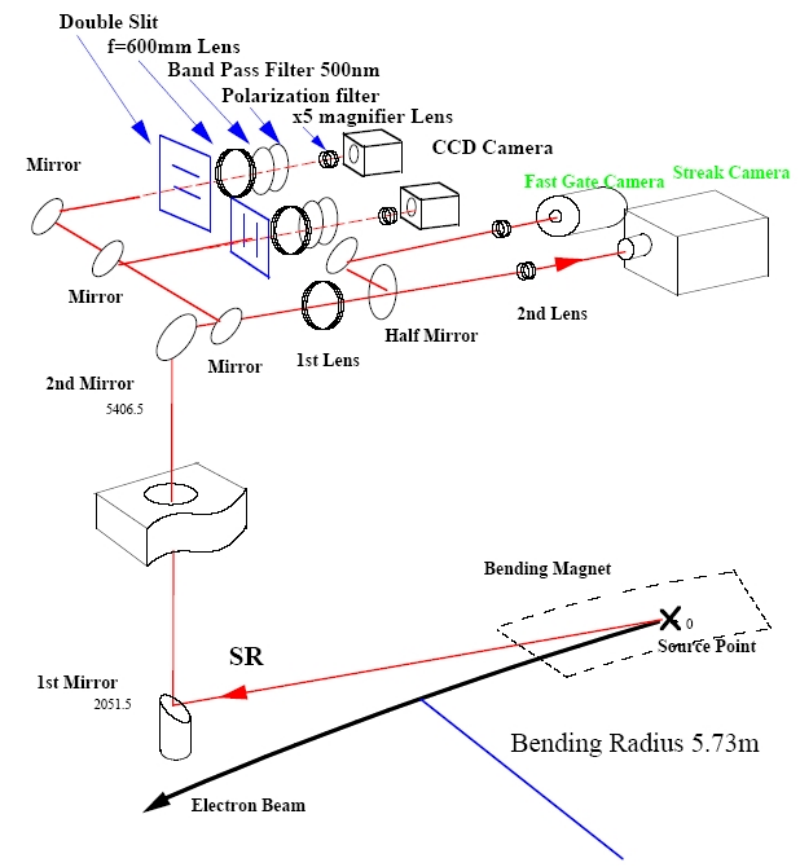

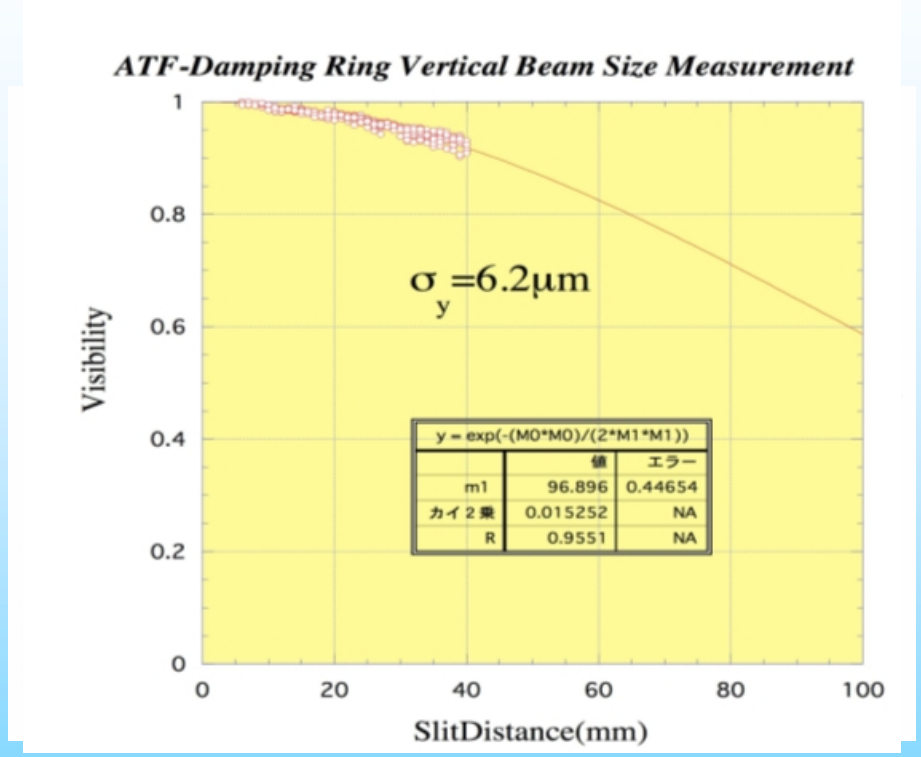

H.Hanyo et al., Proc. of PAC99 (1999), 2143

courtesy of T.Mitsuhashi, KEK

- smallest result: 4.7 μm with 400nm @ ATF, KEK

  accuracy ~ 1 μm

Back to an imaging SR-Monitor: Still not the whole truth:

(Diffraction Limited) Resolution

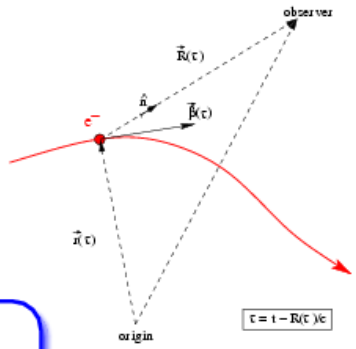

Liénard –Wiechert potentials: $\varphi(t) = \left[\frac{-e}{R(1-\hat{n}\cdot\vec{\beta})}\right]_{ret}$, $\vec{A}(t) = \left[\frac{-e\vec{\beta}}{R(1-\hat{n}\cdot\vec{\beta})}\right]_{ret}$

Liénard –Wiechert fields:

$$\vec{E}(t) = -e\left(\frac{(1-\beta^2)(\hat{n}-\vec{\beta})}{R^2(1-\hat{n}\cdot\vec{\beta})^3} + \frac{\hat{n}\times[(\hat{n}-\vec{\beta})\times\dot{\vec{\beta}}]}{cR(1-\hat{n}\cdot\vec{\beta})^3}\right)_{ret}$$

$$\vec{H}(t) = \hat{n}\times\vec{E}(t)$$

Fourier transform:

$$\vec{E}_\omega \approx -\frac{i\omega e}{cR}\int[\hat{n}\times[\hat{n}\times\vec{\beta}]]\, e^{i\omega(\tau+R(\tau)/c)}\, d\tau$$

point charge on circular orbit

↪ analytical far field expressions for E_σ , E_π

Fourier transform:

$$\varphi_\omega = -e\int\frac{1}{R(\tau)}e^{i\omega(\tau+R(\tau)/c)}d\tau$$

$$\vec{A}_\omega = -e\int\frac{\vec{\beta}(\tau)}{R(\tau)}e^{i\omega(\tau+R(\tau)/c)}d\tau$$

Electric field:

$$\vec{E}_\omega = -\frac{i\omega e}{c}\int\left[\frac{\vec{\beta}-\hat{n}}{R(\tau)} - \frac{ic}{\omega}\frac{\hat{n}}{R^2(\tau)}\right]e^{i\omega(\tau+R(\tau)/c)}\, d\tau$$

numerical near field calculation depending on field geometry

↪ free codes available (SRW, SPECTRA, . . .)

propagation in frame of scalar diffraction theory

$$\vec{E}_{\omega\perp,2} = -i\frac{\omega}{2\pi c}\int\int_\Sigma\frac{\vec{E}_{\omega\perp,1}}{\rho}\exp[i\,\omega/c\,\rho]\, d\Sigma$$

spectral flux density

$$\frac{d^2N_\omega}{dA\, d\omega/\omega} = \frac{\alpha c^2}{4\pi^2 e^2}|\vec{E}_{\omega\perp,2}|^2$$

Classical way:
approximation

Numerical way
Includes real electron path, depth of field and diffraction

Point spread Function

- Fraunhofer diffraction pattern for spherical wave

  ↪ depth of field, orbit curvature: additional contributions

- accounts for the fact that SR is not actually a sperical wave

  ↪ depth of field and orbit curvature included

A. Hofmann and F. Méot, Nucl. Instr. Meth. **203** *(1982) 483*

O. Chubar and P.Elleaume, Proceedings of the EPAC98, Stockholm, Sweden (1998) 1177

Point Spread Function

The **point spread function** (**PSF**) describes the response of an imaging system to a **point source or point object!!!** A more general term for the PSF is a system's impulse response, the PSF being the impulse response of a *focused* optical system. In functional terms it is the spatial domain version of the transfer function of the imaging system. It is a useful concept in many imaging. The degree of spreading (blurring) of the point object is a measure for the quality of an imaging system. In non-coherent imaging systems such as telescopes or optical microscopes, the image formation process is linear in power and described by linear system theory. This means that when two objects A and B are imaged simultaneously, the result is equal to the sum of the independently imaged objects. In other words: the imaging of A is unaffected by the imaging of B and *vice versa*, owing to the non-interacting property of photons. The image of a complex object can then be seen as a convolution of the true object and the PSF. However, when the detected light is coherent, image formation is linear in the complex field. Recording the intensity image then can lead to cancellations or other non-linear effects.

from Wikipedia

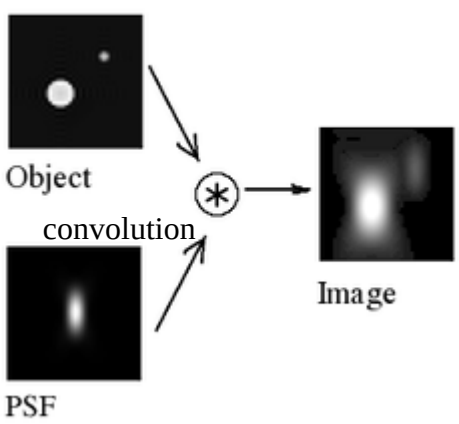

The goal is to minimize the PSF

Because convolution in the spatial domain is equal to multiplication in the frequency domain, convolutions are more easily manipulated by taking their Fourier transform (F).

$$F\{i(x,y,z,t)\} = F\{o(x,y,z,t)\} \times F\{psf(x,y,z,t)\}$$

The frequency domain is characterized by the modulation transfer function MTF or by the optical transfer function OTF with MTF = |OTF|. The MTF is the Fourier transform of the PSF and describes how spatial frequency is affected by blurring.

Theoretically, it should be possible to reverse the convolution of object and PSF by taking the inverse of the Fourier transformed functions. However, deconvolution increases noise, which exists at all frequencies in the image. Many deconvolution algorithms (filters) exist: Richardson-Lucy, van Cittert, Wiener, Blind, ….

Done in astronomy, starting for beam diagnostics

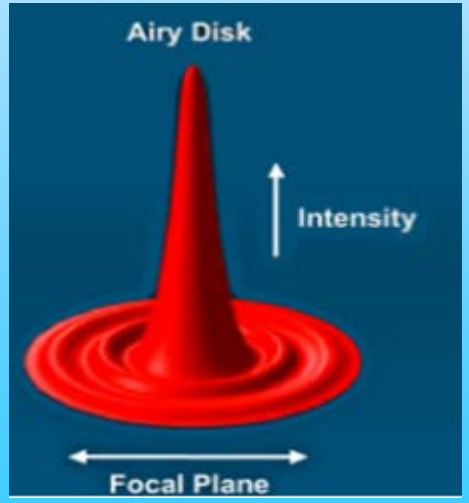

Resolution Broadening Effects for the HERAe Emittance Monitor

determination:

- calculation of spatial SR intensity distribution including beam emittance
- quadratical subtraction of beam size

For ∞ mirror size

horizontal profile

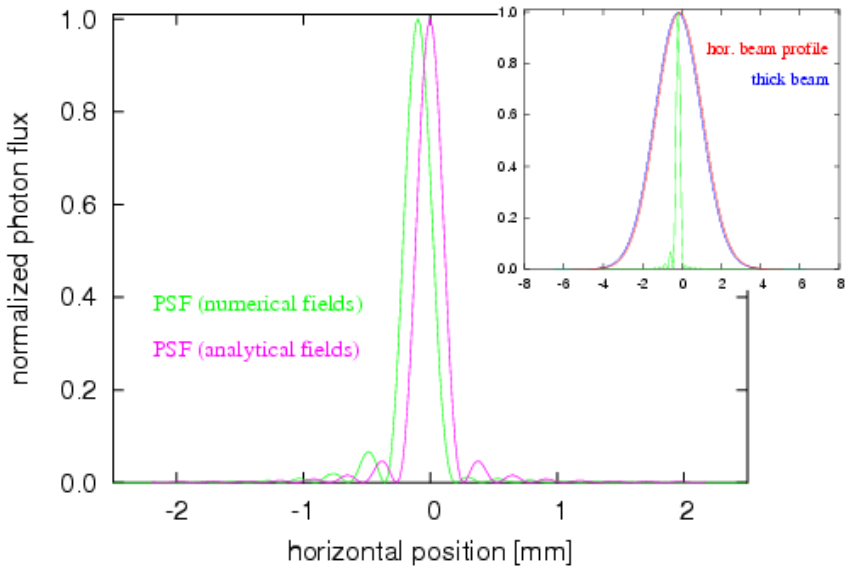

vertical profile

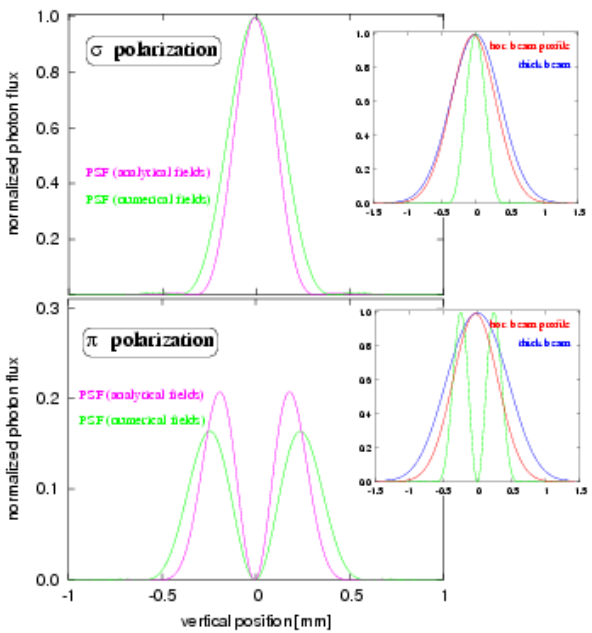

New

broadening contribution: $\sigma_{res} = 203\ \mu m$ numerical

broadening contribution: $\sigma_{res} = 138\ \mu m$

So far

$\sigma_{diffract} = 188\ \mu m$

$\sigma_{dof+curv} = 275\ \mu m$

$\hookrightarrow$ $\sigma_{res} = 333\ \mu m$ analytical

579 ->381-> 333->203 µm

$\sigma_{diffract} = 106\ \mu m$

$\sigma_{dof} = 134\ \mu m$

$\hookrightarrow$ $\sigma_{res} = 171\ \mu m$

617-> 229 ->171-> 138 µm

- *G. Kube, R. Fischer, K. Wittenburg, in Proceedings of BIW2004, AIP Conf. Proc.* **732** *(2004), p.350–357*
- *G. Kube, R. Fischer, Ch. Wiebers, K. Wittenburg, in Proceedings of DIPAC2005*

Comparison

SR-monitor vs Wire scanner

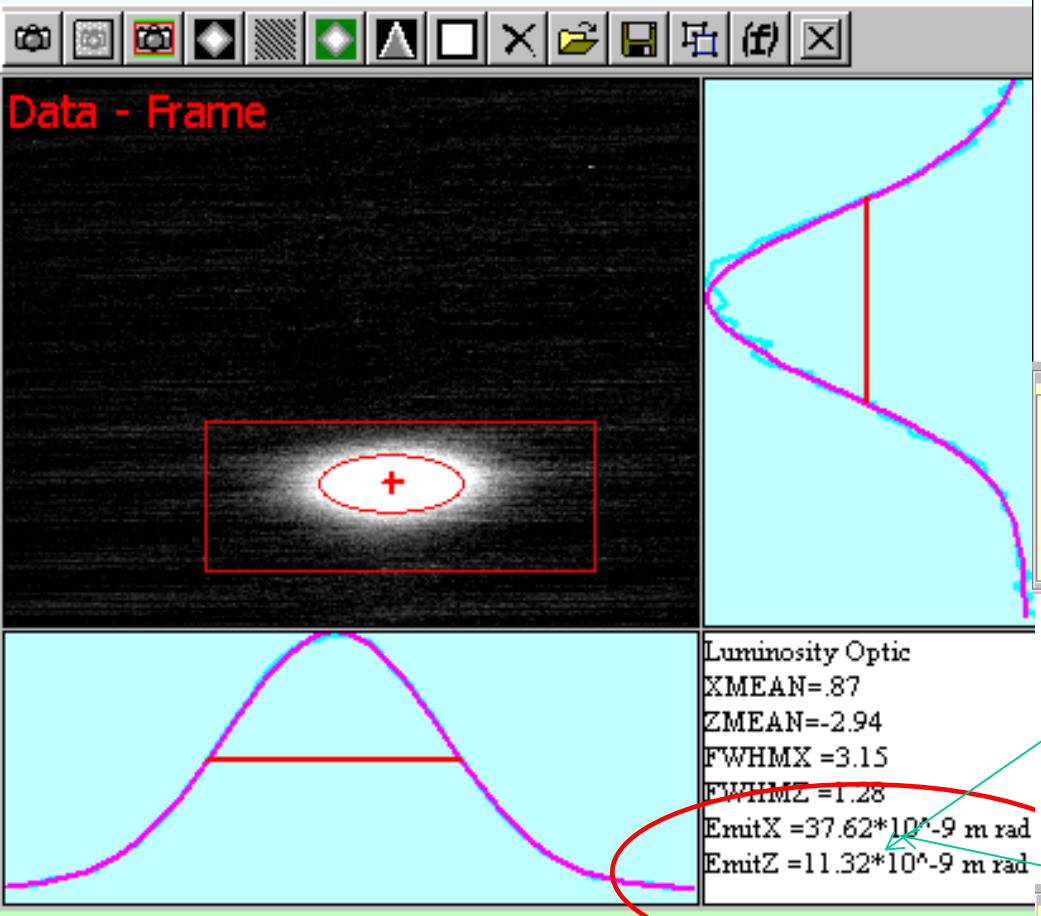

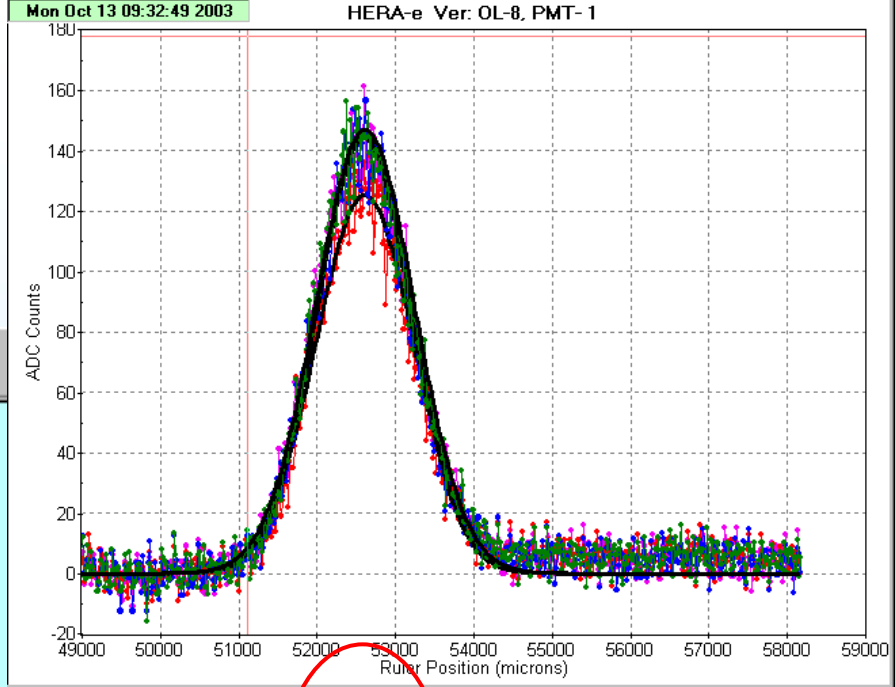

	ε (nm.mrad)	σ(mm)	Mean	Offset	Ampl
Bunch 6	10.65	0.617	52.601	0.000	145.374
Bunch 7	11.01	0.628	52.607	0.000	125.148
Bunch 8	9.96	0.597	52.597	0.000	144.053
Bunch 9	11.07	0.629	52.612	0.000	146.765

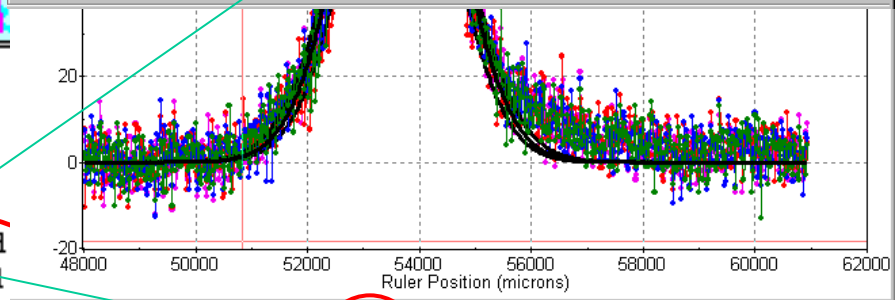

	ε (nm.mrad)	σ(mm)	Mean	Offset	Ampl
Bunch 6	37.18	0.963	53.616	0.000	101.469
Bunch 7	34.25	0.924	53.648	0.000	87.769
Bunch 8	41.71	1.020	53.646	0.000	97.571
Bunch 9	35.90	0.946	53.649	0.000	103.283

$\sigma_v = 542\ \mu m$

End of Synchrotron Light session

and sometimes the beam is watching you …

Reserve

Vertical Resolution for Off–Axis Observation at HERAe

motivation:
- high heat load of extraction mirror
- opening angle Ψ_c for optical SR larger than for X–rays → x-ray miss the mirror

solution:
- observation in off–axis geometry ($y_m \geq 0$)

consequence:
- modification of lower bound in Kirchhoff integral (SR propagation through optical system)

↪ additional resolution broadening

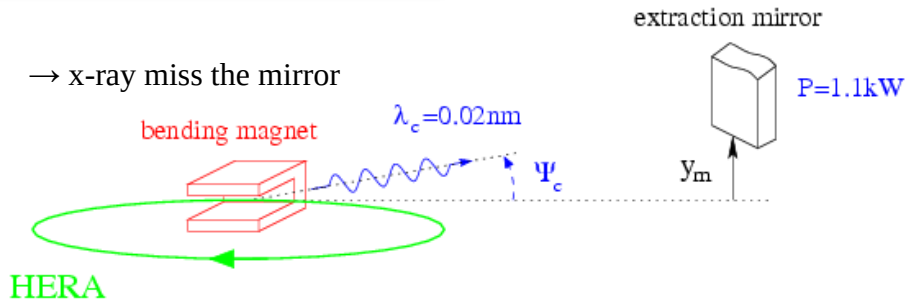

point spread function:

σ polarization π polarization

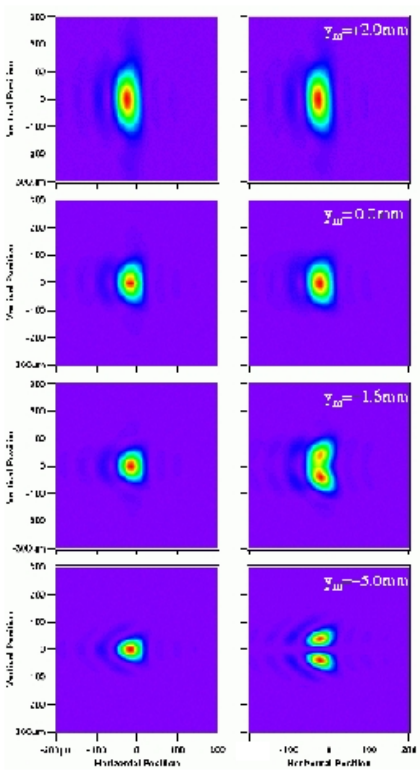

comparison:

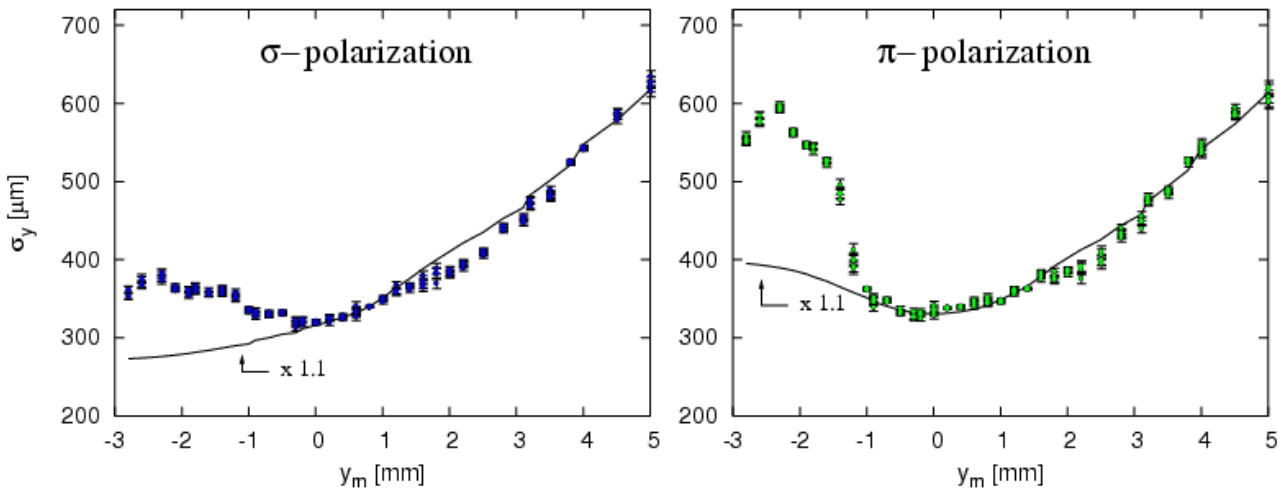

G. Kube, R. Fischer, K. Wittenburg, in Proceedings of BIW2004, AIP Conf. Proc. **732** *(2004), p.350–357*

G. Kube, R. Fischer, Ch. Wiebers, K. Wittenburg, in Proceedings of DIPAC2 005 (in press)

- spectrum characterized by λ_c:
- large p mass $\Longrightarrow$ small $\gamma = E/m_p c^2$

$$\lambda_c = \frac{4\pi}{3}\frac{\rho}{\gamma^3}$$

γ: Lorentz factor

ρ: bending radius

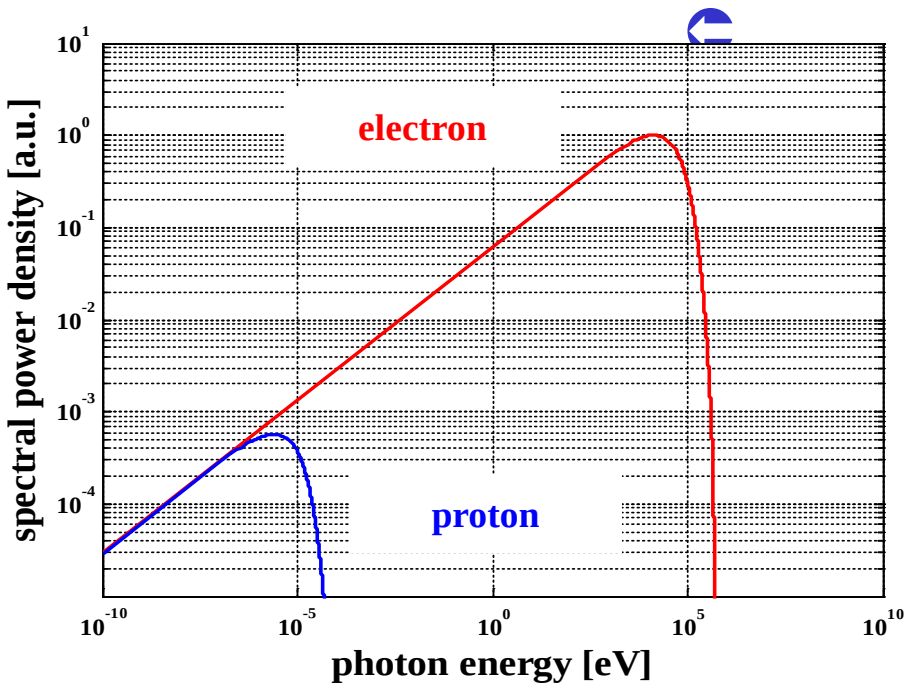

E_{kin} = 20 GeV

ρ= 370 m

HERA-p: E = 40…920 GeV λ_c = 55 mm …4.5 µm

$\Longrightarrow$ large diffraction broadening, expensive optical elements, …

"Frequency Boost" of Synchrotron Radiation

task: production of sufficient synchrotron radiation intensity at high frequencies $\omega \gg \omega_c$

$\hookrightarrow$ intensity: $\boxed{\frac{d^2 W}{d\Omega \, \frac{d\omega}{\omega}} \propto |\vec{E}_\omega|^2}$ with $\vec{E}_\omega = \frac{1}{\sqrt{2\pi}} \int_{-\infty}^{+\infty} dt \, \vec{E}(t) \, e^{i\omega t}$

intuitive approach: synchrotron radiation in time domain

1.) field shape for on–axis observation (i.e. $E_\pi = 0$)

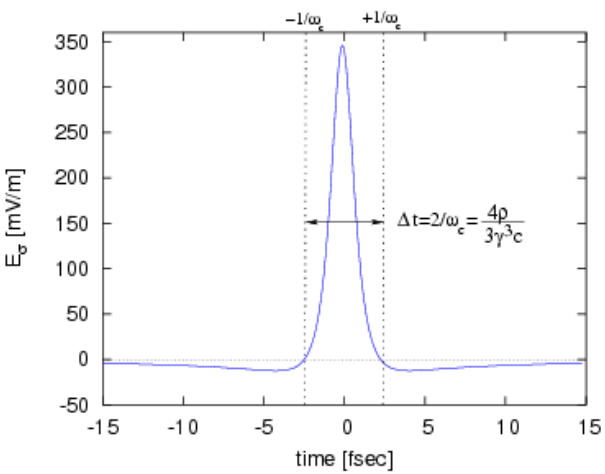

2.) pulse length estimation at fixed observation point

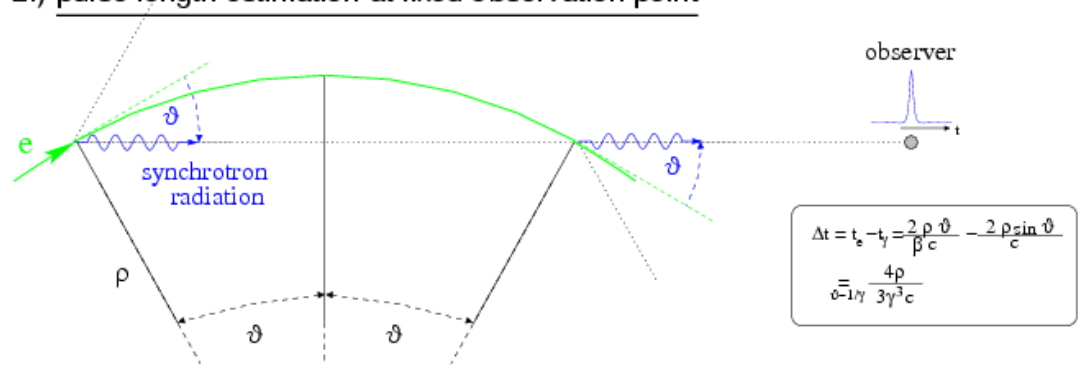

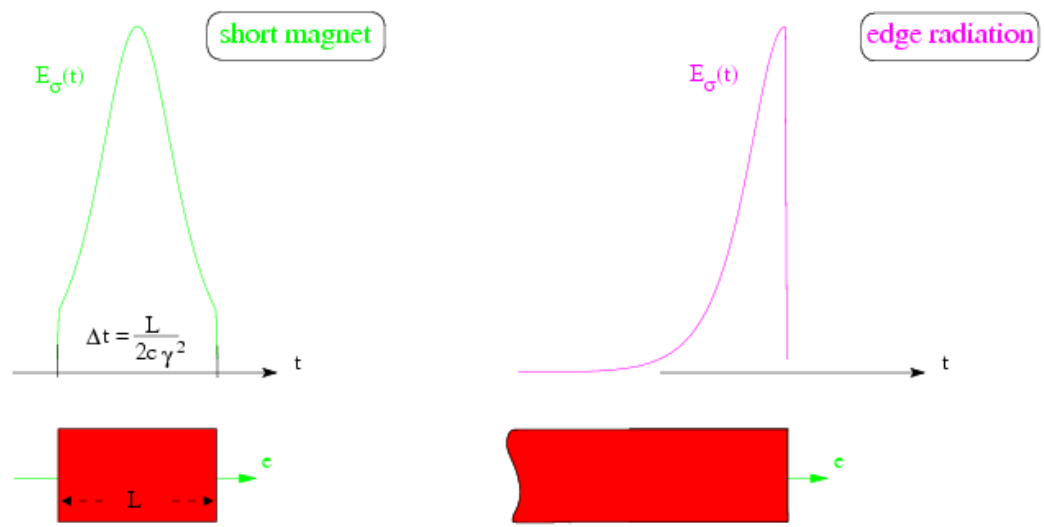

consequence:

Observation time interval defines spectrum (ω_c)

Generation of Frequency Boost

sharp cut-off of wavetrain in time domain

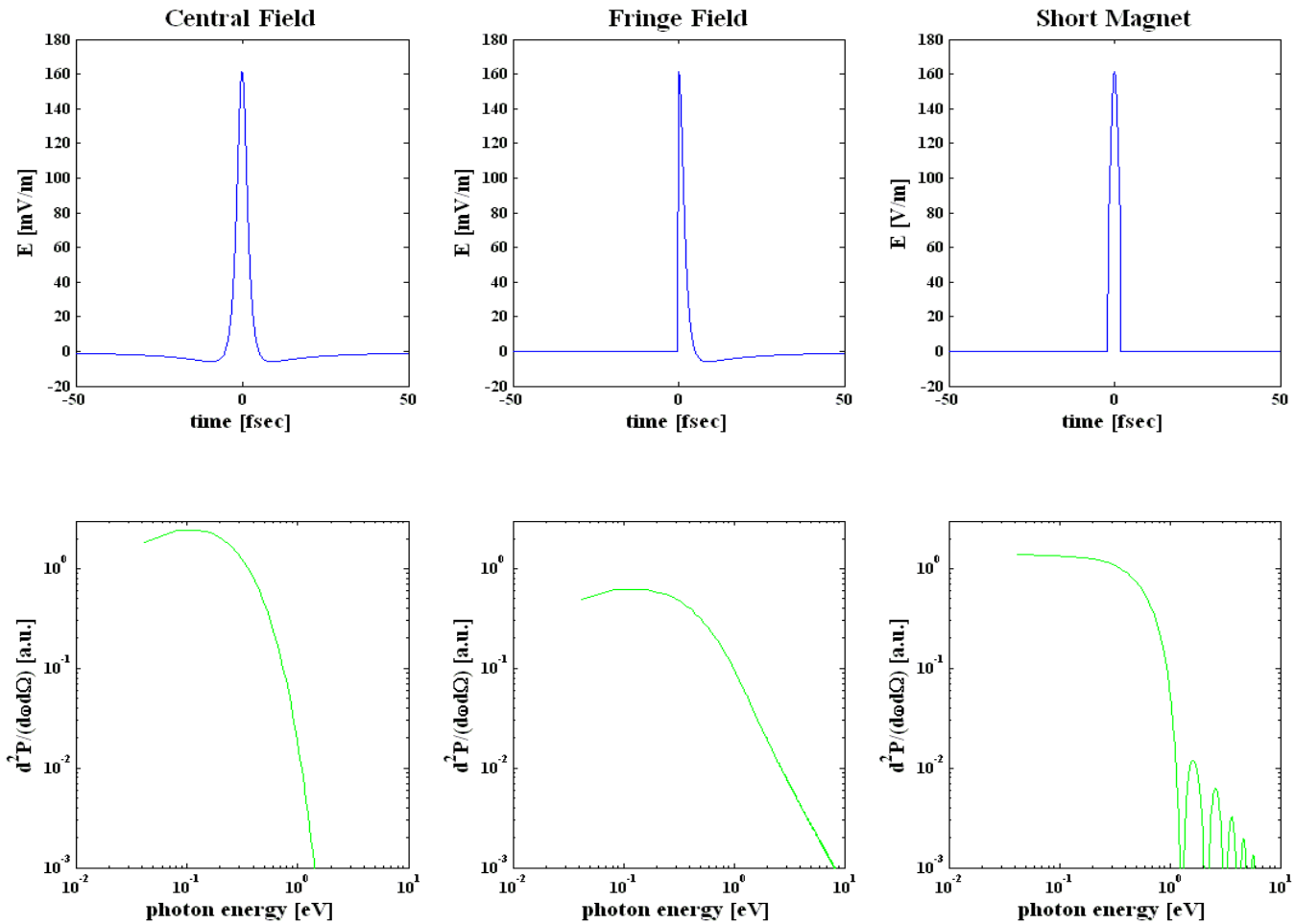

$$\frac{d^2N}{d\Omega\, d\omega/\omega} \propto \left|\vec{E}_\omega\right|^2$$

with

$$\vec{E}_\omega = \frac{1}{\sqrt{2\pi}} \int_{-\infty}^{+\infty} dt\, \vec{E}(t)\, e^{i\omega t}$$

still requires high beam energies (CERN, Tevatron, HERA)

p SyLi Monitor @ HERA (DESY)

fringe field of vertical deflecting dipole

setup :

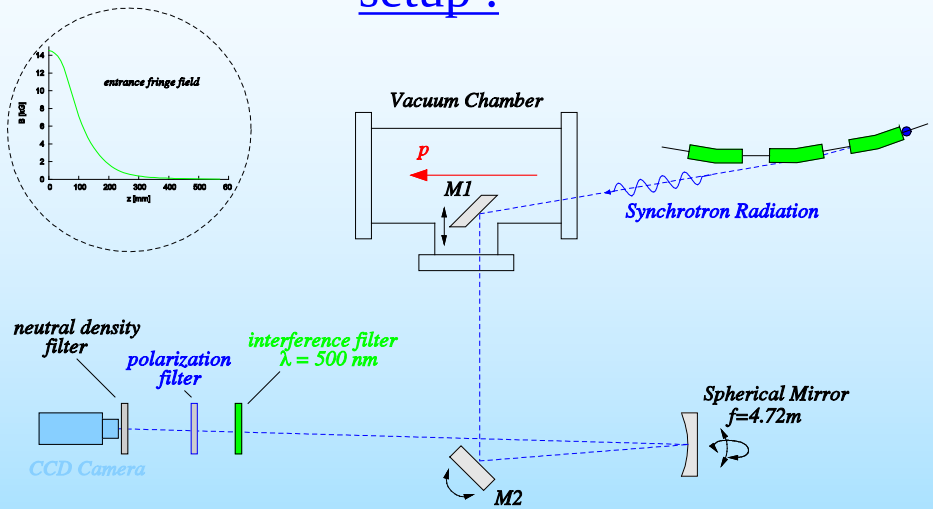

screen shot :

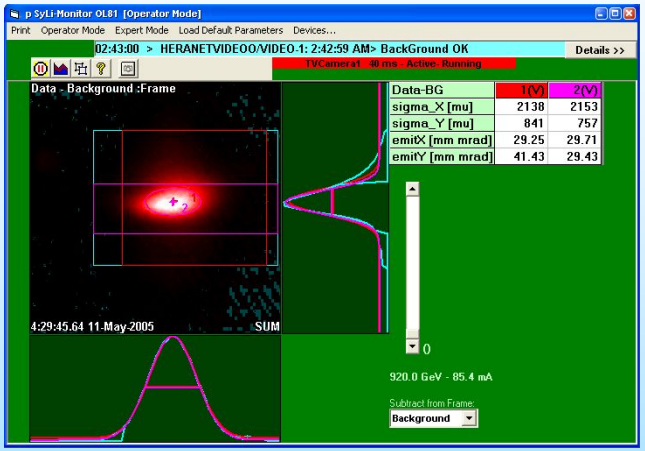

visible light spot for E > 600 GeV

dynamics study:

moving collimators towards the beam

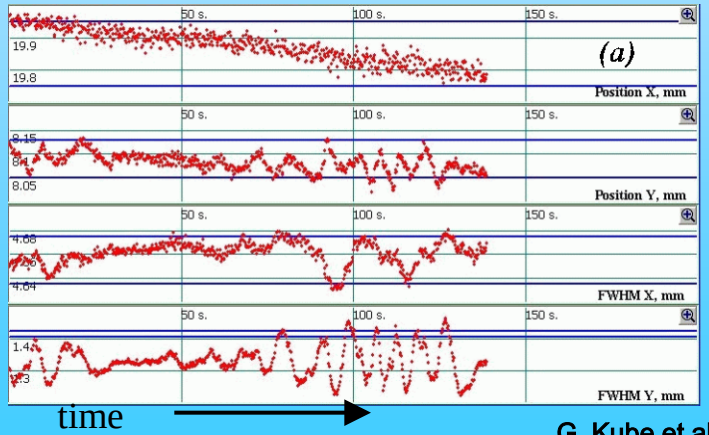

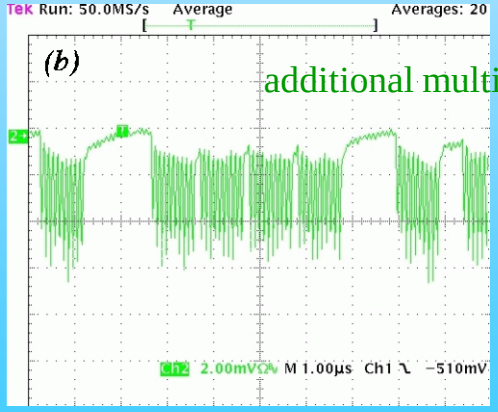

additional multiplier signal

G. Kube et al., Proc. of BIW06 (2006), Batavia, Illinois, p.374

Energy Monitor @ FLASH (DESY)

SR based profile diagnostics in bunch compressor

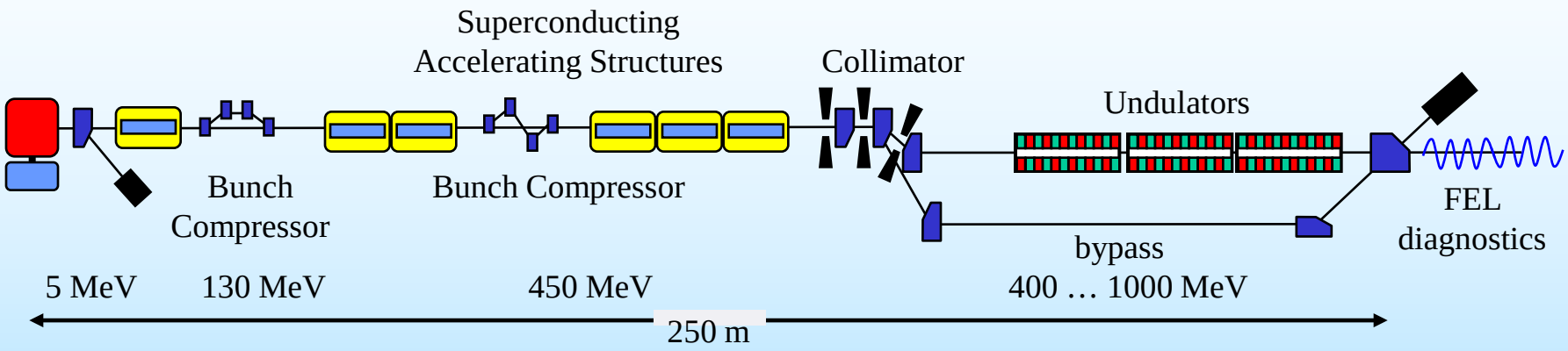

dispersive section ➔ information about energy distribution (and more…)

single bunch

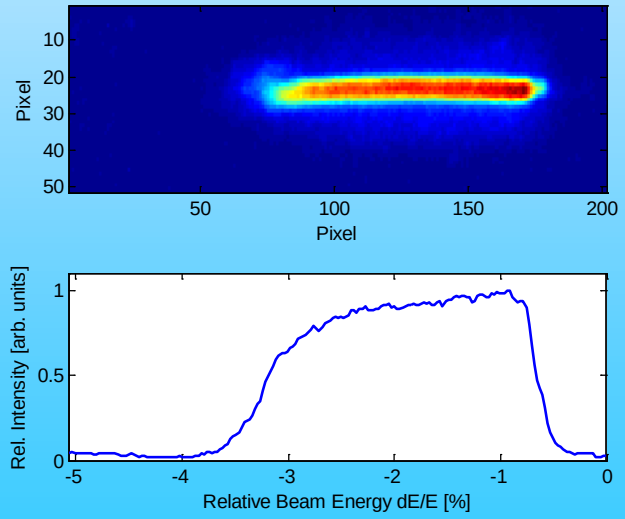

stability :

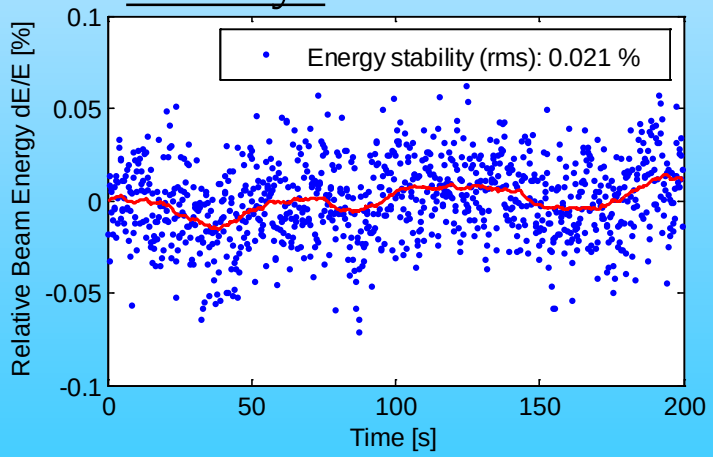

Ch.Gerth, Proc. of DIPAC07 (2007), Venice, p.150

End of Synchrotron Light session

Video

Wire Scanners

Introduction

Conventional wire scanners with thin solid wires (conventional compared with new techniques using, for example, Lasers) are widely used for beam size measurements in particle accelerators.

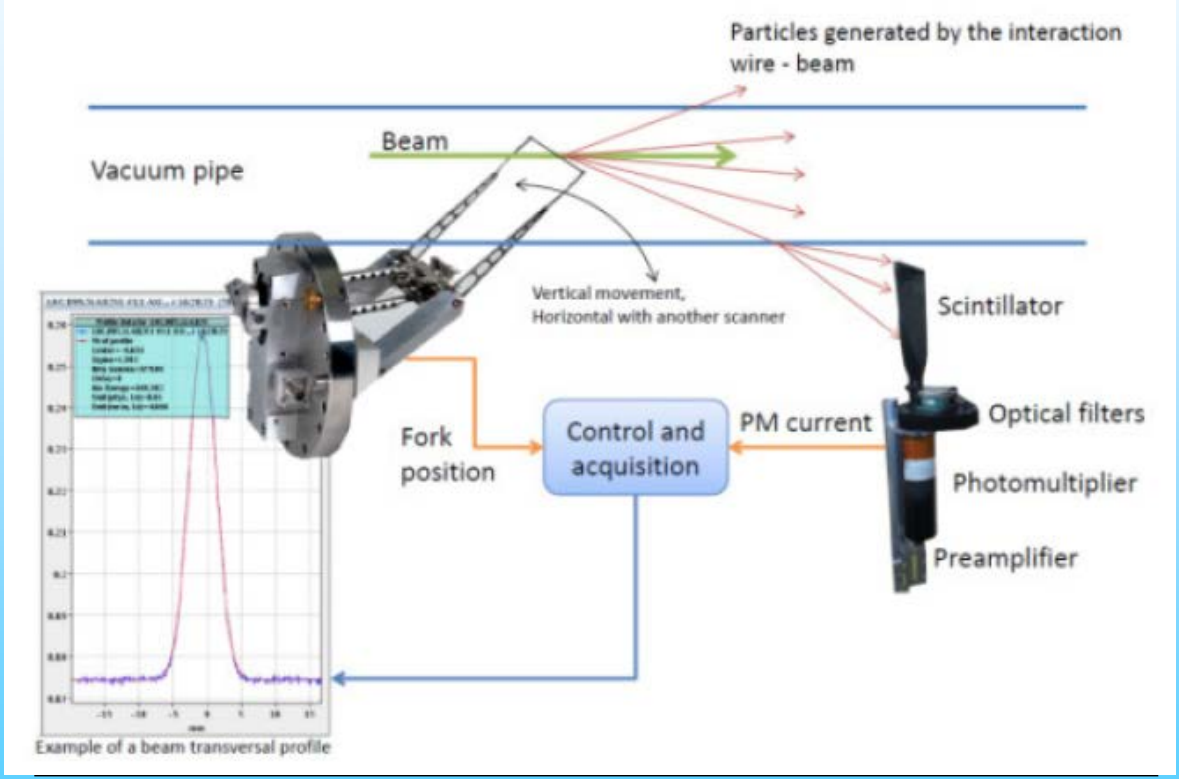

Their advantages:

1) Resolution of down to 1 μm
2) Trusty, reliable
3) Direct

CERN-SPS Wire Scanner Impedance and Wire Heating Studies
E.Piselli, et al. IBIC 2014, Monterey, California, USA September 14-18, 2014.

0.1 micron position resolution is possible

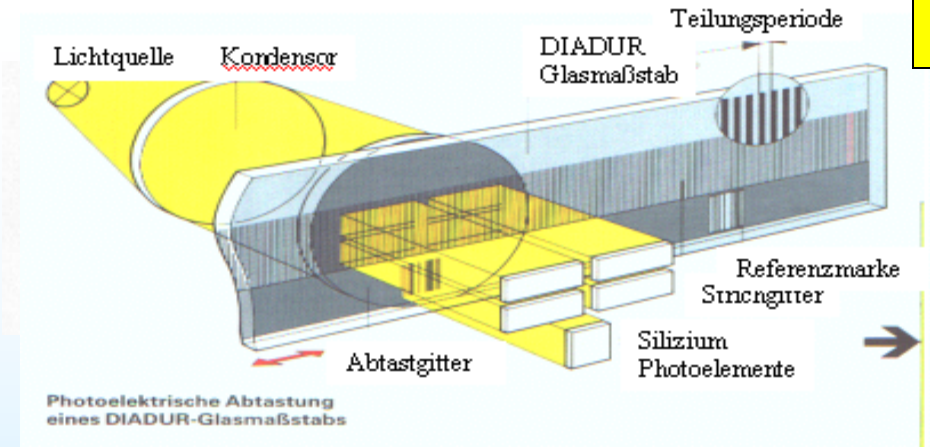

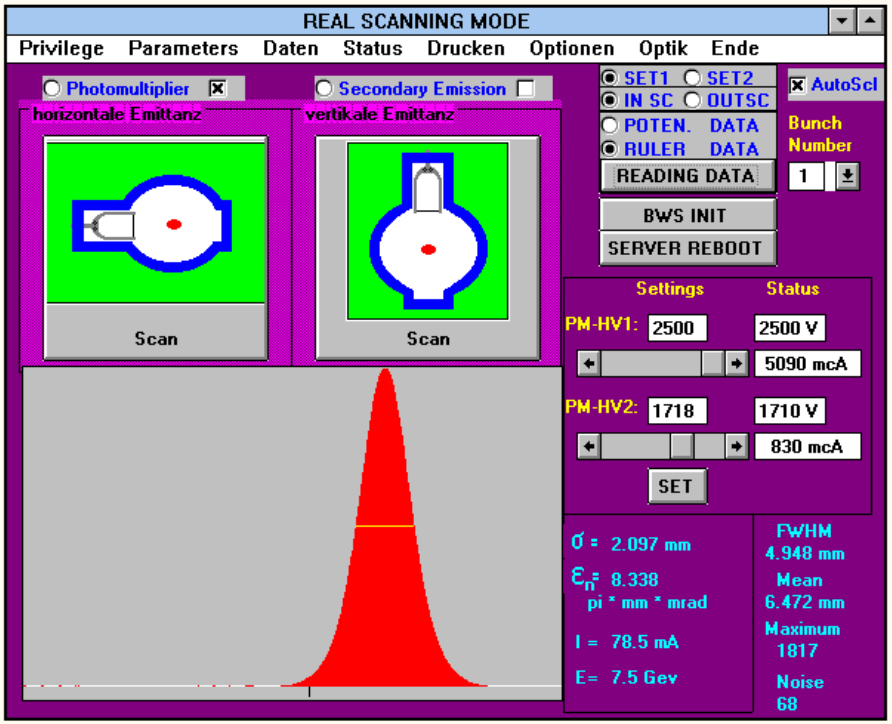

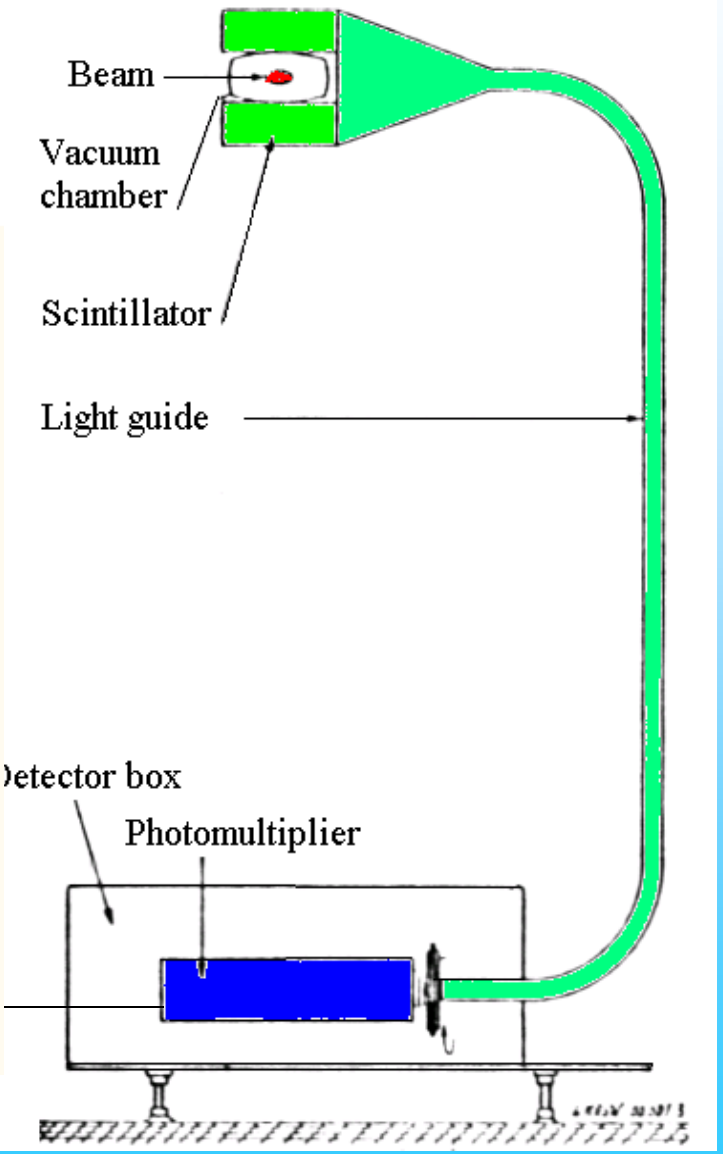

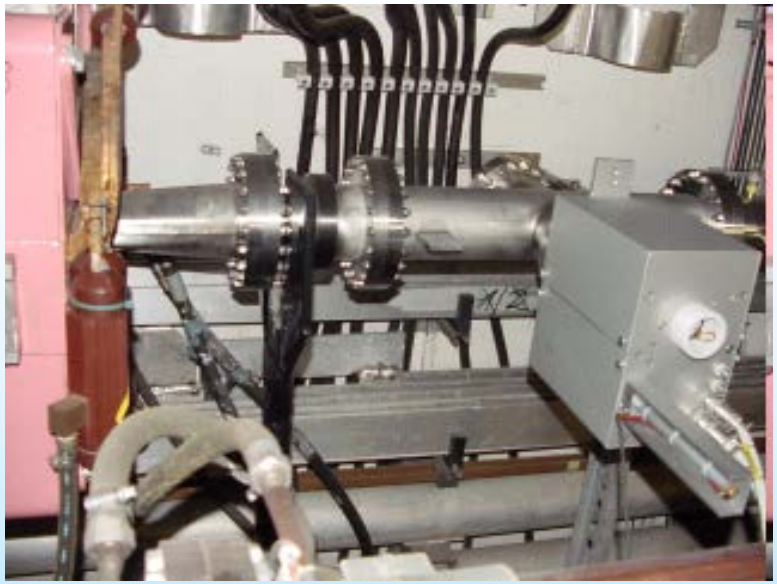

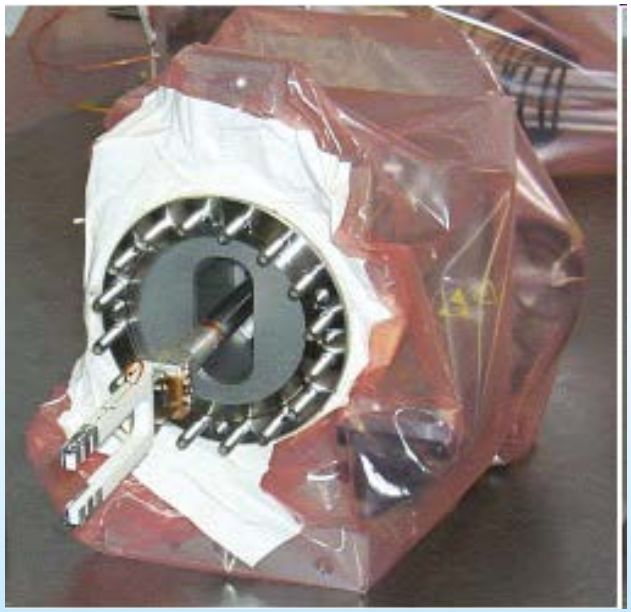

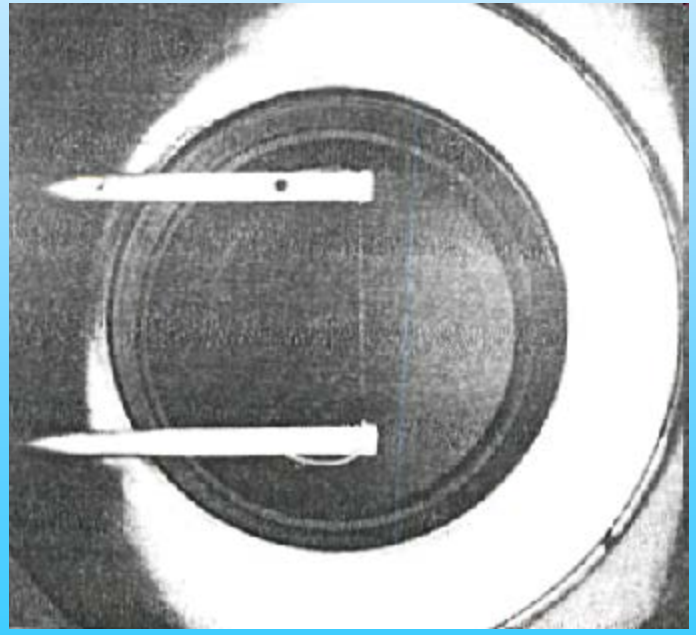

CERN/DESY 1990-2007
FLASH: 2002 - now

Speed: 0 - 1 m/s
Scanning area: approx. 10 cm
Wire material: Carbon/Quartz
Wire diameter: 7 microns
50 μm at Flash
Signal: shower

1 micron resolution

Where one should locate the Scintillator?

Projected angular distribution could be approximated by Gaussian with a width given by

$$\Theta_{mean} = \frac{0.014\,GeV}{pc} \cdot \sqrt{\frac{d'}{L_{rad}}} \cdot \left(1 + 1/9 \cdot \log_{10} \frac{d'}{L_{rad}}\right)$$

$d' = 1.5\times10^{-3}$ cm – the thickness of the target, X_0=12.3 cm – quartz-wire radiation length, $x/X_0 = 1.22\times10^{-4}$

It is corresponding to:

$$\Theta_{mean} \approx 3.0\times10\text{-}6 \text{ rad}$$

for electron momentum of 30GeV/c.

Scattered particles will arrive vacuum chamber of radius R = 2 cm at:

$$z \approx \frac{R}{\Theta_{mean}\sqrt{2}} \approx 4.9km!!!!$$

What to do?

Monte Carlo simulations for finding best location of scintillators

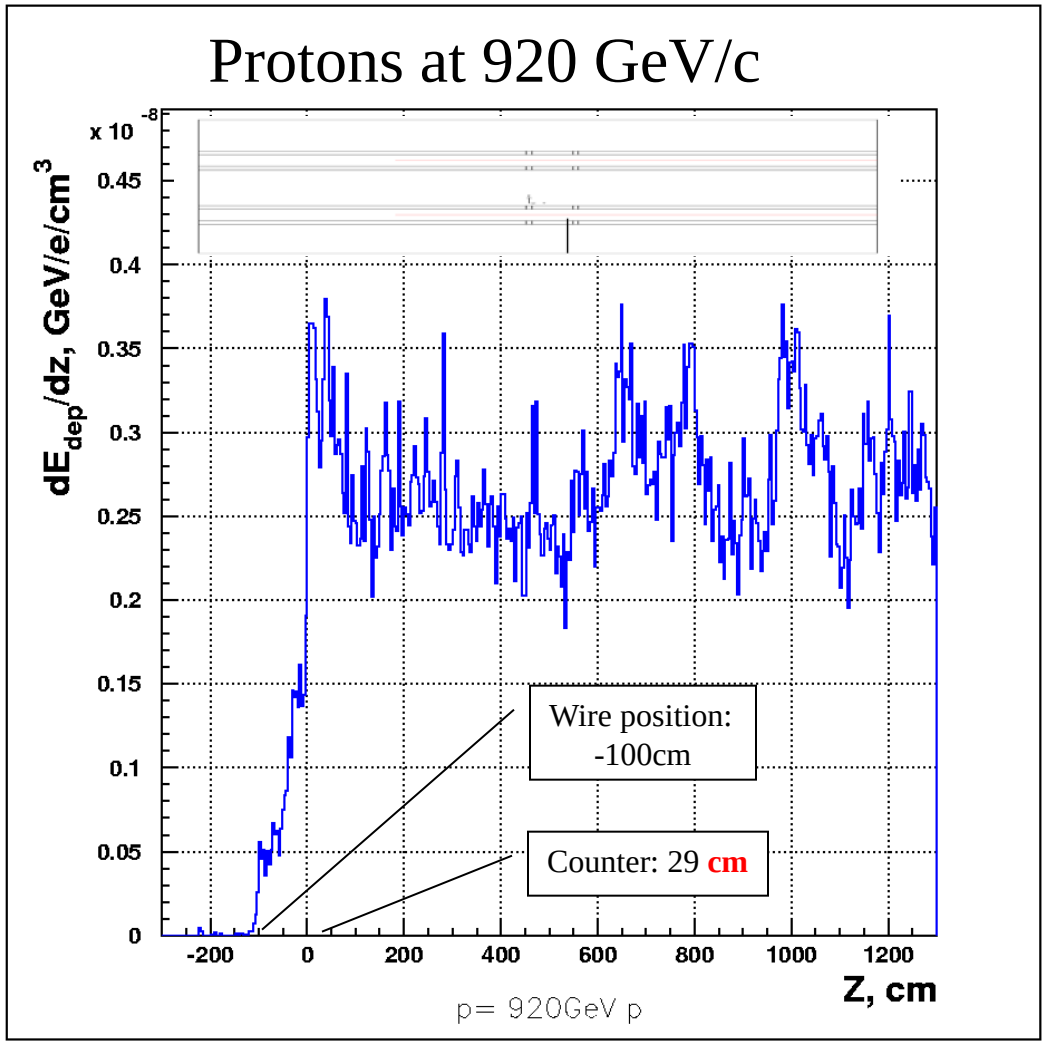

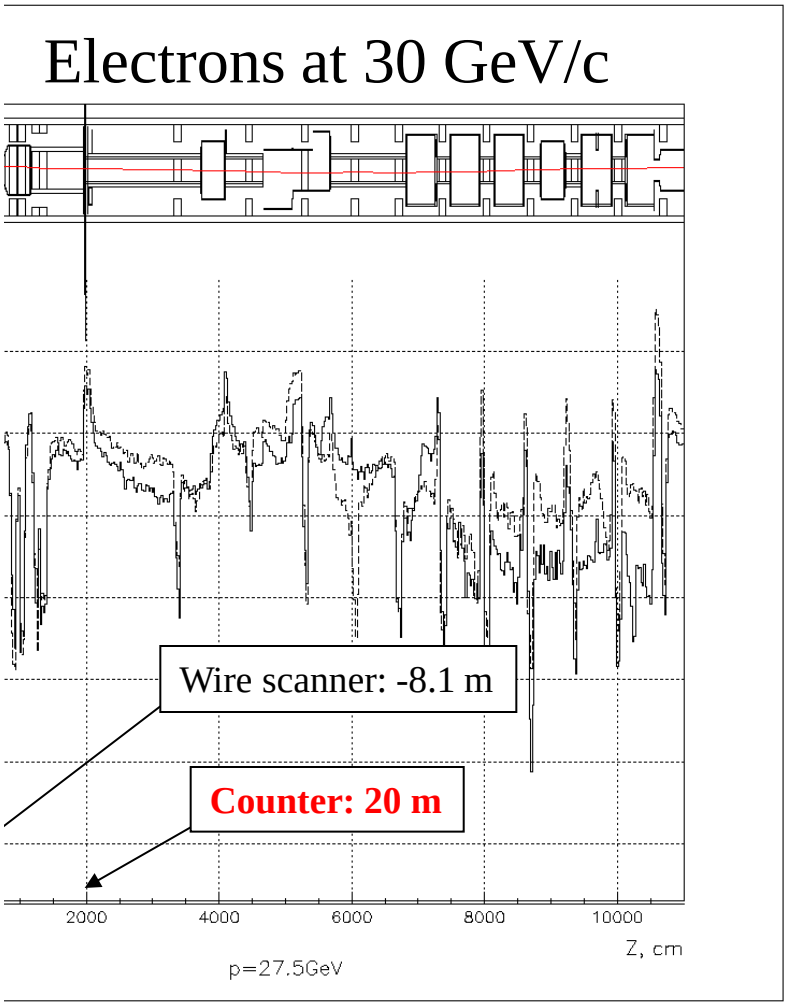

Simulation includes <u>all magnetic fields</u>

as well as <u>all elastic and inelastic scattering cross sections</u>

Wire Scanner at low energies

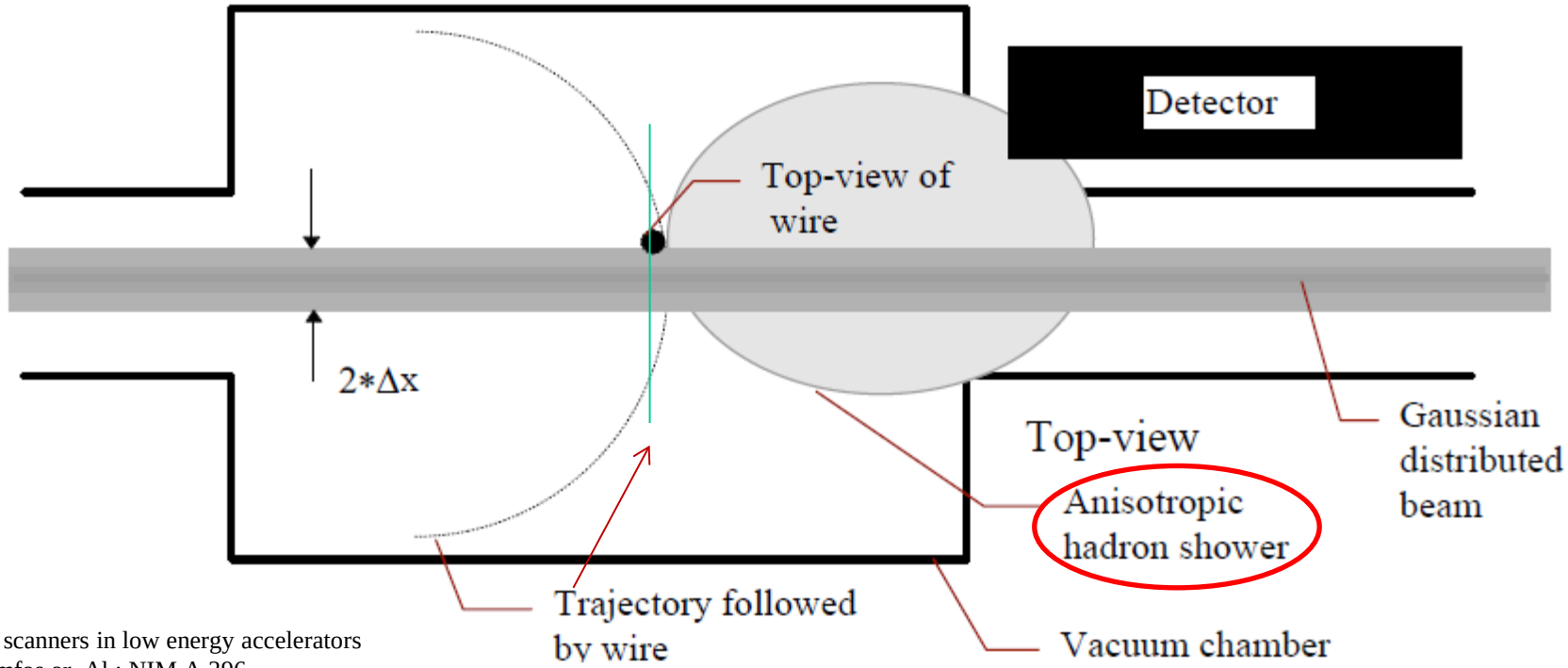

Wire scanners in low energy accelerators
P. Elmfos ar. Al.; NIM A 396

Wire Scanner at low energies

2) Secondary electron emission (SEM) .

- This method is often used at <u>low energy beams</u> where the scattered particles cannot penetrate the vacuum pipe wall (below pion threshold).

- Avoid cross talk of wires

- In this low energy regime the hadron beam particles stop in the wire, so that the signal is a <u>composition</u> of the stopped charge (in case of H^-: proton and electrons) and the secondary emission coefficient. Therefore the <u>polarity of the signal may change</u>, depending on the beam energy and particle type (true also for grids!).

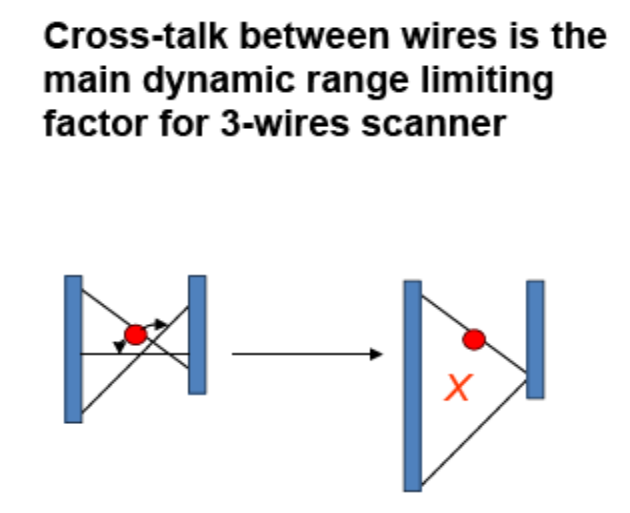

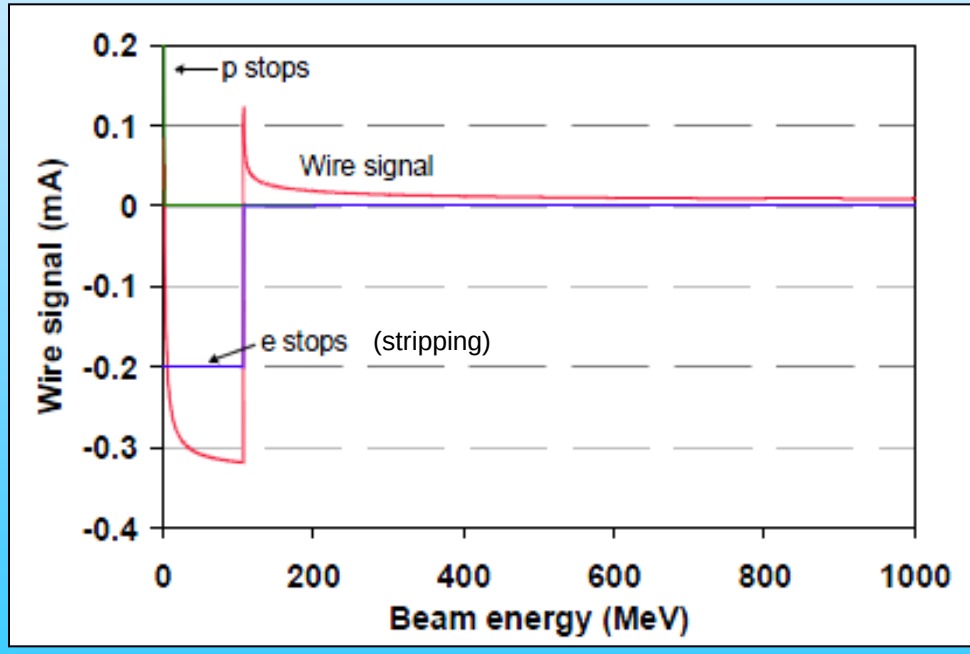

M. A. Plum, et al, SNS LINAC WIRE SCANNER SYSTEM, Signal Levels and Accuracy; LINAC2002

Wire scanner's limitations are?

1. The smallest measurable beam size is limited by the finite wire diameter of a few microns,

2. Higher Order Modes may couple to conductive wires and can destroy them,

3. High beam intensities combined with small beam sizes will destroy the wire due to the high heat load.

4. Emittance blow up

Limitations:

1. Wire size

The smallest achievable wires have a diameter of about 5-6 µm.
An example of the error in the beam width determination is shown for a 36 µm wire.

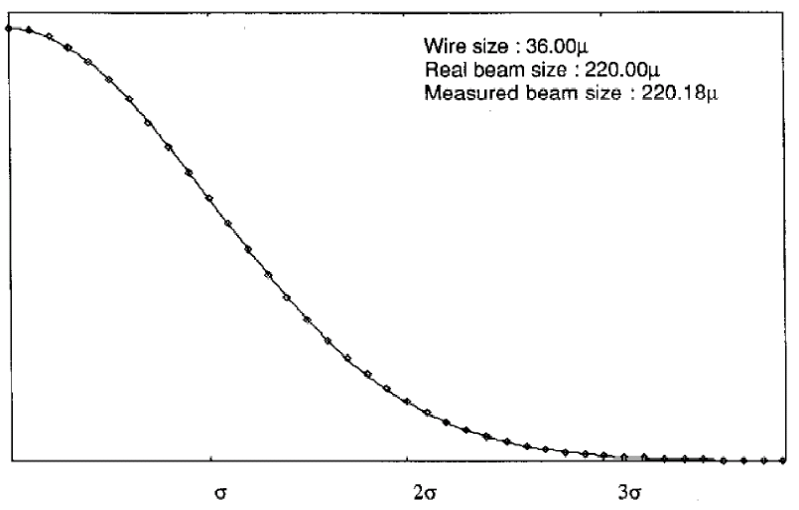

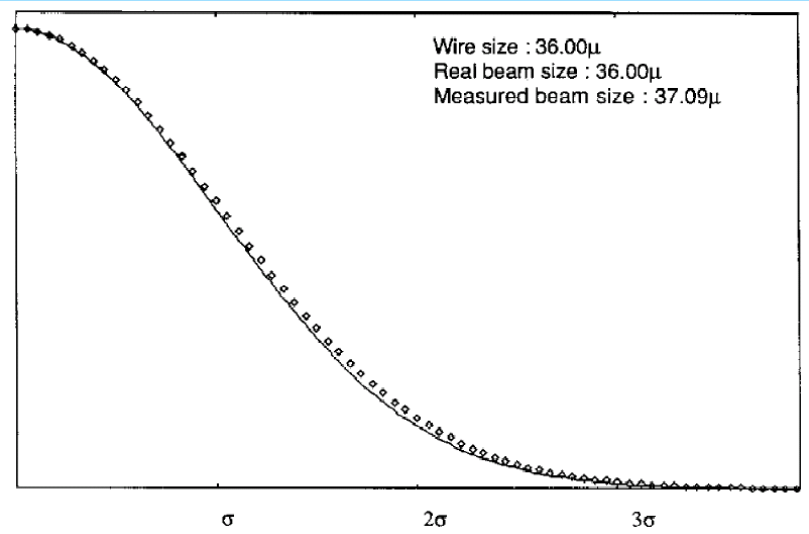

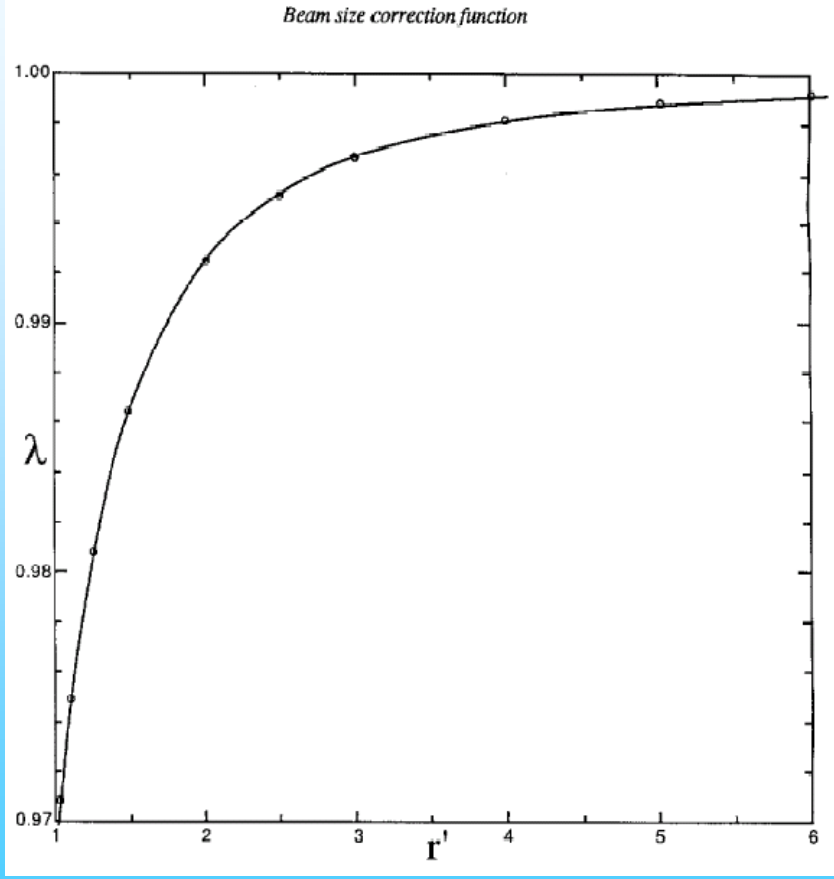

Influence of the wire diameter on the measured beam width.
(All figures from: Q. King; **Analysis of the Influence of Fibre Diameter on Wirescanner Beam Profile Measurements**, SPS-ABM-TM/Note/8802 (1988))

Limitations:

2. Higher Order modes

An early observation (1972 DORIS) with wire scanners in electron accelerators was, that the wire was always broken, even without moving the scanner into the beam. An explanation was that Higher Order Modes (HOM) were coupled into the cavity of the vacuum chamber extension housing the wire scanner fork. The wire absorbs part of the RF which led to strong RF heating.

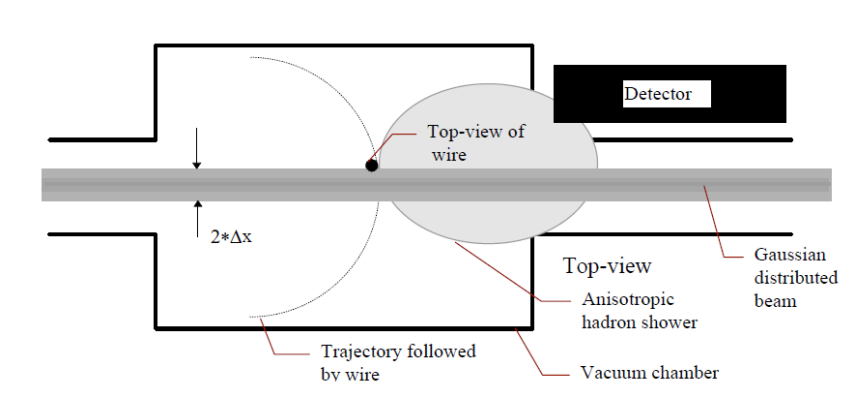

Exercise WIRE1:

1) Discuss methods of proving this assumption.

Methods:

1. Measurement of thermo-ionic emission
2. Measurement of wire resistivity
3. Optical observation of glowing wire
4. Measurement of RF coupling in Laboratory with spectrum analyzer

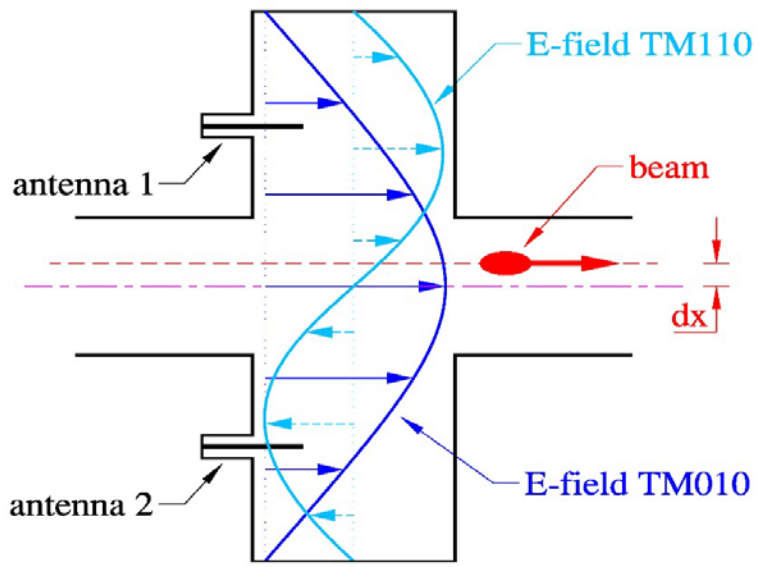

1a. Measurement of thermo-ionic emission, during scan

CERN SPS 2012

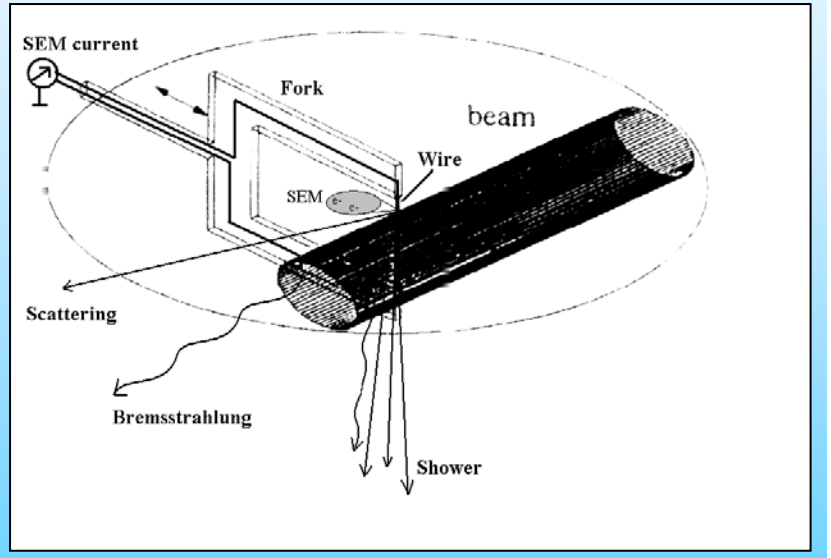

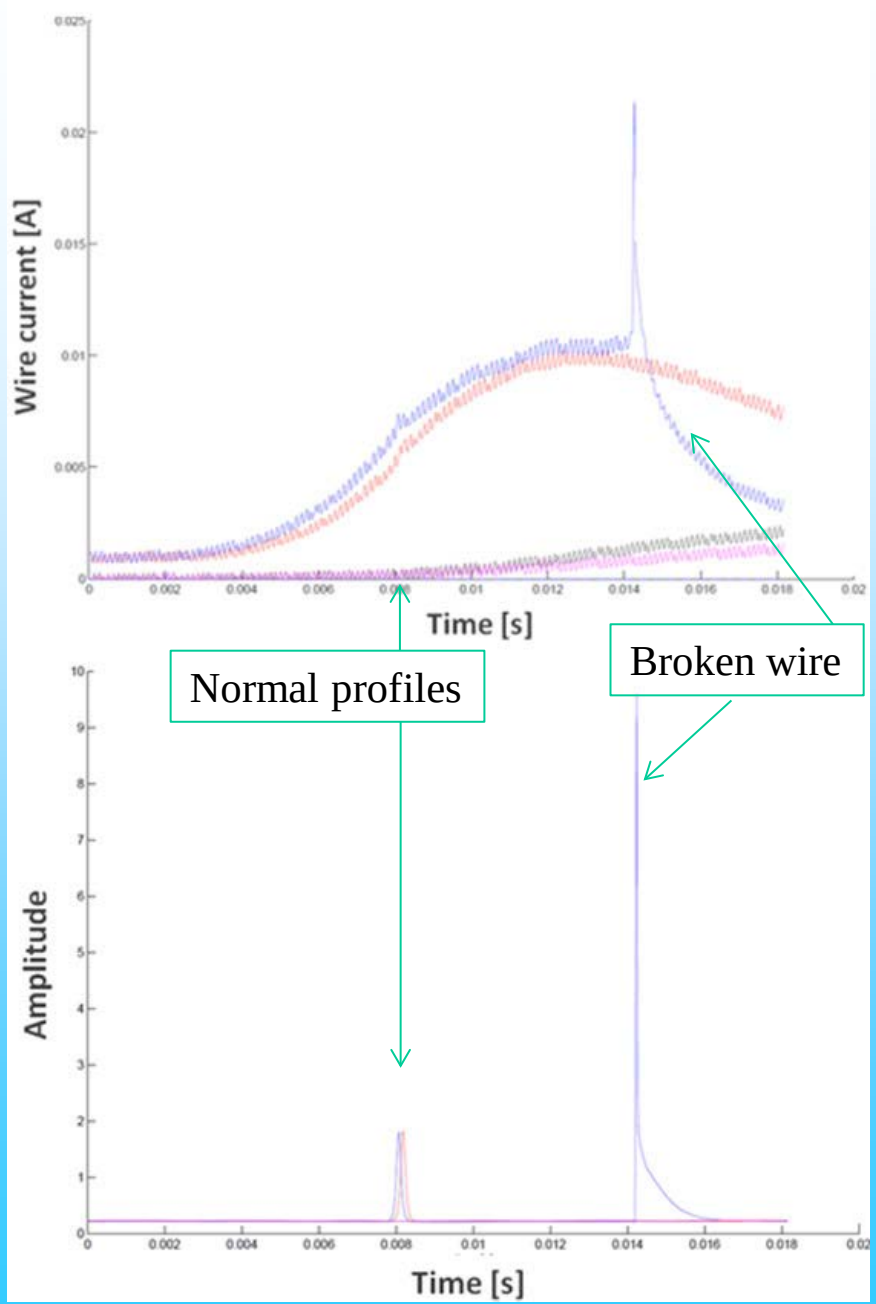

CERN-SPS Wire Scanner Impedance and Wire Heating Studies
E.Piselli, et al. IBIC 2014, Monterey, California, USA September 14-18, 2014.

1b. Measurement of thermo-ionic emission, no scan

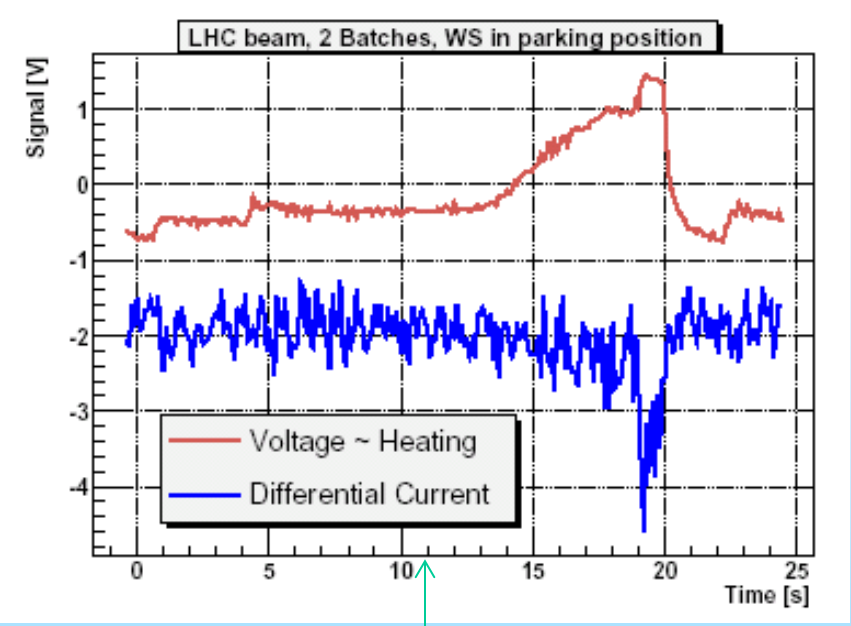

Wire heating due to the LHC beam injection in the SPS (**No scan, wire in parking position**).
The beam energy ramp/**bunch length decreasing begin t=11 s**.

A constant current was supplied to the wire and the voltage drop across it was fed to a digital scope together with the difference between the input and output currents. The differential current (I_{out}-I_{in}) grow up is due to the wire heating and consequent emission of electrons for thermionic effect. Fig. WIRE5 shows such voltage and differential current evolutions during the SPS cycle with LHC type beam. **No scans were performed along this cycle.** It is thus evident that the wire heating does not depend on the direct wire-beam interaction only.

(From **CAVITY MODE RELATED WIRE BREAKING OF THE SPS WIRE SCANNERS AND LOSS MEASUREMENTS OF WIRE MATERIALS**
F. Caspers, B. Dehning, E.Jensen, J. Koopman, J.F. Malo, CERN, Geneva, Switzerland
F. Roncarolo, CERN/University of Lausanne, Switzerland; DIPAC03)

2. Measurement of wire resistivity

The wire resistivity will change depending on the temperature of the wire, even without scanning.

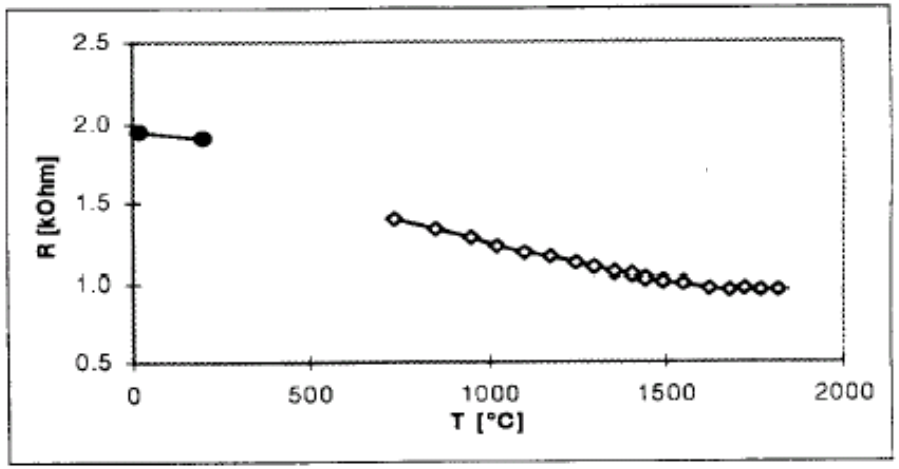

Fig 4: Measured wire resistance variations with temperature.

Here: 8 μm Carbon wire

(from OBSERVATION OF THERMAL EFFECTS ON THE LEP WIRE SCANNERS. By J. Camas, C. Fischer, J.J. Gras, R. Jung, J. Koopman (CERN). CERN-SL-95-20-BI, May 1995. 4pp. Presented at the 16th Particle Accelerator Conference - PAC 95, Dallas, TX, USA, 1 - 5 May 1995. Published in IEEE PAC 1995:2649-2651)

3. Optical observation of glowing wire

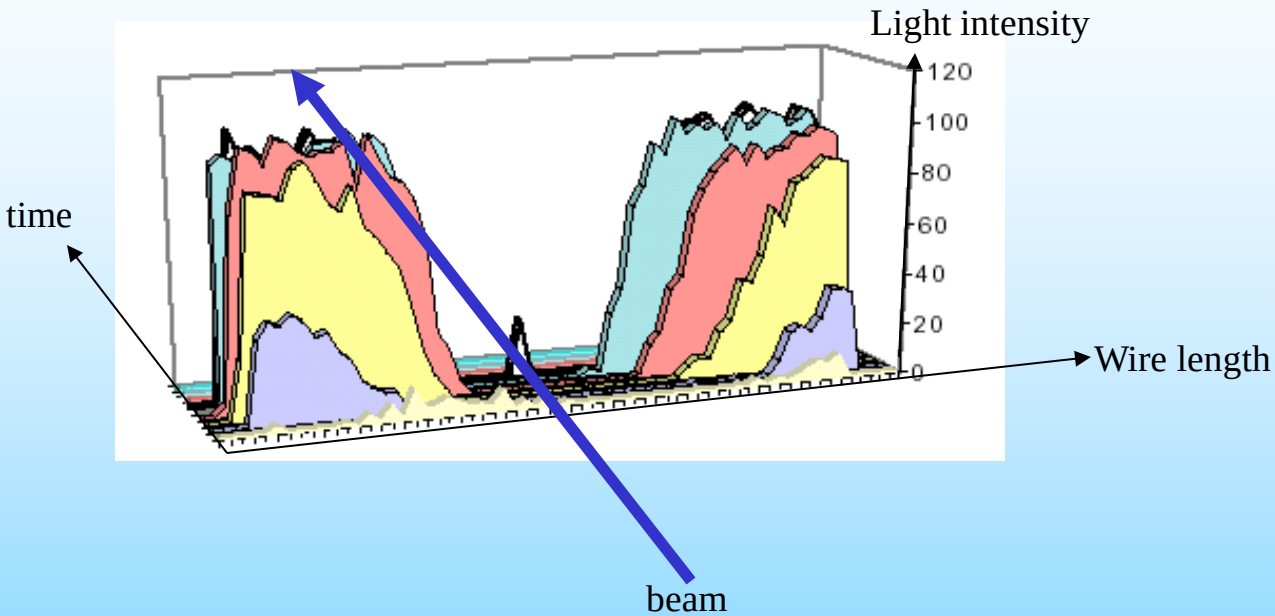

Digitized video recording of an 8 μm carbon wire scanning a 0.8 mA beam. The wire is parallel to the horizontal axis, and the light intensity is plotted along the vertical axis (arbitrary units). Successive profiles are separated by 20 ms. The central spot corresponds to the passage of the wire through the beam. Thus, RF heating led to (huge) thermal glowing before the beam interacts with the wire.

(from: QUARTZ WIRES VERSUS CARBON FIBERS FOR IMPROVED BEAM HANDLING CAPACITY OF THE LEP WIRE SCANNERS.
By C. Fischer, R. Jung, J. Koopman (CERN). CERN-SL-96-09-BI, May 1996. 8pp. Talk given at 7th Beam Instrumentation Workshop (BIW 96), Argonne, IL, 6-9 May 1996.

4. Measurement of RF coupling with spectrum analyzer

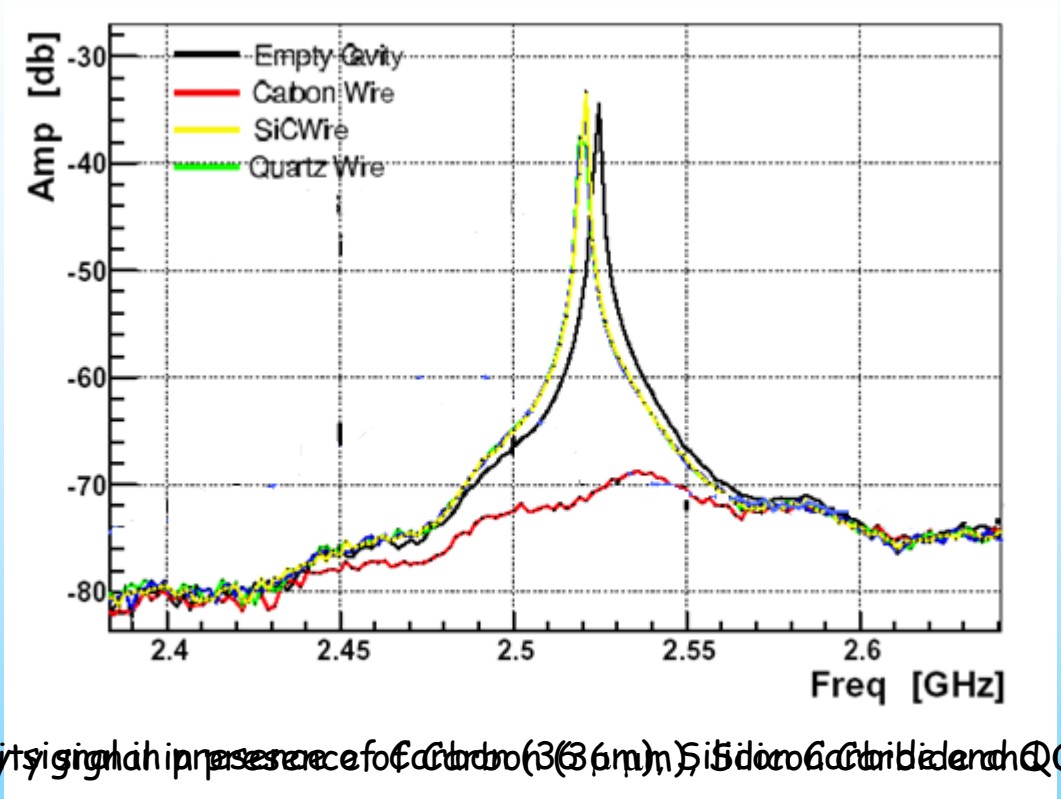

Resonant cavity signal in presence of Carbon (36 µm), Silicon Carbide and Quartz wires

The plot qualitatively proves the RF power absorption of Carbon, the Absorbed energy is mainly converted into Quartz. Absorbed energy is mainly converted into heat.

What are solutions for the problems 1-4?

- Damping of Higher Order Modes with Ferrites **etc.**
- **Non conducting wires**

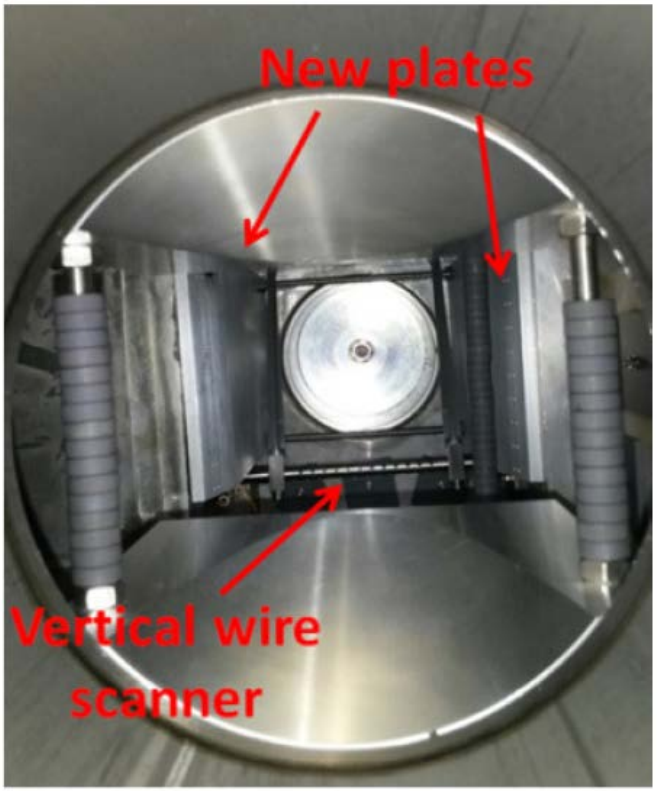

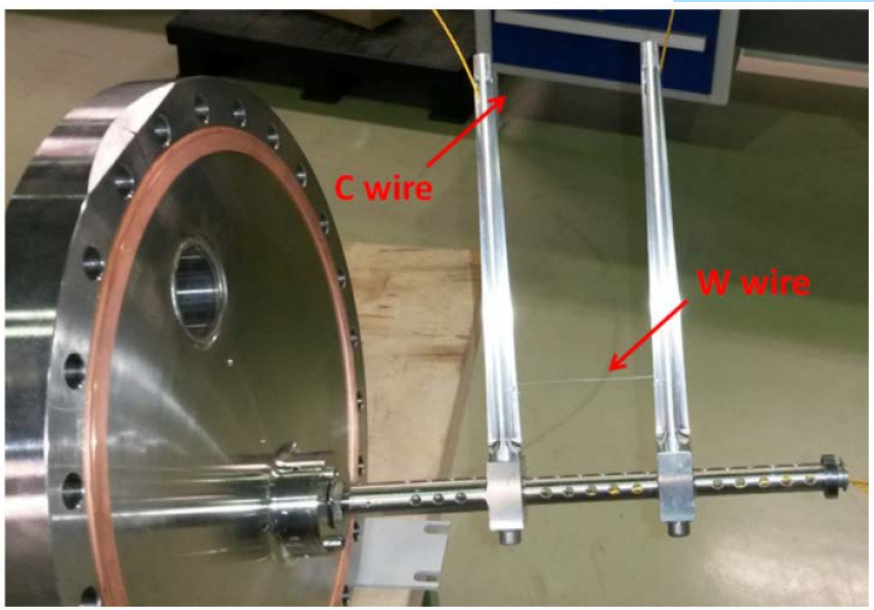

Lab. Measurements

CST Simulations

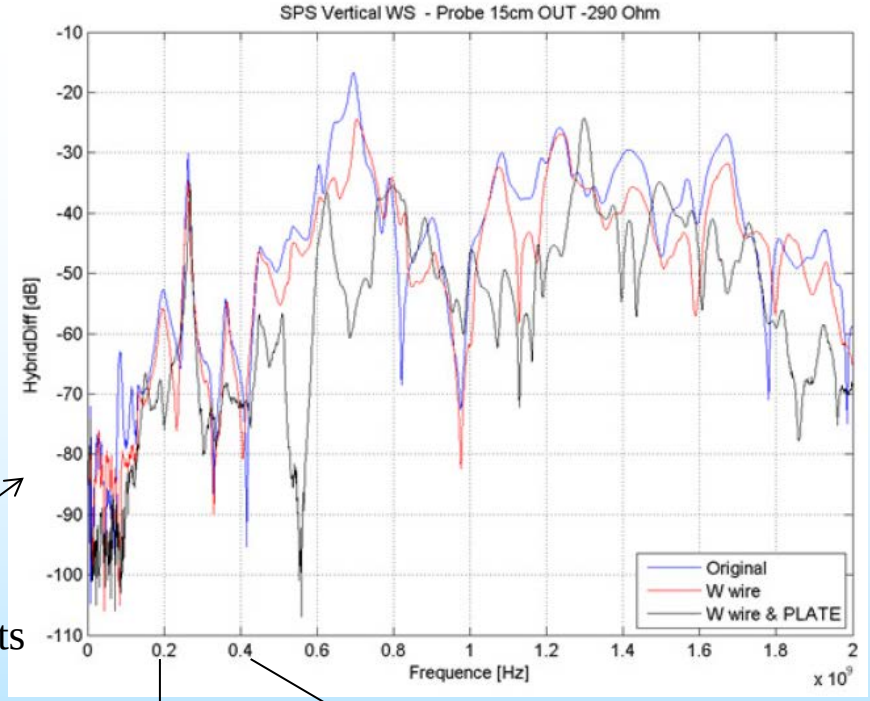

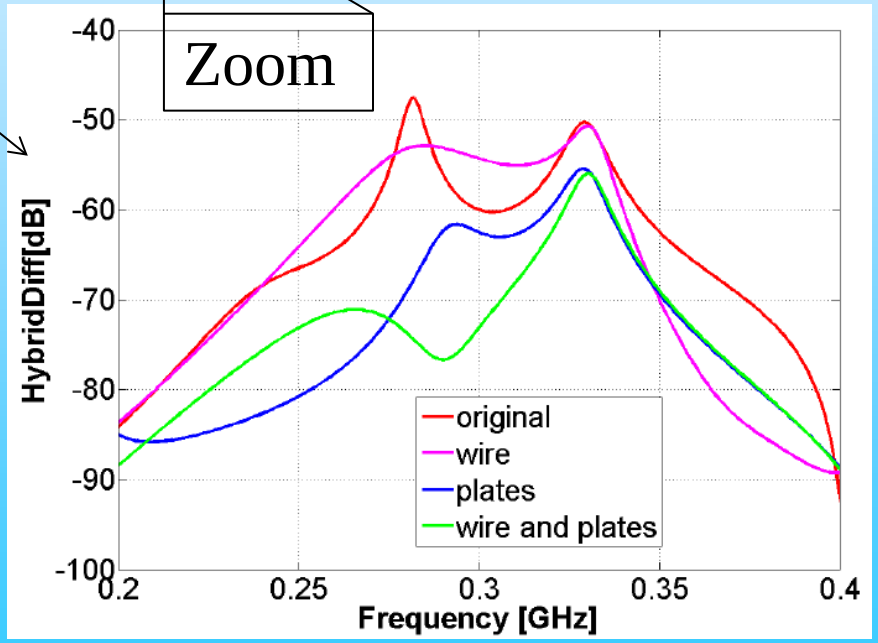

CERN-SPS Wire Scanner Impedance and Wire Heating Studies
E.Piselli, et al. IBIC 2014, Monterey, California, USA September 14-18, 2014.

Limitations:

3. Wire heat load

According to Bethe-Blochs formula, a fraction of energy dE/dx of high energy particles crossing the wire is deposit in the wire. Each beam particle which crosses the wire deposits energy inside the wire. The energy loss is defined by dE/dx (minimum ionization loss) and is taken to be that for a minimum ionizing particle.

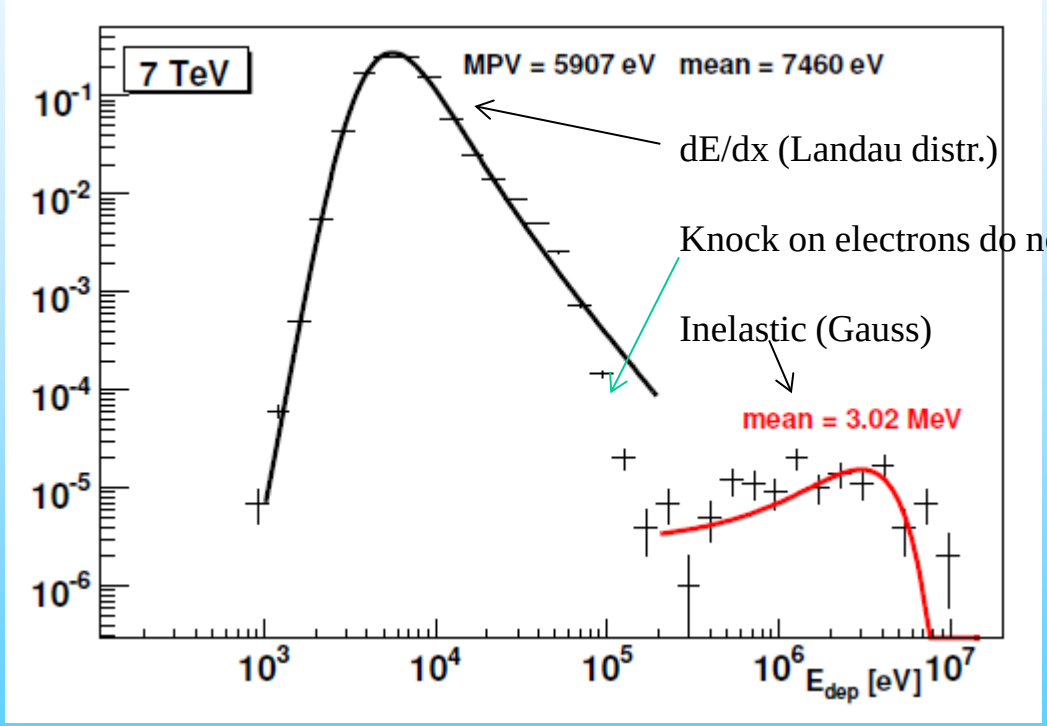

Geant Simulation: Distribution of 7 TeV proton energy deposit in 33 micron carbon fiber.

Limitations:

3. Wire heat load

According to Bethe-Blochs formula, a fraction of energy dE/dx of high energy particles crossing the wire is deposit in the wire. Each beam particle which crosses the wire deposits energy inside the wire. The energy loss is defined by dE/dx (minimum ionization loss) and is taken to be that for a minimum ionizing particle. In this case the temperature increase of the wire can be calculated by:

unknown

$$T = C \cdot dE/dx_m \cdot d' \cdot N \cdot \frac{1}{c_p \, G} \quad [^0C]$$

where N is the number of particles hitting the wire during one scan, d' is the thickness of a quadratic wire with the same area as a round one and G [g] is the mass of the part of the wire interacting with the beam. The mass G is defined by the beam dimension in the direction of the wire (perpendicular to the measuring direction):

Estimation of the wire temperature after one scan with speed v (assume no cooling mechanisms):

Solving G: G [g] is the mass of the part of the wire interacting with the beam. The mass G is defined by the beam dimension in the direction of the wire (perpendicular to the measuring direction) and by the wire diameter d':

$$G = wire\ volume \cdot \rho = 2 \cdot \sigma_v \cdot d'^2 \cdot \rho \quad [g]$$

Solving N:

The number of particles N hitting the wire during one scan depends on the speed of the scan (~1/v), the revolution frequency (~f_{rev}), the wire diameter (~d') and the beam current (~NB · n_{bunch}):

$$N = \frac{d' \cdot f_{rev}}{v} \cdot (NB \cdot n_{bunch})$$

The figure shows the a graphical representation of the parameters. The quotient d·f/v is the ratio of the scanned beam area or, in other words, like a grid seen by one bunch, assuming that all bunches are equal. However, the ratio can exceed the value 1 (a foil) if the scanning distance between two bunches is smaller than the wire diameter. Note that N does not depend on the beam widths σ.

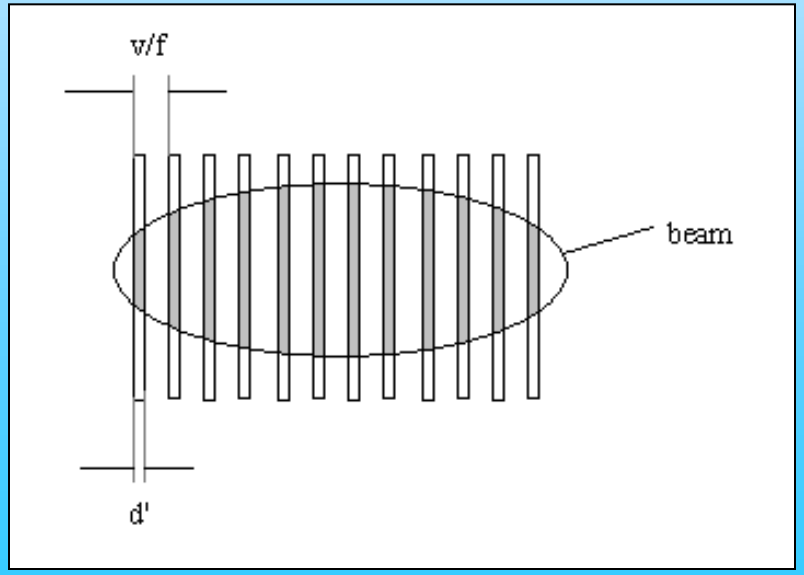

Geometrical meaning of the parameters v/f and d'

Therefore, the temperature increase of the wire after one scan becomes:

$$T = C \cdot dE/dx_m \cdot d' \cdot N \cdot \frac{1}{c_p \cdot G} \quad [^0C]$$

In MeV/cm

$$Mass\,G = wire\ volume \cdot \rho = 2 \cdot \sigma_v \cdot d'^2 \cdot \rho \quad [g]$$

$$N = \frac{d' \cdot f_{rev}}{v} \cdot (NB \cdot n_{bunch})$$

$$T_h = C \cdot dE/dx_m \cdot \cancel{d'} \cdot \frac{\cancel{d'} \cdot f_{rev}}{v} \cdot (NB \cdot n_{bunch}) \cdot \frac{1}{c_p \cdot 2 \cdot \sigma_v \cdot \cancel{d'^2} \cdot \rho} \cdot \alpha \quad [^0C]$$

$$with \quad \frac{dE/dx_m}{\rho} = dE/dx \left[\frac{MeV \cdot cm^2}{g}\right] \quad and \quad f_{rev} \cdot NB = f_{bunch}$$

$$\Downarrow$$

$$T_h = C \cdot dE/dx \cdot n_{bunch} \cdot \frac{f_{bunch}}{v} \cdot \frac{1}{c_p \cdot 2 \cdot \sigma_v} \cdot \alpha \quad [^0C]$$

Where h, denotes the horizontal (h) scanning direction. The cooling factor 'α' is described in the next section. **Note that the temperature does not depend on the wire diameter and that it depends on the beam dimension perpendicular to the measuring direction. The temperature increase is inverse proportional to the scanning speed**, therefore a faster scanner has a correspondingly smaller temperature increase.

Exercise WIRE2: Which kind of wire Material you will prefer for a wire scanner in this accelerator?

Parameter table

The wire minimal for a choice of

The beam parameters used in this exercise are shown in the following table:

Parameter	Symbol	Unit	Value
circumference of accel.	circ.	m	300
particle		Proton	
Beam particle momentum	p	GeV/c	0.3-7
Beta function	$\beta_h = \beta_v$	m	11.8
Emittance	$\varepsilon_h = \varepsilon_v$	π mm mrad	15
revolution Frequency	f_{rev}	MHz	0.93
Bunch spacing	t_{bunch} f_{bunch}	ns MHz	98 10.2
Number of bunches in accel.	NB		11
Bunch charge	n_{bunch}	1/e	$1.1 \cdot 10^{11}$
Beam width measurement [1]	σ_h	mm	1.5
Beam width perpendicular to meas. [1]	σ_v	mm	1

Table WIRE2: Parameters of Beam

TableWire3: calculated Temperatures

From Table WIRE3 follows, that even the best material (Carbon) will be a Factor 2.2 above its melting temperature.

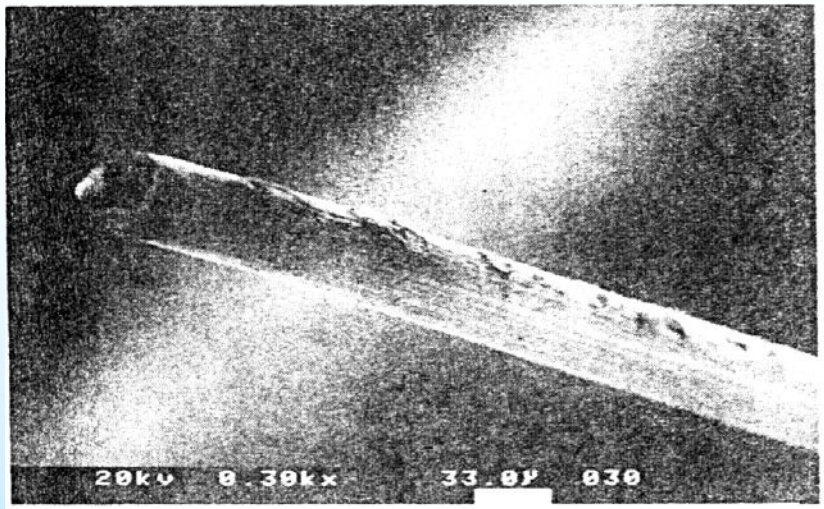

Small pit marks seen near the end of the wire are further evidence for arcing.

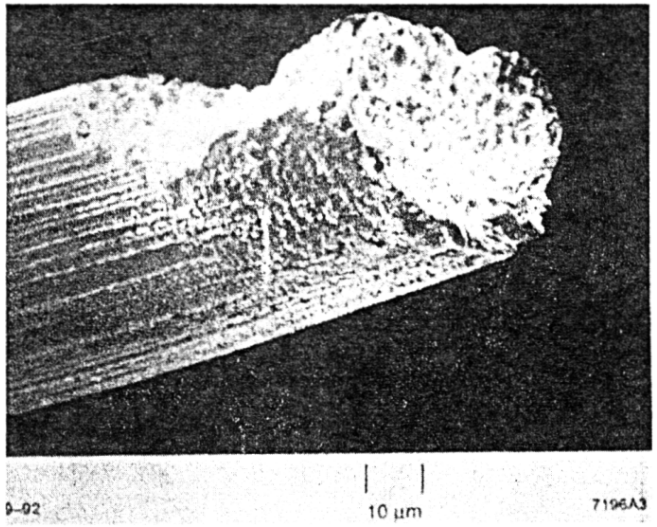

Figure 3. Electron microscope picture of a 40 µm tungsten wire break. This wire was installed in an SLC linac wire scanner.

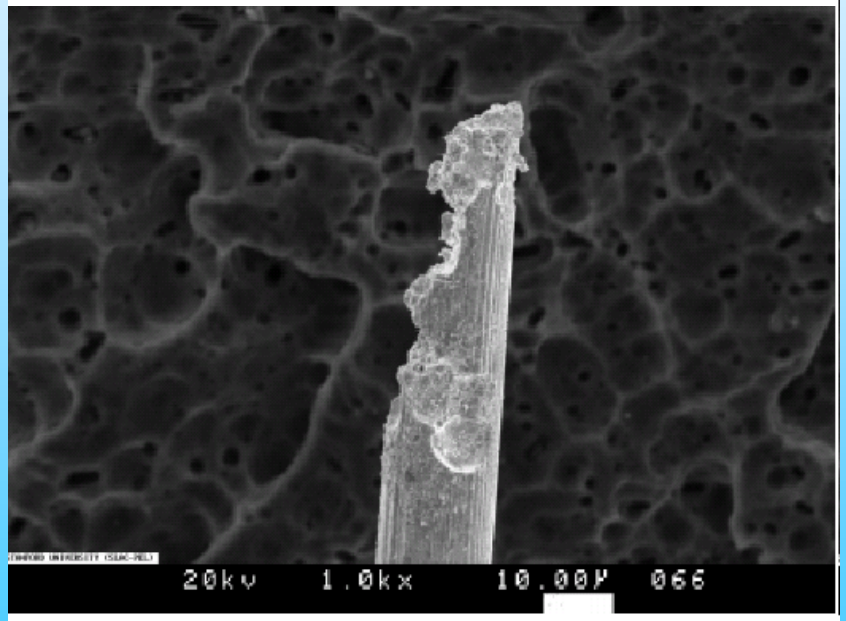

FIGURE 3. Failed 15 µm diameter tungsten wire showing the rough surface resulting from many discharges.

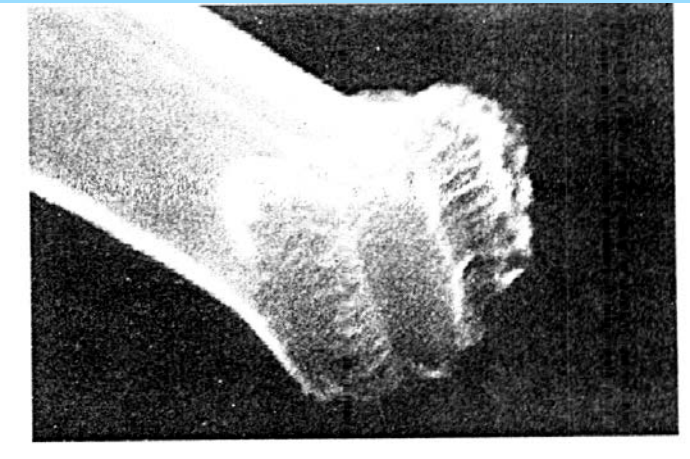

Burned by the e-beam at SLC

Exercise WIRE2a: Discuss cooling mechanisms which will cool the wire.

1) Secondaries emitted from the wire
2) Heat transport along the wire
3) Black body radiation
4) Change of c_p with temperature
5) Thermionic emission
6) Sublimation

Wire type	Approximation Q (μJ)	Monte Carlo Q (μJ)
10 μm graphite	0.140	0.169 ± 0.002
10 μm tungsten	1.01	2.19 ± 0.04
15 μm tungsten	2.27	4.90 ± 0.05
50 μm tungsten	25.3	32.0 ± 0.1

Heat deposited in various wire types by a passing bunch of 1 nC. The approximated value follows (1), the "Monte Carlo" result is obtained by the simulation of an electromagnetic shower with Fluka.

Thermal Load on Wirescanners
Lars Fröhlich
37th ICFA Advanced Beam Dynamics Workshop on Future Light Sources; May 15-19, 2006 in Hamburg, Germany

1) Secondaries:

Some energy is lost from the wire by secondary particles. In the work in (J. Bosser et al.; The micron wire scanner at the SPS, CERN SPS/86-26 (MS) (1986)) **about 70% is assumed**. In DESY III (example above) no carbon wire was broken during more than 10 years of operation. At HERA, the theoretical temperature of the carbon wire (without secondaries) exceeds the melting temperature after a scan by far (T = 12800 ^{0}C). Considering the loss by secondaries of 70%, the temperature reaches nearly the melting point. In practice, the wire breaks about once in 2 months. The observation is that the wire becomes thinner at the beam center. This may indicate, that during a scan some material of the wire is emitted because of nuclear interactions or is vaporized because it is very close to the melting temperature. This supports the estimate of the 70% loss and one has to multiply the factor α = 0.3 in the equation above

2) Heat transport:

The transport of heat along the wire does not contribute **to short time cooling** of the wire (P. Lefevre; CERN PS/DL/Note 78-8). However, frequent use of the scanner heats up also the ends of the wire and its connection to the wire holders (fork).

For small temperatures (low repetition rates (LINACs)) this is the major cooling mechanism.

$$P_{cool}^{cond} = -\lambda(T) A_d \frac{dT}{dx}$$

with λ = thermal cond. , A = Surface

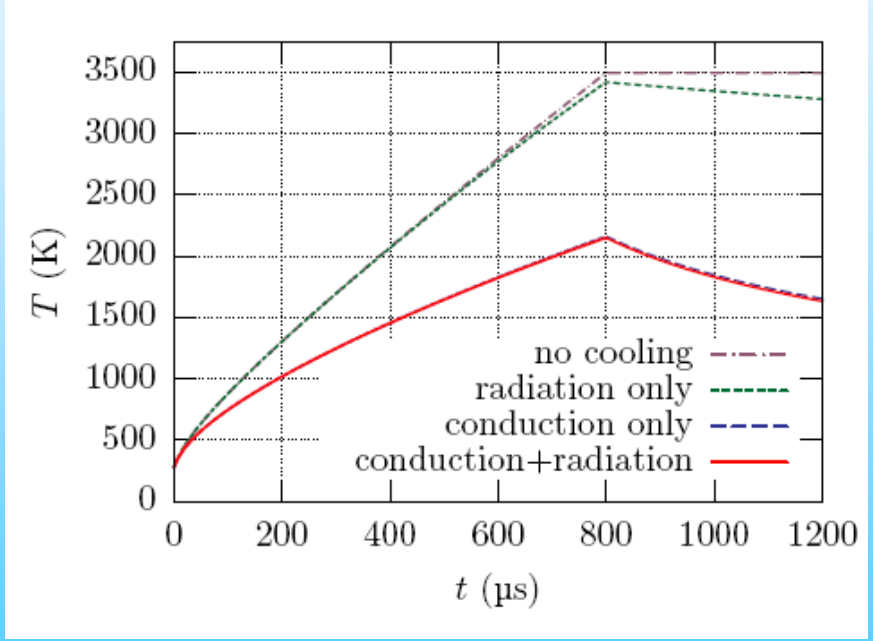

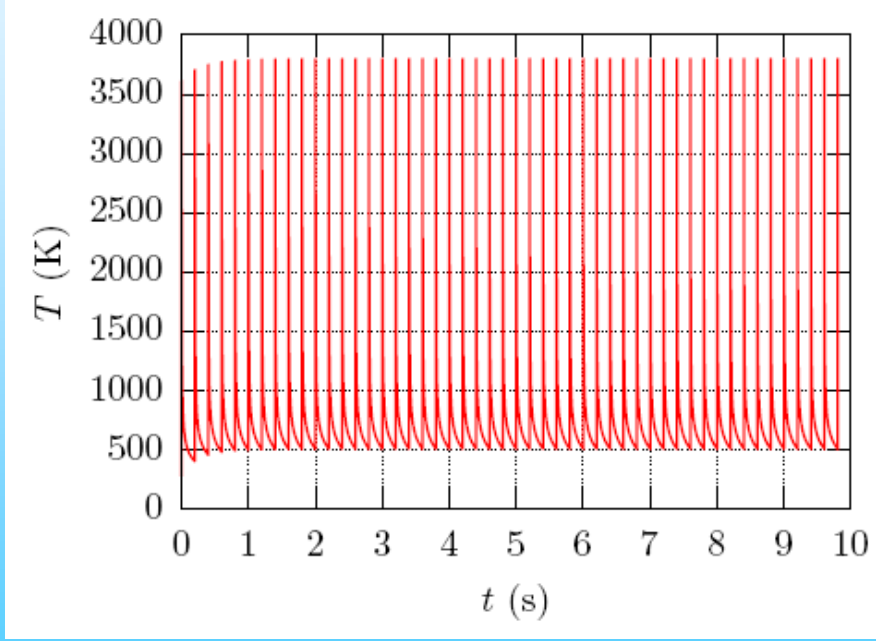

10 µm graphite wire bombarded with 800 bunches at 1 MHz; simulated with various combinations of cooling mechanisms, 5 Hz rep. rate.

3) Black body radiation: The temperature T_{bb} at which the radiated power is equal to the deposited power in the wire during one scan P_{dep} [MeV/s] can be calculated from the Stefan-Bolzmann-law:

$$T_{bb} = \sqrt{\sqrt{\frac{P_{dep}}{s \cdot A}}}$$

where s = 35.4 MeV / (s^1 cm^2 $^0K^4$) is the Stefan-Bolzmann-constant and A is the area of radiating surface. The surface of the heated wire portion A is $2 \cdot \sigma_v \cdot d \cdot \pi$ [cm^2]. The power can be calculated by:

$$P_{dep\ h,v} = \alpha \cdot dE/dx \cdot d' \cdot n_{bunch} \cdot \frac{f_{bunch} \cdot d'}{v} \cdot \frac{1}{t_{scan}} \quad [MeV/s]$$

where $t_{scan} = 2 \cdot \sigma_{h,v} / v$ is the time for a scan (in the assumpion of 2 σ it is neglected that only about 70% of the power is concentrated within 2 σ). α is the expected loss from secondaries.

For the example above: T_{bb} = 3900 ^{0}C.

$$\boxed{P_{cool}^{rad} = A \cdot s(T^4 - T_{env}^4)}$$

4) $c_p(T)$: The heat capacitance is a function of the temperature. The figure shows the increase of c_p for Carbon with T. The expected temperature after a scan is inversely proportional to c_p. **Therefore one can expect a slightly smaller resulting temperature because of this dependence.**

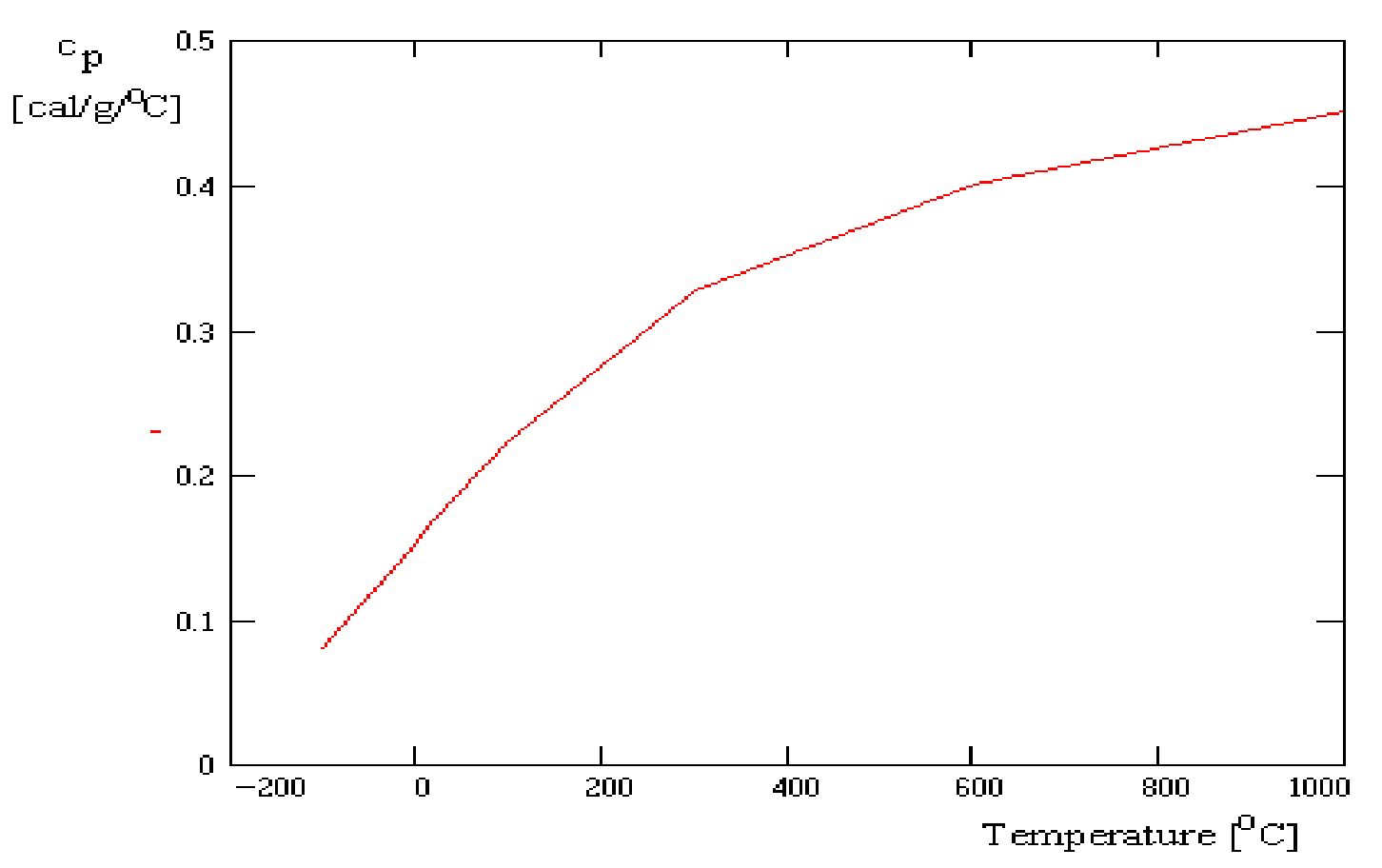

5) Thermionic emission

The thermionic emission is a dominant cooling process for temperatures above 3200 K. It determines the wire temperature for scans of the high intensity beams. The electric current emitted by the hot body is described by Richardson-Dushman Equation:

$$J_{th} = A_R \cdot T^2 \cdot e^{-\frac{\Phi}{k_B T}} \quad or \quad \boxed{P_{cool}^{th} = A_R(\Phi + \frac{2k_b T}{q}) J_{th}}$$

where A_R is Richardson constant and Φ is the material work function. The power dissipated by the thermionic current is proportional to the surface of the wire and depends exponentially on the temperature. The thermionic emission removes electrons which are replaced by a current flowing from the fork supporting the wire. This current has a negligible contribution as an additional source of heating.

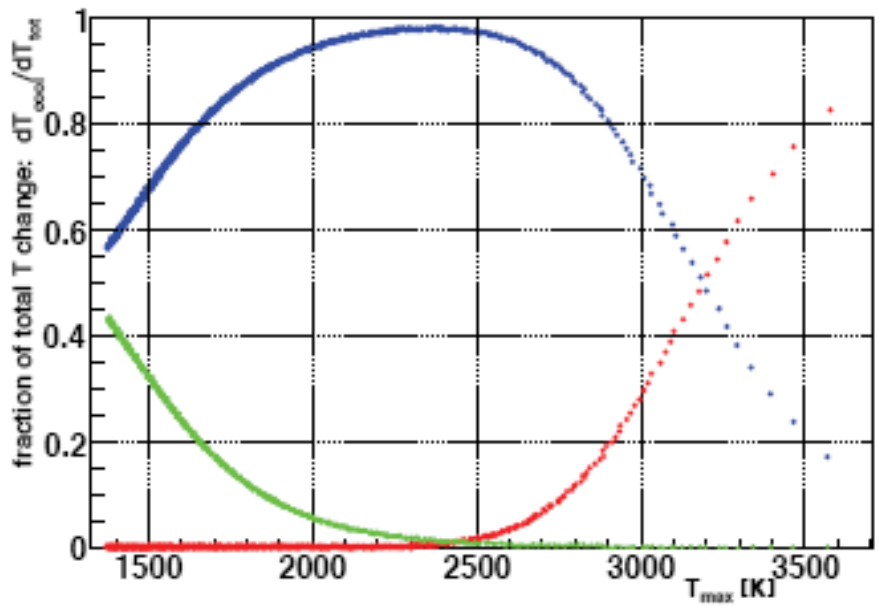

Relative contribution of cooling processes to the total temperature change as a function of temperature. Blue points are for radiative cooling, red for thermionic emission and green are for the heat transfer.

Operational Limits of Wire Scanners on LHC Beam
Mariusz Sapinski, Tom Kroyer (CERN, Geneva)
2008 Beam Instrumentation Workshop (BIW08) held on May 4-8, 2008 at the Granlibakken Conference Center and Lodge in Tahoe City, CA, USA, pp.383-388

5) Sublimation Cooling

The material behavior in high temperatures and in a vacuum can be read from a phase diagram. Materials which sublimate under these conditions have an advantage because the sublimation temperature and sublimation heat are higher than melting temperature and heat. Sublimation removes the hottest fraction of the material from the surface, what is equivalent to a cooling, which is weak in comparison to other cooling processes.

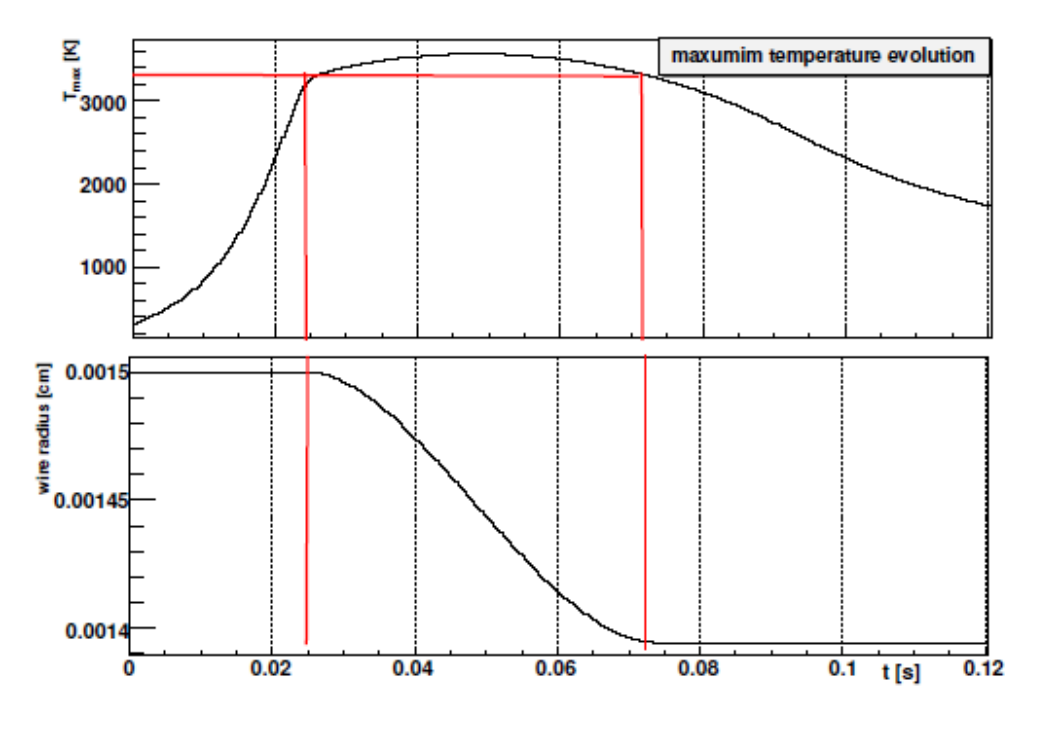

$$P_{cool}^{sub} = H_{sub} \frac{\Delta n}{\Delta t}$$

With:
H_{sub}= Entalpie of Sublimation,
Δn = amount of material sublimated

$$P_{total} = P_{dep} - \sum P_{cool}$$

Evolution of the wire temparature during a scan of the beam is shown together with decrease of the wire diameter due to sublimation.

Temperature of the wire (v=1m/s)

	Num. of part.	Typ. Beam diam.	Temp. after scan [C]	Eqi. - Temp [Celsius]
HERAp	1 *10^13	0.7 mm	3900	5100
HERAe	6.5 * 10^12	0.2 mm	4800	4500
PETRAp	4.8*10^12	2 mm	980	3500
PETRAe	1.5*10^12	0.1 mm	4700	6800
DESYIII	1.2*10^12	1 mm	3400	5300
TTF fast	2.8*10^13	0.05 mm	4000	7400
TTF slow	2.8*10^13	0.05 mm	286 000	2900

Melting temperature = 3500 °C for Carbon
= 1700 °C for Quartz

The wire in DESY III existed with 200 mA = $1.25 \cdot 10^{12}$ p for all times.

In HERAp we exchanged the wires every 2 month after "normal" use. Unusual frequent use destroyed the wires much earlier.

Reason: Sublimation of material:

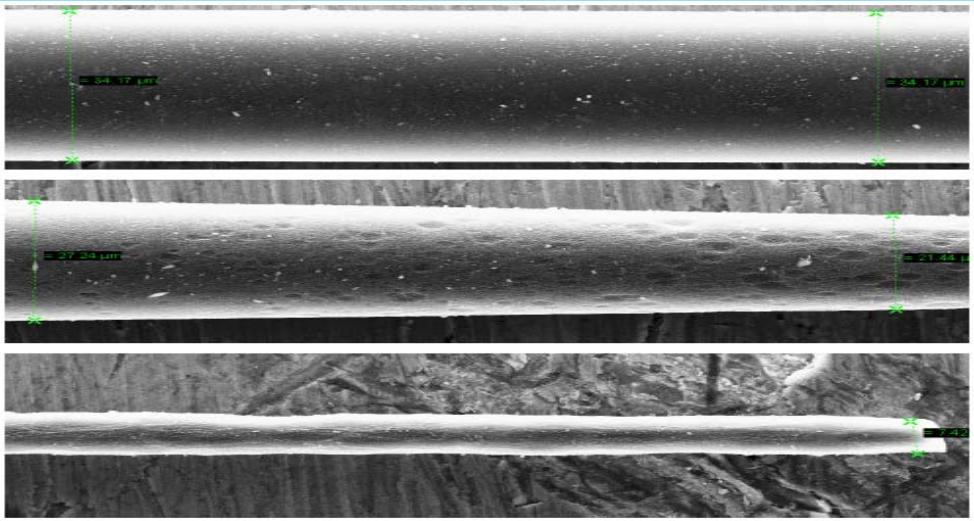

Fiber fracture at three distances from the beam impact location: 1 mm (upper plot), 0.5 mm (middle plot) and at beam center location (bottom plot).

CERN-BE-2009-028
Carbon Fiber Damage in Accelerator Beam
Sapinski, M ; Dehning, B ; Guerrero, A ; Koopman, J ; Métral, E ; DIPAC09, Basel

New concept to reach v=20 m/s and a resolution of 5 microns

$$T_h = C \cdot dE/dx \cdot n_{bunch} \cdot \frac{f_{bunch}}{v} \cdot \frac{1}{c_p \cdot 2 \cdot \sigma_v} \cdot \alpha \quad [^0C]$$

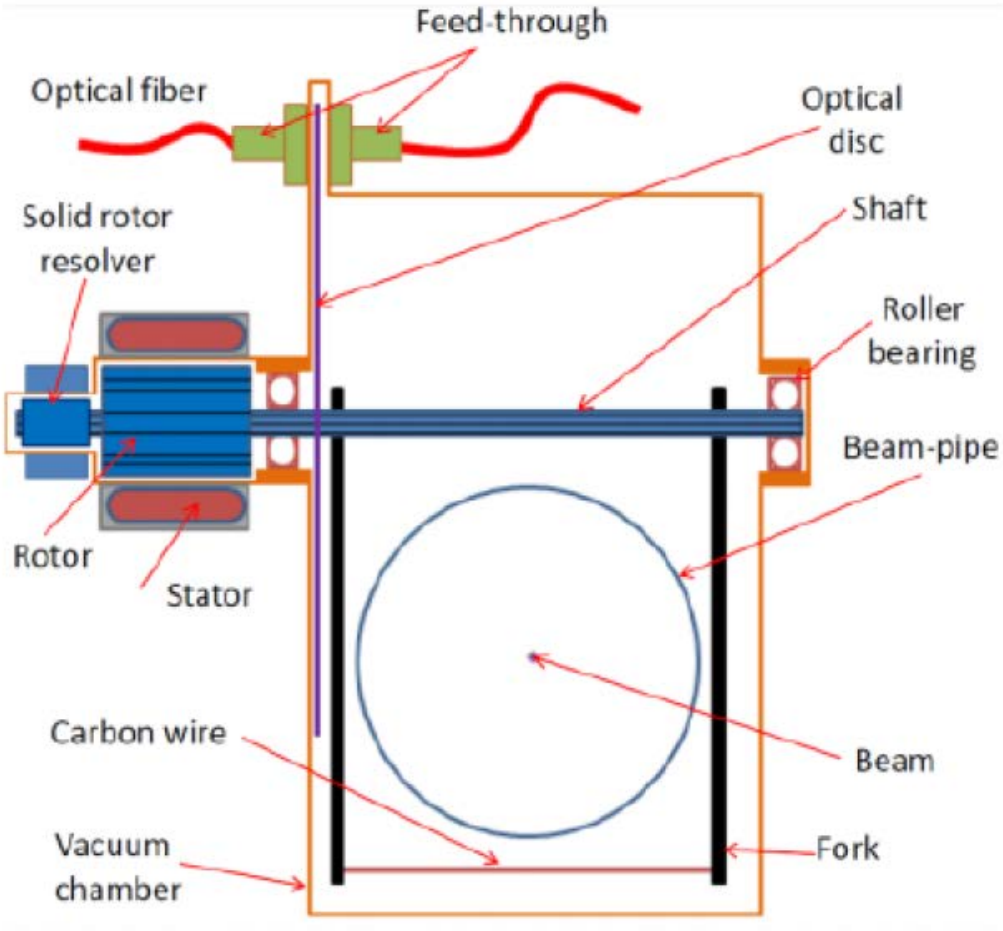

Figure 1: Fast Wire Scanner concept.

Design of a High-precision Fast Wire Scanner for the SPS at CERN
R. Veness, N. Chritin, B. Dehning, J. Emery, J.F. Herranz Alvarez, M. Koujili, S. Samuelsson, J.L. Sirvent Blasco; CERN, Geneva, Switzerland
IBIC2012, Tsukuba, Japan, Oct 1-4, 2012,

Limitations
4: Emittance blow up

Parameter table

Exercise WIRE3: Calculate the emittance blowup of the proton beam after one scan at a position with β = 11.8 m for p =0.3 and 7 GeV/c (Carbon wire): Assume a measurement position close to a Quadrupole (α=0)

For small deflection angles a good approximation for average root mean square scattering angle is given by:

$$\delta\Theta = \frac{0.014\,GeV}{pc}\cdot\sqrt{\frac{d'}{L_{rad}}}\cdot\left(1+1/9\cdot\log_{10}\frac{d'}{L_{rad}}\right)$$

Remember:

$$\gamma(s)y^2 + 2\alpha(s)yy' + \beta(s)y'^2 = \varepsilon$$

A fraction Ψ of the circulating beam particles will hit the wire:

$$\Psi = \frac{d'\cdot f_{rev}}{v}$$

=> Θ = Ψ ▪ δΘ ≈ y'

(see exercise WIRE2) | mean deflection angle

The resulting emittance blowup is than (7 GeV/c):

$$\delta\varepsilon_{rms} = \sqrt{2\pi}\cdot\delta\Theta^2\cdot\Psi^2\cdot\beta(s)$$
$$= 5.1\cdot10^{-2}\,\pi\,mm\,mrad$$

$\sqrt{2\pi}$ from Literature

Gas: emittance growth due to residual gas per hour (P=10^{-9} mbar)

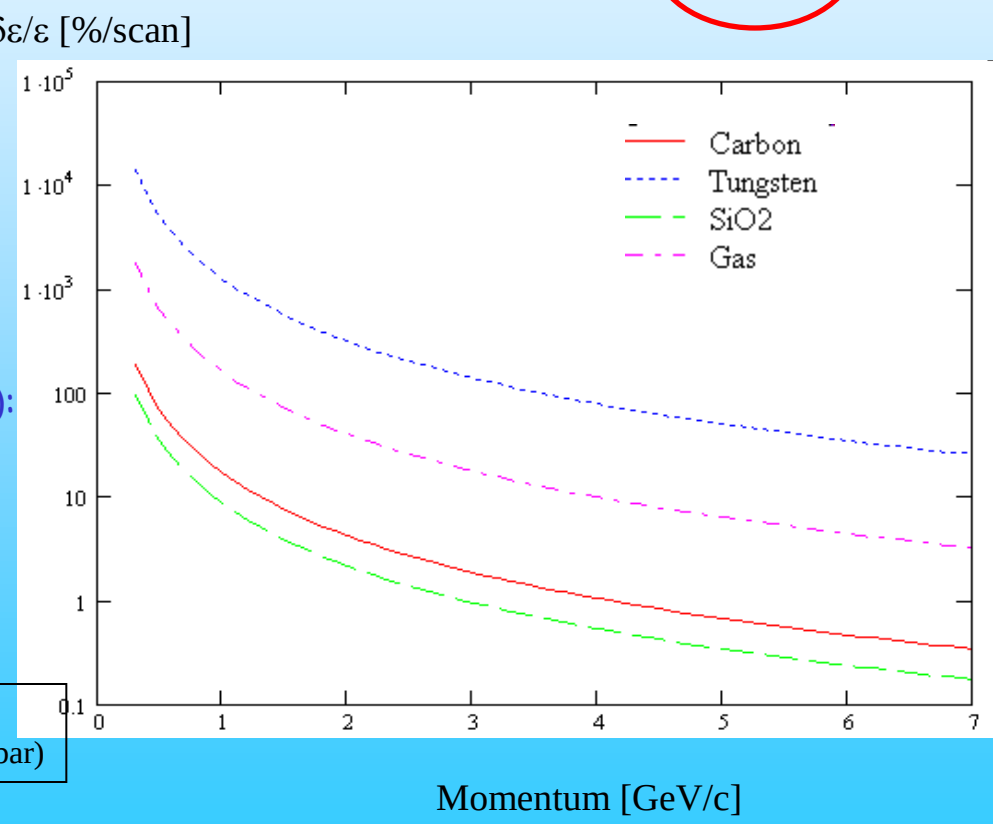

D. Möhl, Sources of emittance growth (also P. Bryant; CAS, Beam transfer lines):

$$\delta\varepsilon = \pi \frac{1}{2} \cdot \Theta_{rms}{}^{2} \cdot \beta$$

Averaging over all Betatron-phases

Unit of phase space emittance

M. Giovannozzi (CAS 2005)

$$\delta\varepsilon = \pi \frac{1}{4} \cdot \Theta_{rms}{}^{2} \cdot \beta$$

D. Möhl, Sources of emittance growth, 2007:

$$\delta\varepsilon_{\sigma} = \frac{1}{2} \cdot \Theta_{rms}{}^{2} \cdot \beta$$

The End of Wire Scanner Session

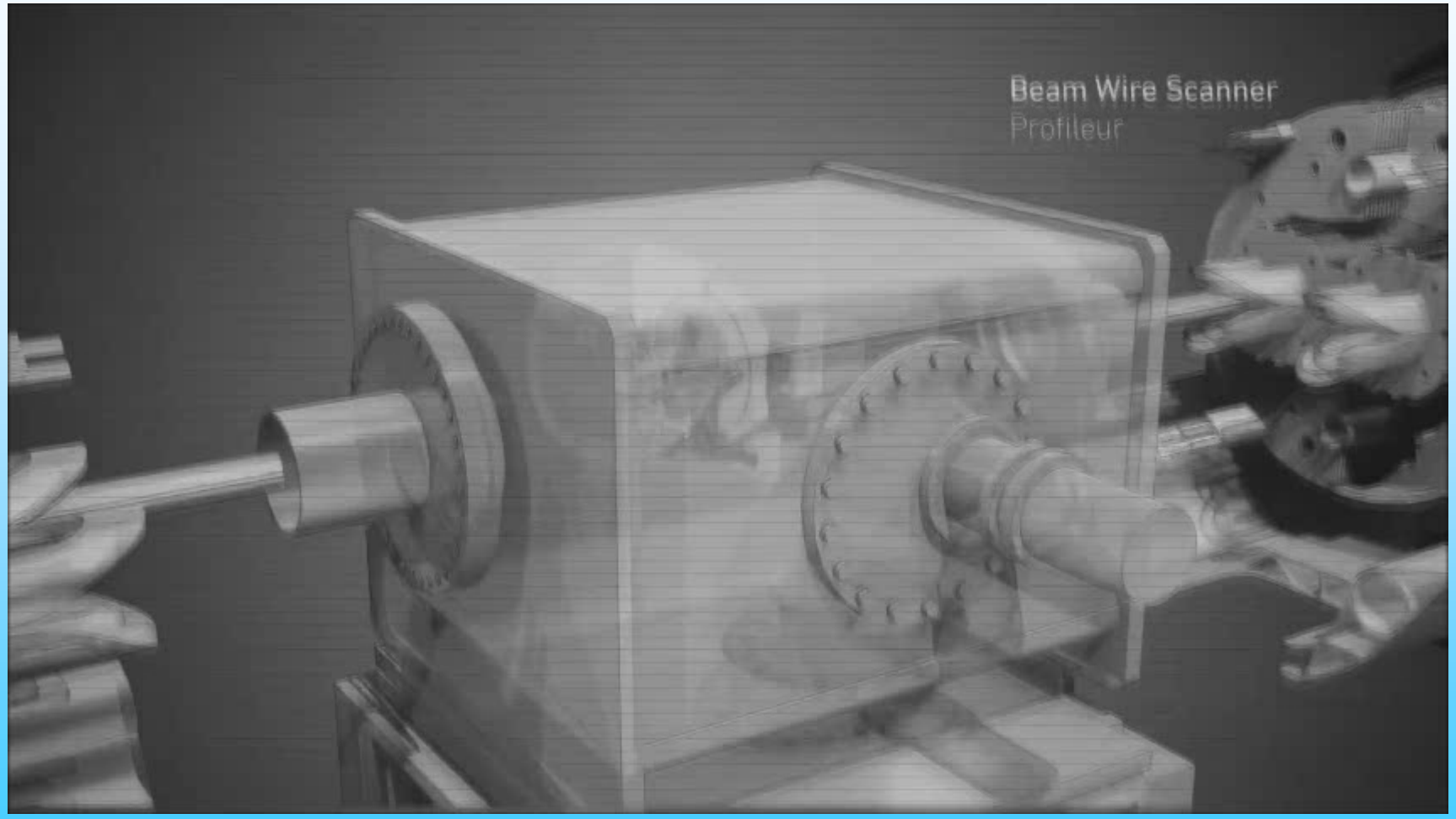

Wire Parameters

Parameter	Symbol	Unit	wire material				
			AL	W	Carbon	Beryllium	Quartz (SiO_2)
wire diameter	d $= 7 \cdot 10^{-4}$	cm					
mean wire diameter	$d' = d/2 \cdot \sqrt{\pi}$ $= 5.5 \cdot 10^{-4}$	cm					
Conversion	0.239	cal/Joule					
Conversion factor	$C = 3.8 \cdot 10^{-14}$	MeV / cal					
Speed of wire	v = 100	cm/s					
specific heat capacity*	c_p	cal / g / ^{0}C	0.21	0.036	0.42 (>400^{0}C) 0.17 (< 400^{0}C)	0.43	0.18
Energy loss of min. ion. part. (MIPs)	dE/dx dE/dx_m	MeV cm^2 / g MeV/cm	1.62 4.37	1.82 35.13	2.3 5.3	1.78 3.3	2.33 5.3
density	ρ	g/cm^3	2.7	19.3	2.3	1.85	2.29
melting temp.	T_m	^{0}C	650	3400	ca. 3500	1200	1700
Heat conductivity	l	W/(m K)	230	100-160	30-3000	200	1.2-1.4
Radiation length	l_{rad}	cm	8.9	0.35	18.8	34.7	12.3
Nuclear coll length	lnuc	cm	26	9.6	34	30	25.4

Table WIRE1: Parameters of wire materials. *> 500 ^{0}C

The beam parameters used in this exercise are shown in the following table:

Parameter	Symbol	Unit	Value
circumference of accel.	circ.	m	300
particle		Proton	
Beam particle momentum	p	GeV/c	0.3-7
Beta function	$\beta_h = \beta_v$	m	11.8
Emittance	$\varepsilon_h = \varepsilon_v$	π mm mrad	15
revolution Frequency	f_{rev}	MHz	0.93
Bunch spacing	t_{bunch} f_{bunch}	ns MHz	98 10.2
Number of bunches in accel.	NB		11
Bunch charge	n_{bunch}	1/e	$1.1 \cdot 10^{11}$
Beam width measurement [1]	σ_h	mm	1.5
Beam width perpendicular to meas. [1]	σ_v	mm	1

Table WIRE2: Parameters of Beam

LINACS/Transport Lines Emittance Measurement

Recapitulation of 'Emittance'

In a transfer line, the beam passes once and the shape of the ellipse at the entry to the line determines its shape at the exit. **Thus α and β, γ depend on the input beam and their propagation depends on the structure.** Any change in the structure will only change the α and β, γ values downstream of that point. … The input ellipse must be chosen by the designer and should describe the configuration of all the particles in the beam.

In the following let's assume a transport line or the part of the Linac where no acceleration takes place. What about the emittance?

If no energy is transferred to the beam (Hamiltonian systems), the emittance is conserved.

Recapitulation of 'Emittance'

Emittance is only constant in beamlines without acceleration

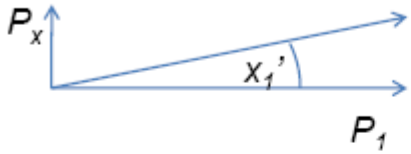

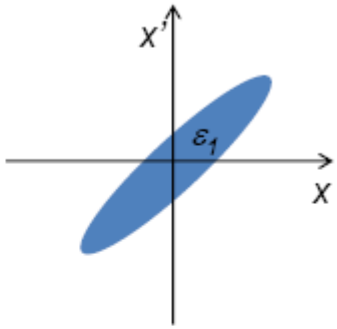

acceleration

$$\varepsilon_2 = \varepsilon_1 \frac{P_1}{P_2} \quad \text{with} \quad P = m\beta_{rel}\gamma_{rel}\, c$$

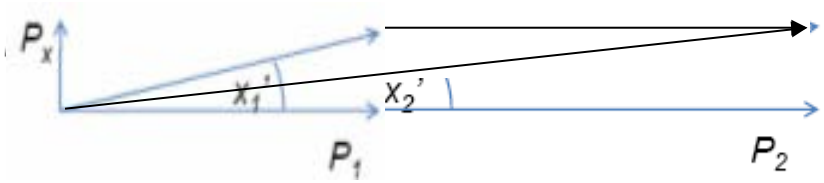

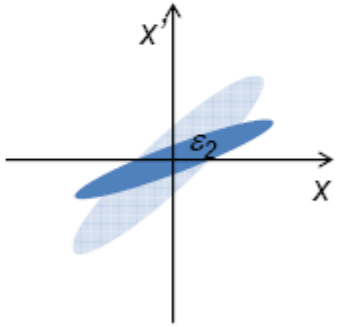

<u>normalised emittance</u> $\varepsilon_N = \beta_{rel}\gamma_{rel}\ \varepsilon$ preserved with acceleration !

To distinguish from normalised emittance ε_N , ε is quoted as "geometric emittance" !

Exercise: Draw radiation damping by Synchrotron Radiation

Recapitulation of ‘Emittance’

Exercise: Draw radiation damping by Synchrotron Radiation

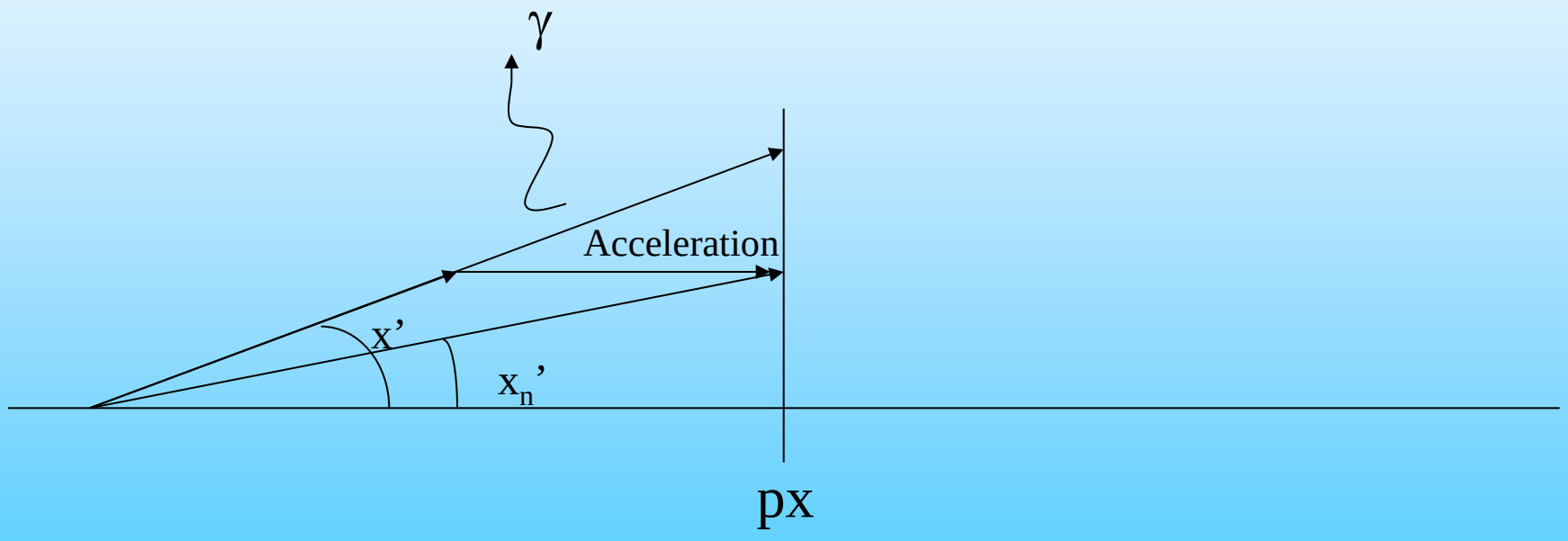

Recapitulation of ‘Emittance’

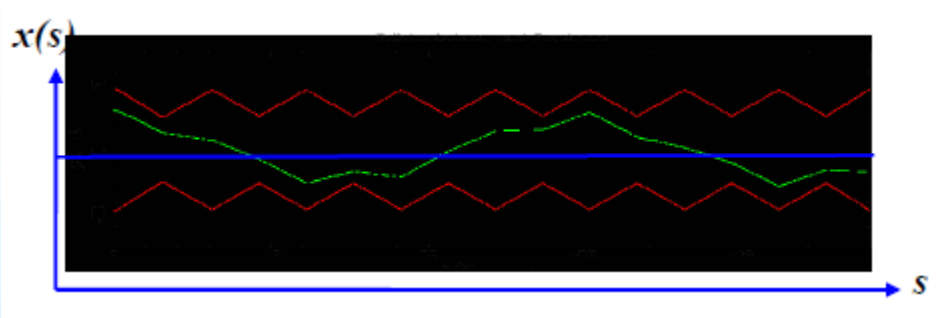

Q = irrational

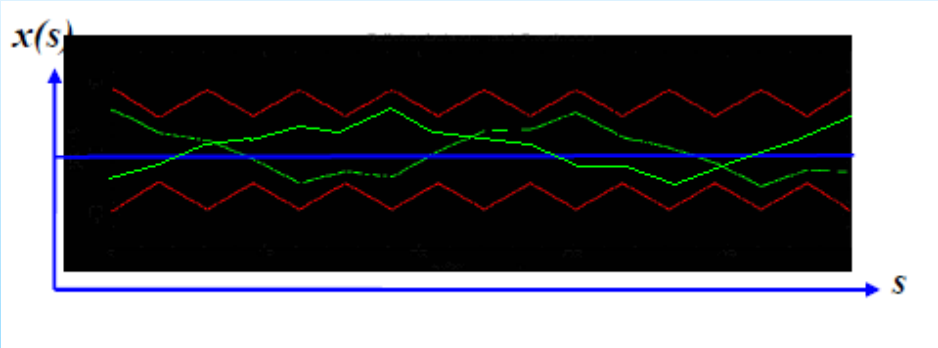

$$x(s) = \sqrt{\varepsilon} * \sqrt{\beta(s)} * \cos(\psi(s) + \phi)$$

How the profile looks like?

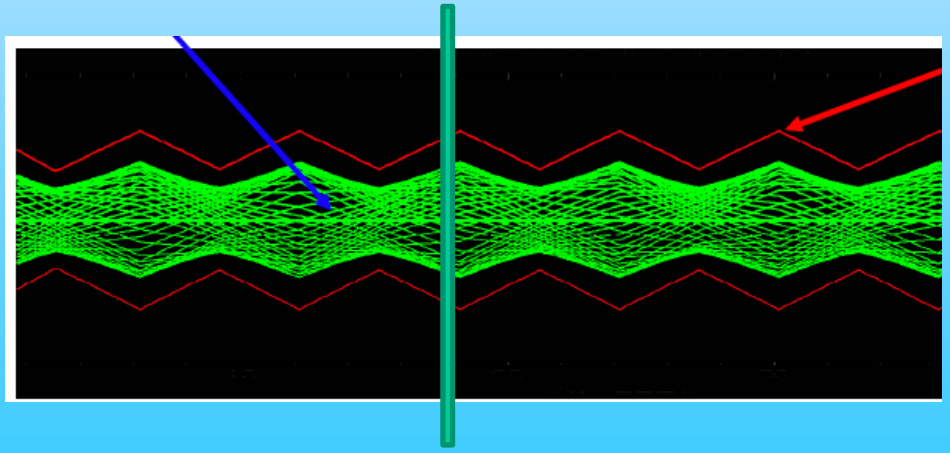

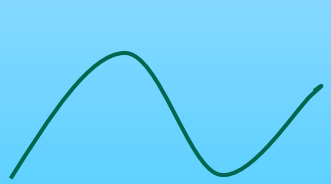

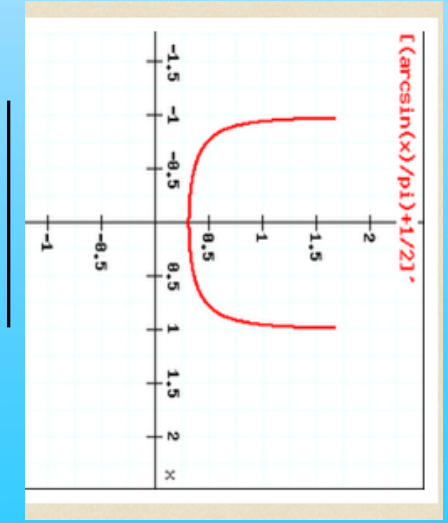

Recapitulation of 'Emittance'

The Ellipse and the Twiss parameter:

diverging beam: $\alpha<0$
waist or lens: $\alpha=0$
converging beam $\alpha>0$

$\beta>0$ by definition [mm/mrad]
$0<\varepsilon=$ constant [mm·mrad]
$0<\gamma=\left(1+\alpha^2\right)/\beta$ [mrad/mm]

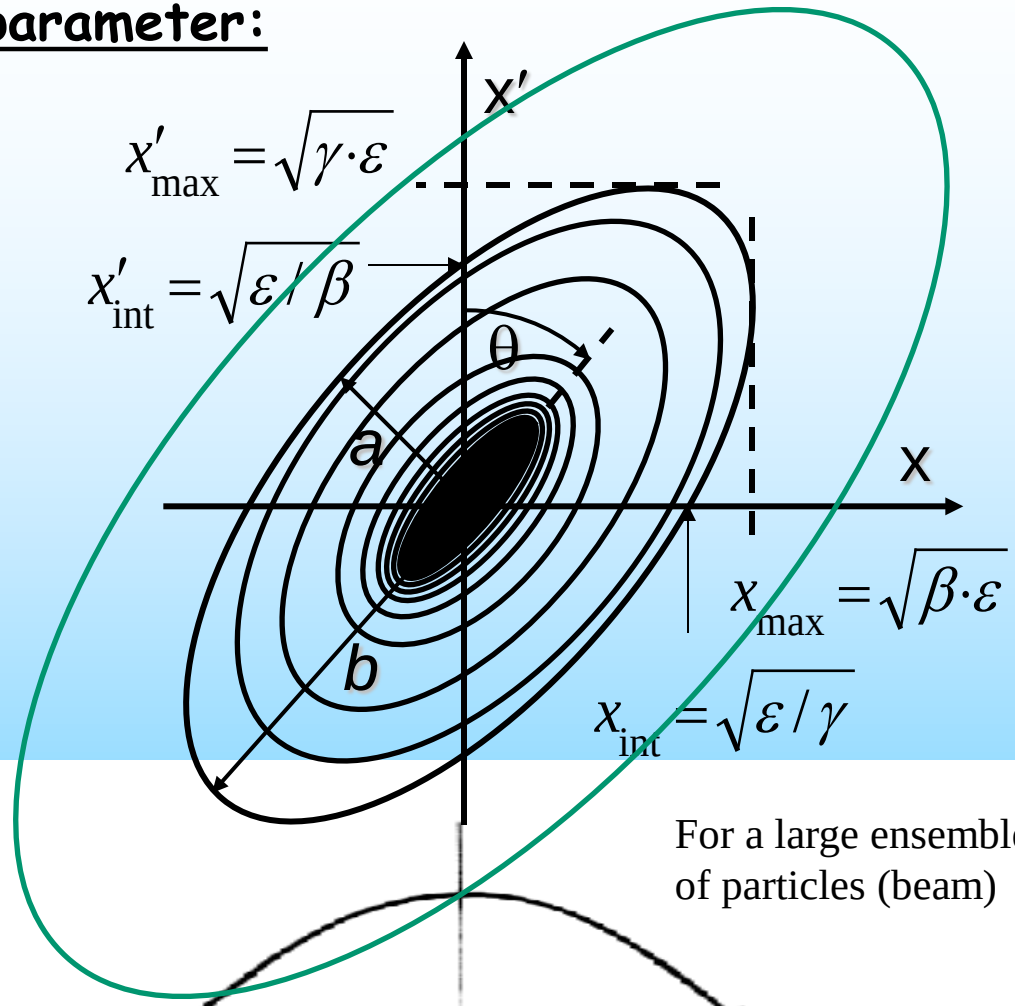

Divergence:

$$x'_{max}=\sqrt{\gamma\cdot\varepsilon}=\sqrt{\left(1+\alpha^2\right)\cdot\varepsilon/\beta}$$

Beam radius (Profile):

$$x_{max}=\sqrt{\beta\cdot\varepsilon}$$

For a large ensemble of particles (beam)

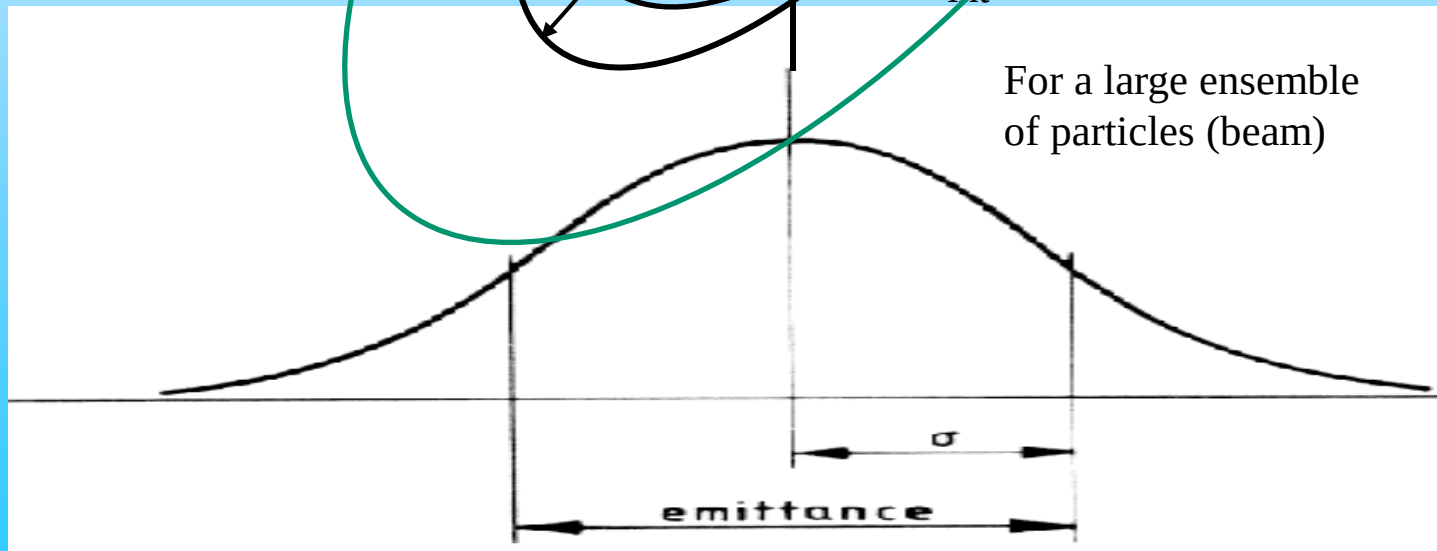

Recapitulation of 'Emittance'

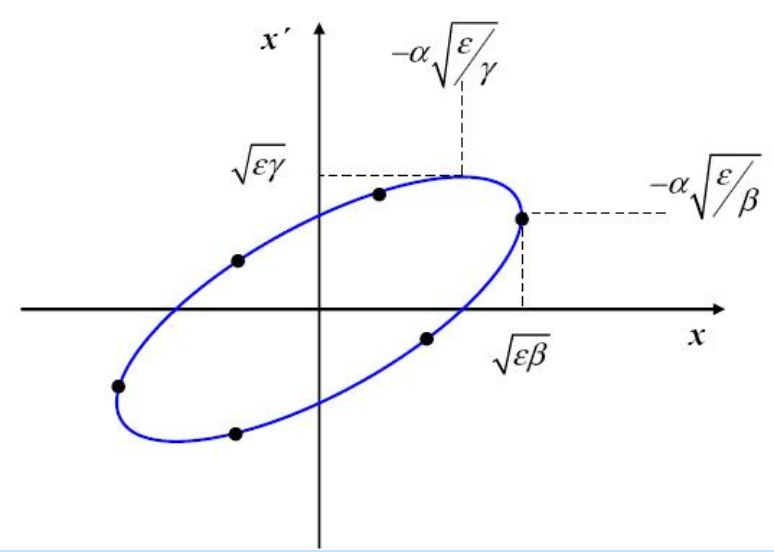

- via Twiss parameters

$$\varepsilon = \gamma x^2 + 2\alpha x x' + \beta x'^2$$

- statistical definition

P.M. Lapostolle, IEEE Trans. Nucl. Sci. NS-18, No.3 (1971) 1101

$$\varepsilon_{rms} = \sqrt{\langle x^2 \rangle \langle x'^2 \rangle - \langle x x' \rangle^2}$$

2nd moment of beam distribution ρ(x)

$$\langle x^2 \rangle = \frac{\int_{-\infty}^{\infty} dx\, x^2 \cdot \rho(x)}{\int_{-\infty}^{\infty} dx\, \rho(x)}$$

- ε_{rms} is measure of spread in phase space
- root-mean-square (rms) of distribution

$$\sigma_x = \langle x^2 \rangle^{1/2}$$

- ε_{rms} useful definition for non-linear beams
  → usually restriction to certain range
  (c.f. 90% of particles instead of [-∞,+∞])

- beam matrix

$$\sigma = \begin{pmatrix} \sigma_{11} & \sigma_{12} \\ \sigma_{21} & \sigma_{22} \end{pmatrix} = \begin{pmatrix} \langle x^2 \rangle & \langle x x' \rangle \\ \langle x x' \rangle & \langle x'^2 \rangle \end{pmatrix} = \varepsilon \begin{pmatrix} \beta & -\alpha \\ -\alpha & \gamma \end{pmatrix}$$

$$\varepsilon_{rms} = \sqrt{\det \sigma} = \sqrt{\sigma_{11}\sigma_{22} - \sigma_{12}^2}$$

○ = beam size

- transformation of beam matrix σ by transportmatrix M

$$\sigma^1 = M \sigma^0 M^T \quad M = \begin{pmatrix} M_{11} & M_{12} \\ M_{21} & M_{22} \end{pmatrix}$$

Recapitulation of 'Emittance'

While the area is constant, the emittance ellipse shape and orientation changes. It is described by:

$$\gamma \cdot x^2 + 2 \cdot \alpha \cdot x \cdot x' + \beta \cdot x'^2 = A/\pi = \varepsilon$$

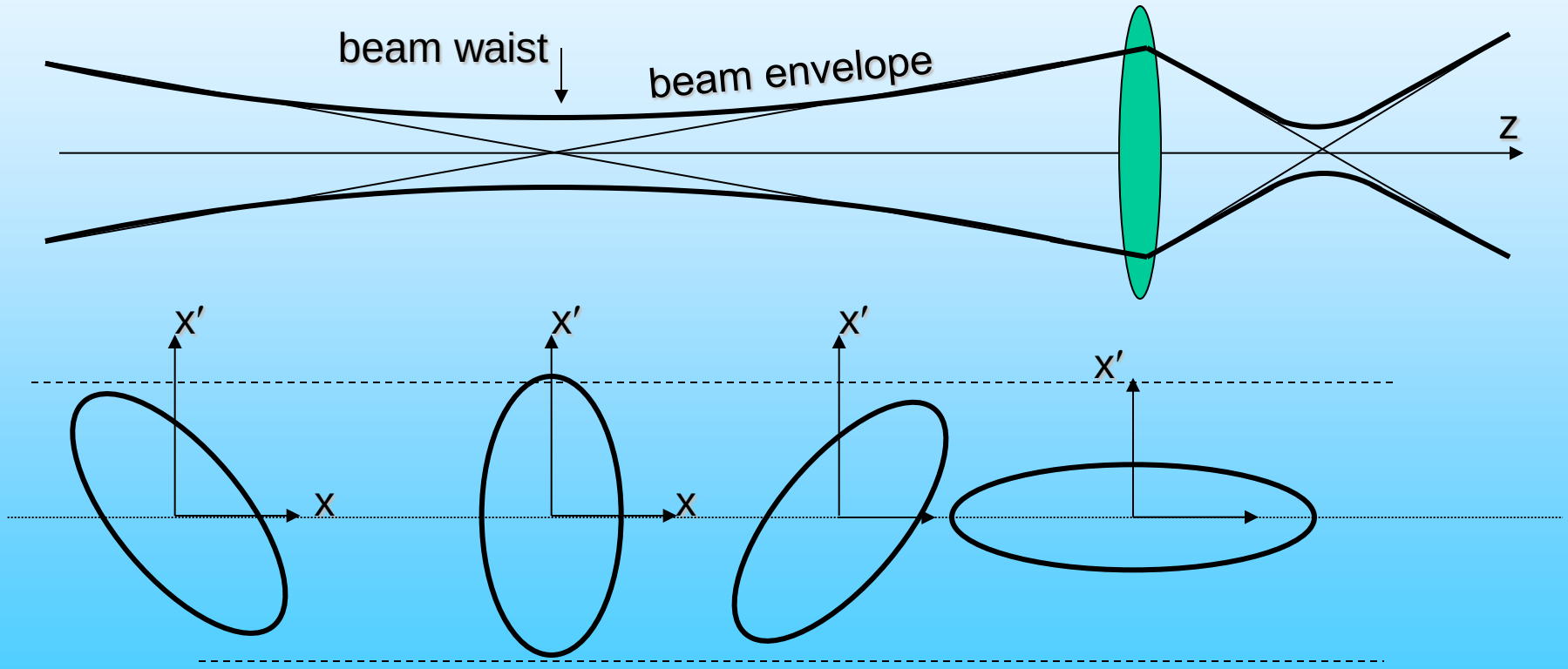

End of Recapitulation of ‘Emittance’

Next: Explain ways of measuring the emittance of a charged particle beam in a Linear Accelerator or a transport line without knowing the beam optic parameters α, β, γ.

Exercise L1: Which is (are) the preferable method(s) for a high energy proton transport line (p > 5 GeV)?

Solution: 3 (thin) **screens** or **SEM** grids or varying quadrupole which measure the different beam widths σ. For **pepper pot or slits** one needs a full absorbing aperture.

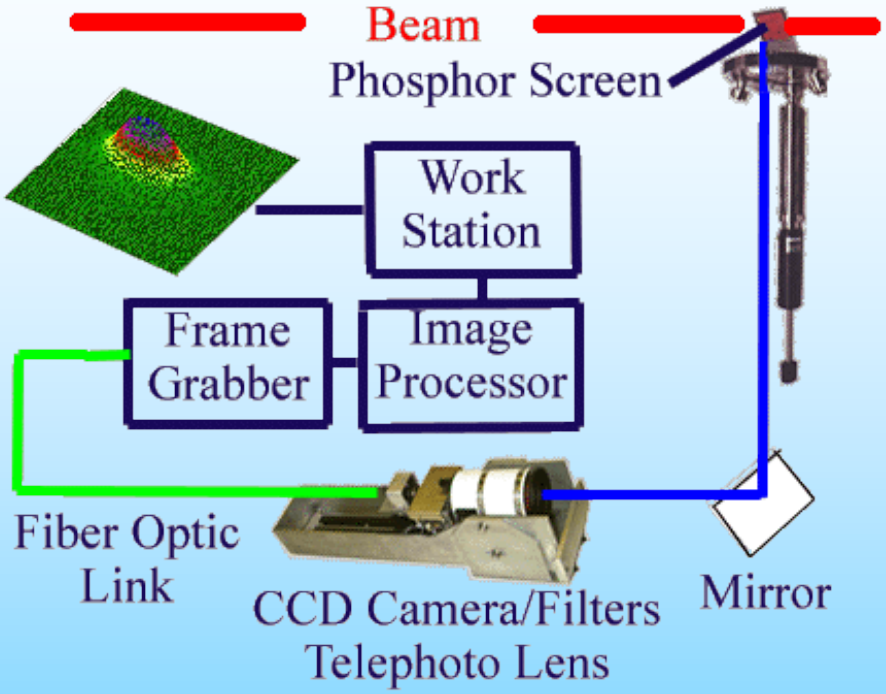

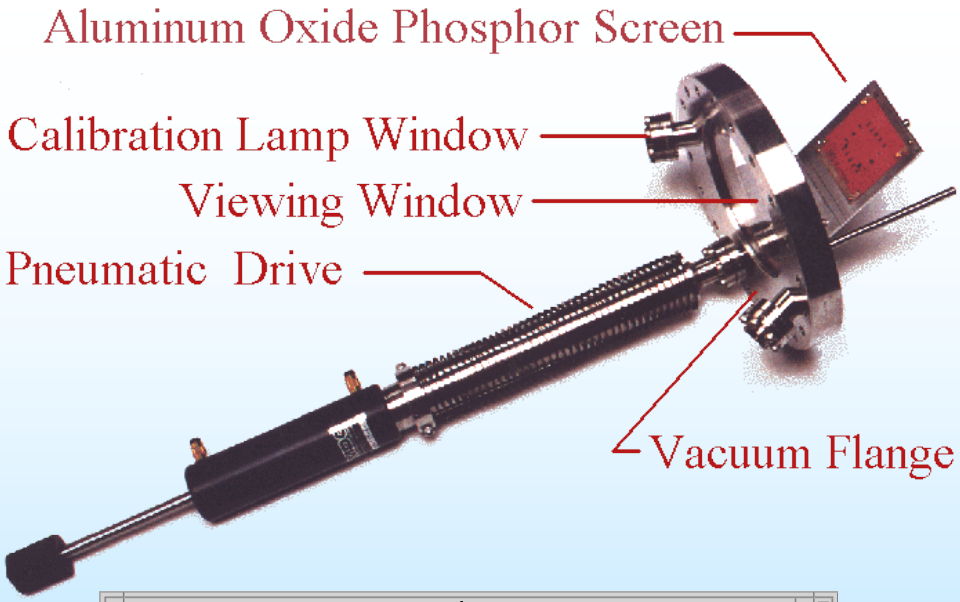

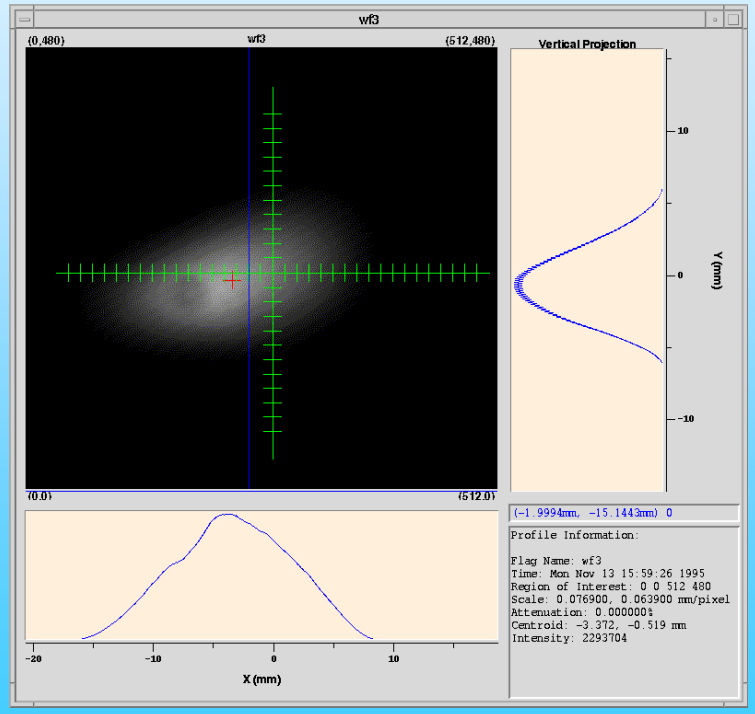

Substrate: Aluminum Foil, 0.001" thick

http://accelconf.web.cern.ch/AccelConf/p95/ARTICLES/TPB/TPB26.PDF

http://www.rhichome.bnl.gov/RHIC/Instrumentation/Systems/InjProfile/flags.html

XFEL-Screens (ca. 50 Stations)

Idea 1: 90^0 /45^0 Geometrie for removing (C)OTR

Idea 2: “Scheimpflug” Prinziple from Large-Picture-Photography to remove depth-of-field

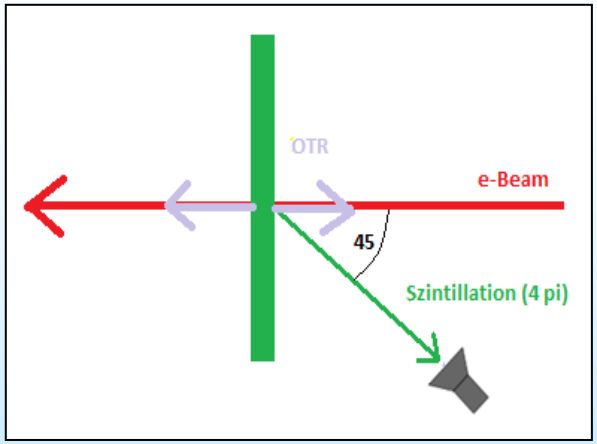

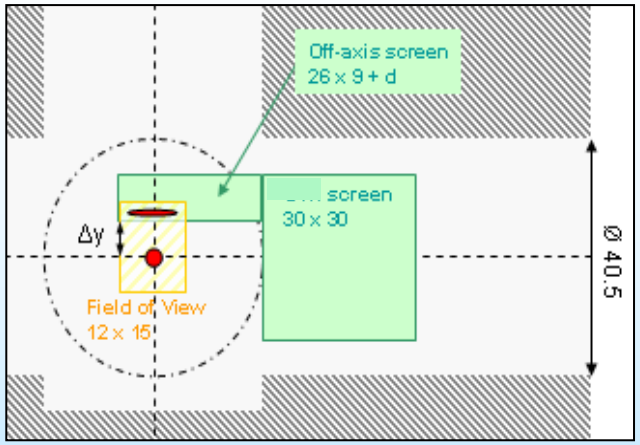

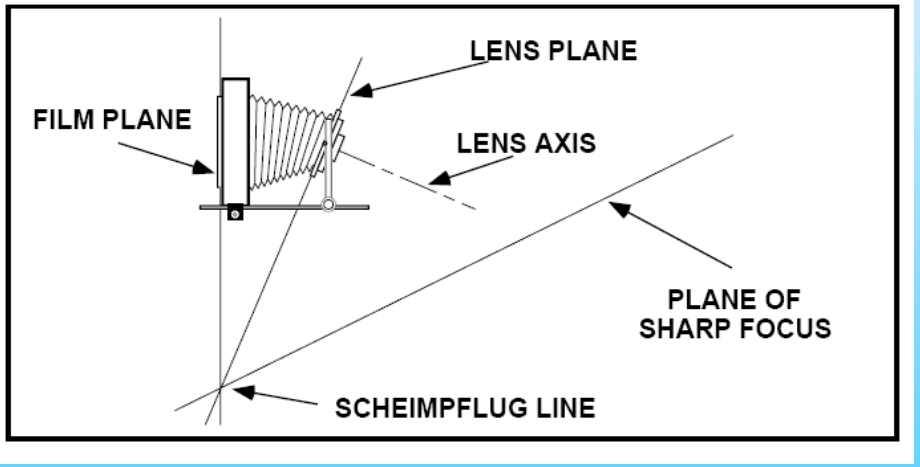

“Get a sharp image of an entire plane, if focus, image, and object plane cut in a single line.“

Scintillating Screen Applications in Beam Diagnostics

Unfortunately for the moment there is **no clear recommendation** for "the best" material for the use in high current applications and further studies are still needed and ongoing. Lot of details at: **http://www-bd.gsi.de/ssabd/**

4.8 MeV/u ← Same pulse energy → 11.4 MeV/u

(~similar flux [ions/(cm² s)])

$4.3*10^{10}$ ppp $1.8*10^{10}$ ppp

Ion beam: Ca^{10+},

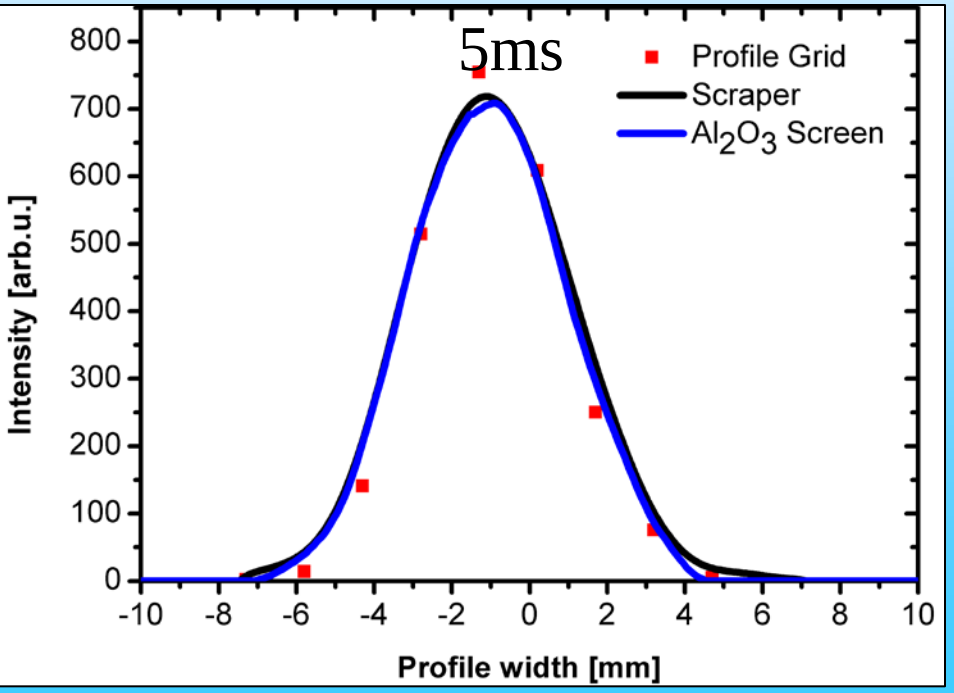

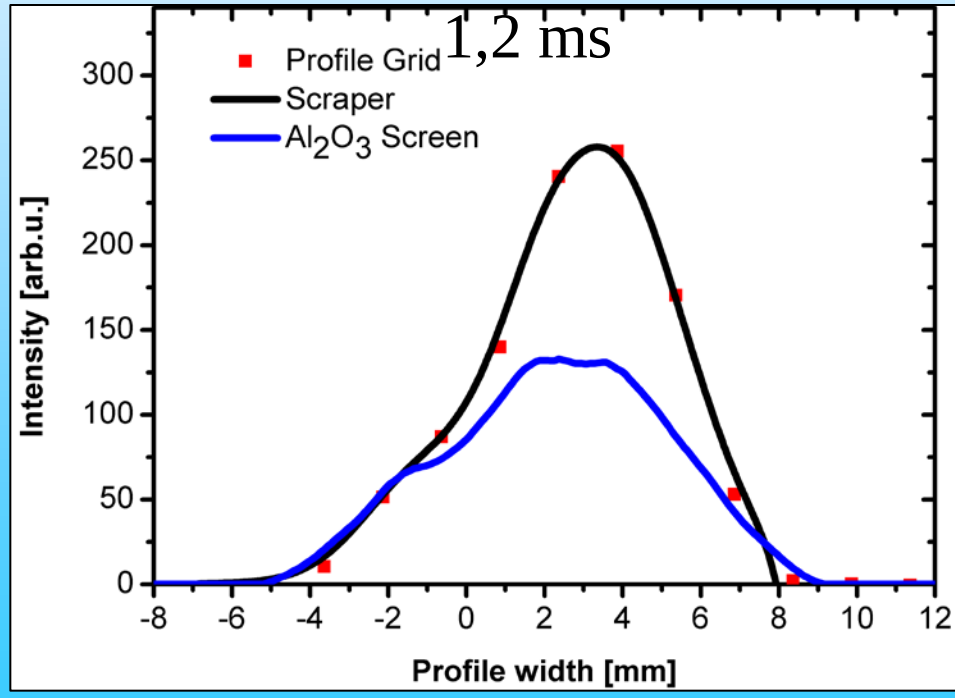

Wire scanner vs Screen
XFEL@1597m

Beam size measured from Screen:

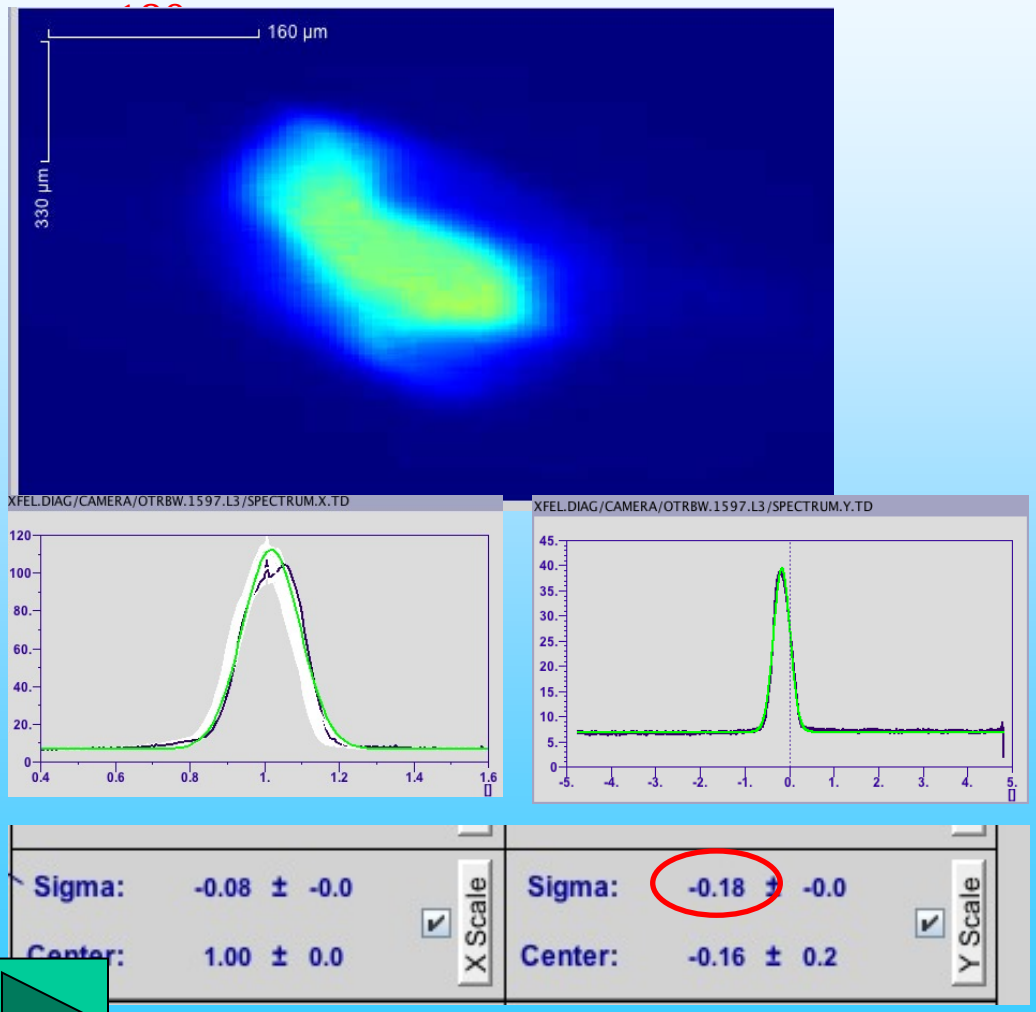

Vertical wire scanner

σ_y = 161.47um

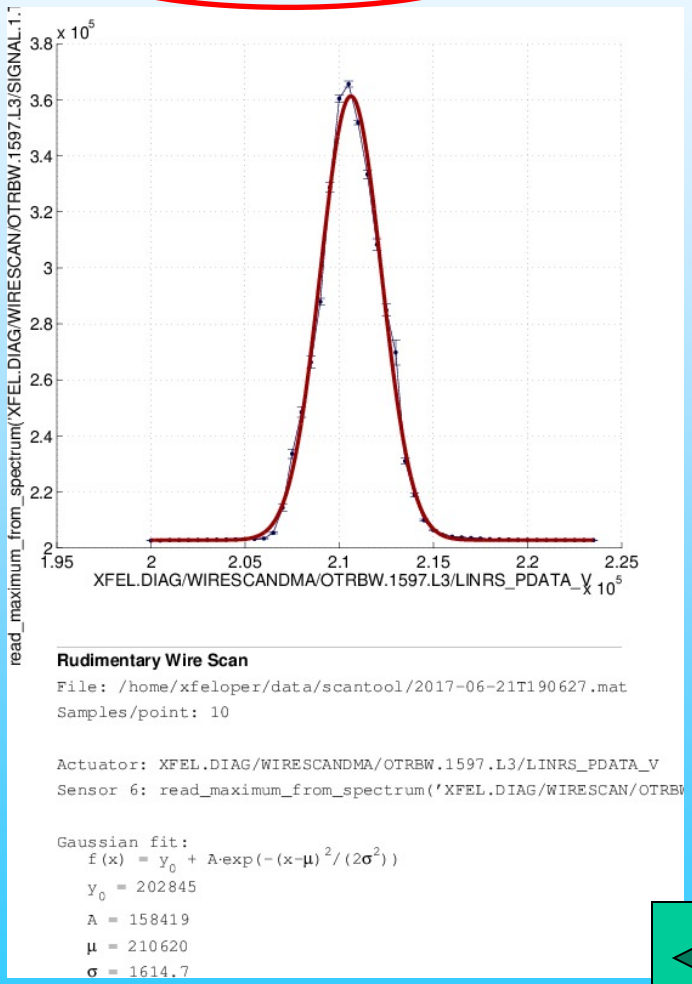

Measurement with –Harps-

- Each individual wire is connected to an electrical vacuum feedthough and an amplifier.
- Beam particles hitting a wire create secondary electrons of 20 – 100 eV from its surface.
- The secondary electron yield Y varies between about 300% for low energy ions (e.g. 40 keV) to about 2% for minimum ionizing particles for most common metals.
- The SEM current is linear over many orders of magnitude.
- The spacing and the diameter of the wire defines the resolution of the instrument. Typical values of both are between 20 µm to about 2 mm.
- Materials are tungsten and titanium due to their good mechanical and thermal properties but also carbon and aluminum.
- Low-Z materials have the advantage of lower beam losses

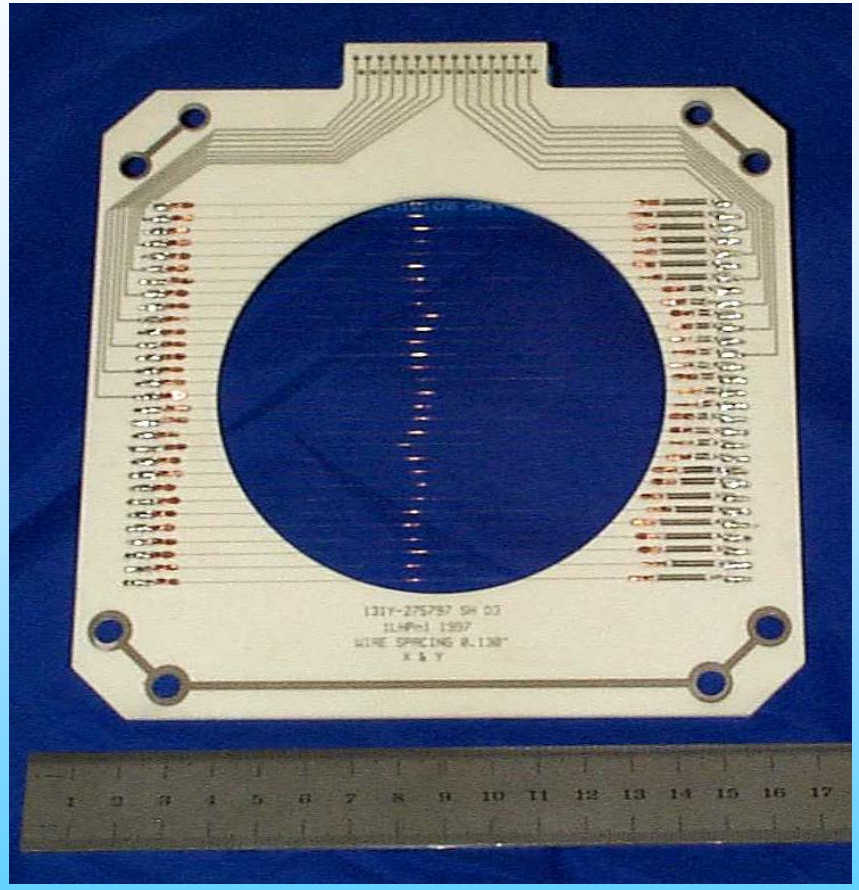

Harps in high radiation environments
11th ICFA International Mini-Workshop on Diagnostics for High-Intensity Hadron Machines, 2002, by Mike Plum

Measurement with –Harps-

- A negative bias voltage on the wires or positive collection electrodes avoids recollection of the secondary electrons by the same or another wire.
  => Avoid signal coupling (also electrical).
- The dynamic range of a SEM harp is limited the electronic noise on the low beam current end and by thermal electron emission due to heating of the wire at the high beam current end.
- Beside thermal electron emission the wire itself or its support (e.g. soldering) may melt and the elongation of the wires changes with heat.
- A SEM Harp (or a thin screen) is quite transparent for not too low energetic beams and successive harps are possible.

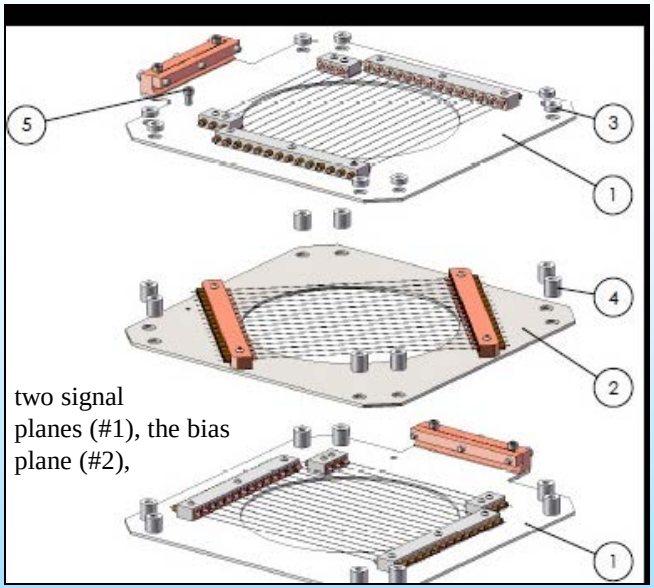

two signal planes (#1), the bias plane (#2),

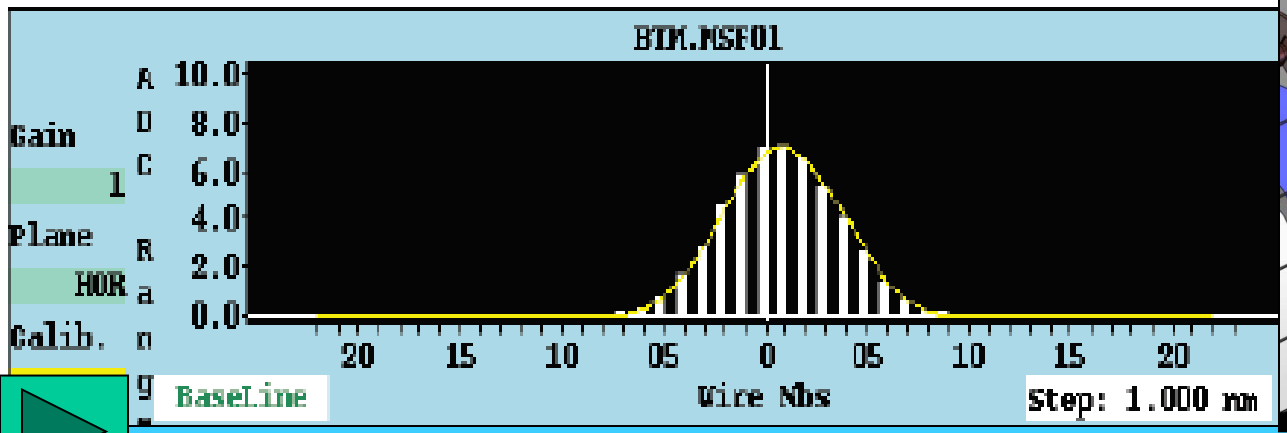

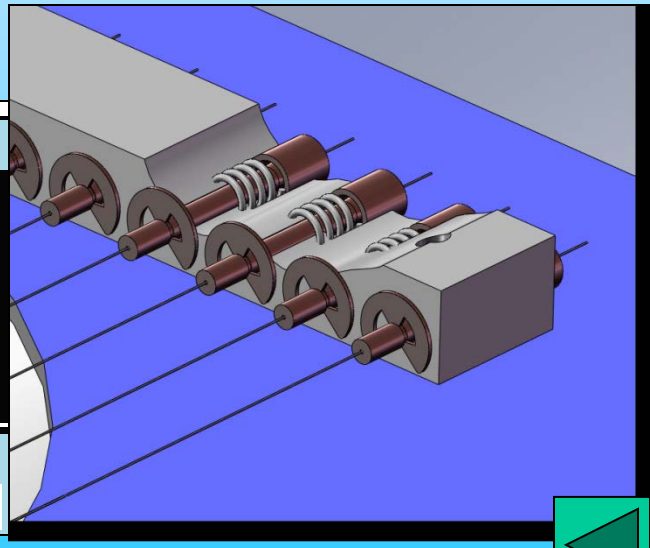

LANSCE Harp Upgrade, J. Douglas et. al, BIW2010

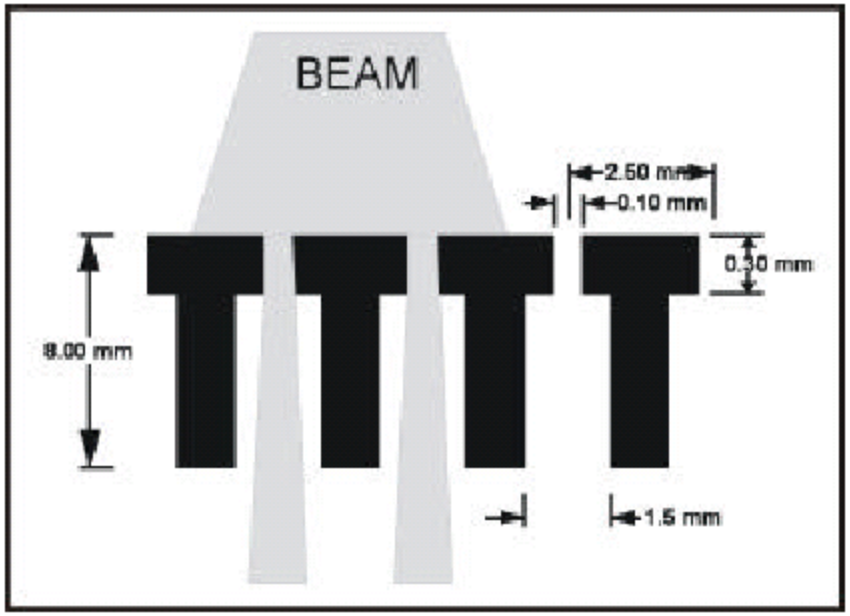

Scheme of the pepperpot plate in a cross sectional view and relevant dimensions

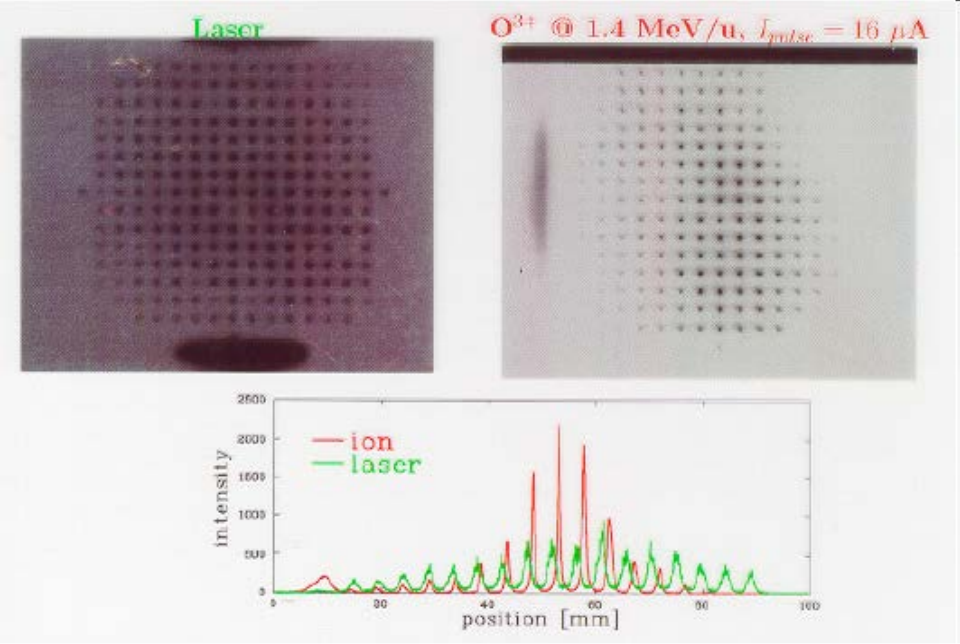

Light spots observed on the viewing screen of a Pepperpot device. Top left: Spots generated for calibration using a laser beam. Top right: Spots from an oxygen beam. Bottom: Intensity distribution along one line.

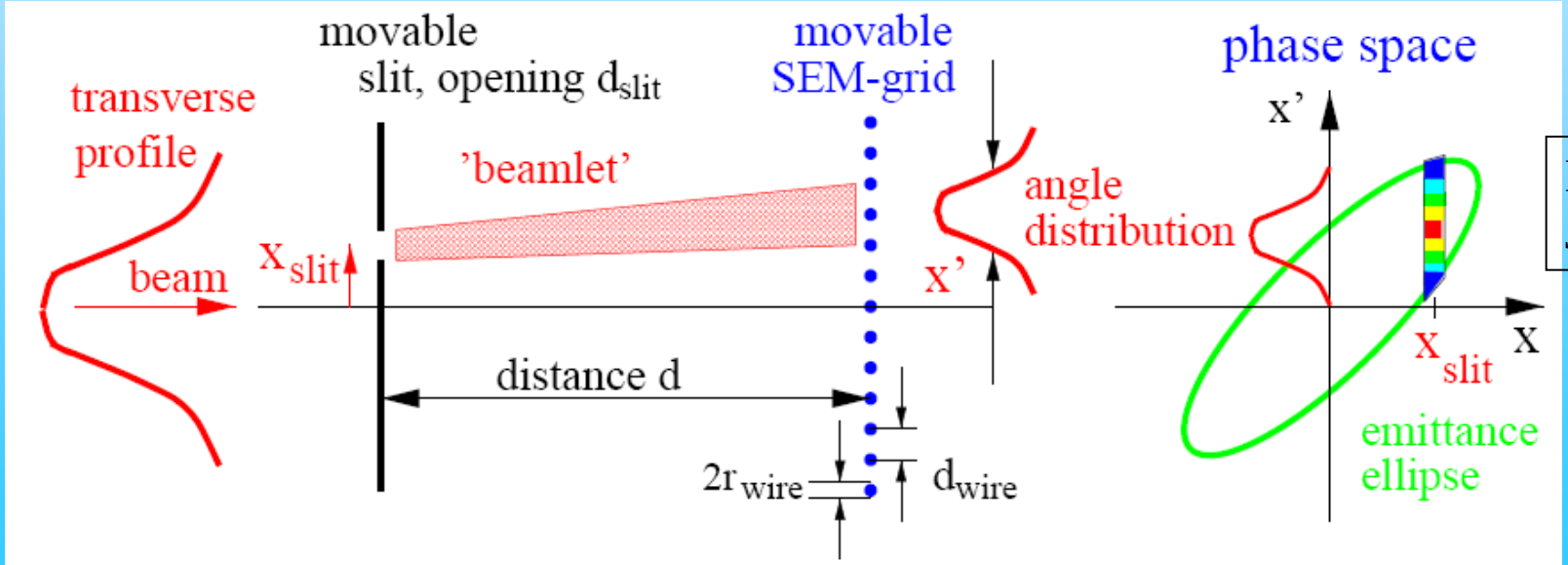

By P. Forck
Juas 2009

The Slit and Grid Method

3-dim plot:

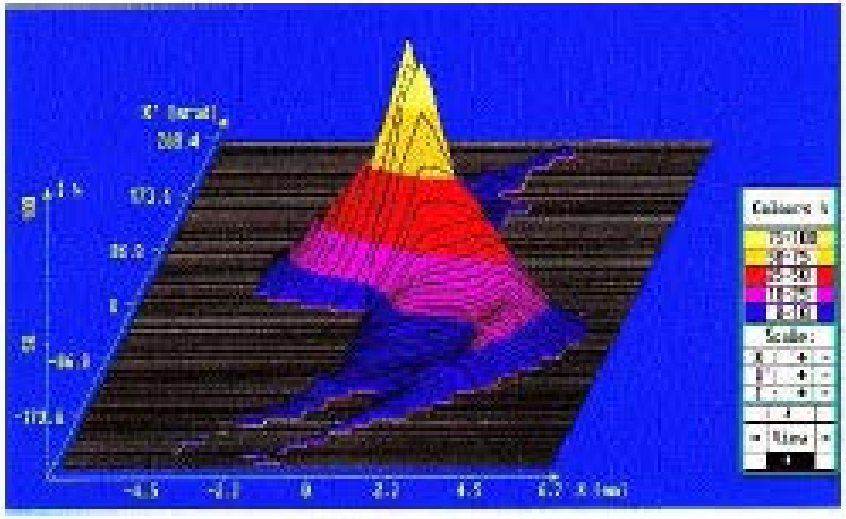

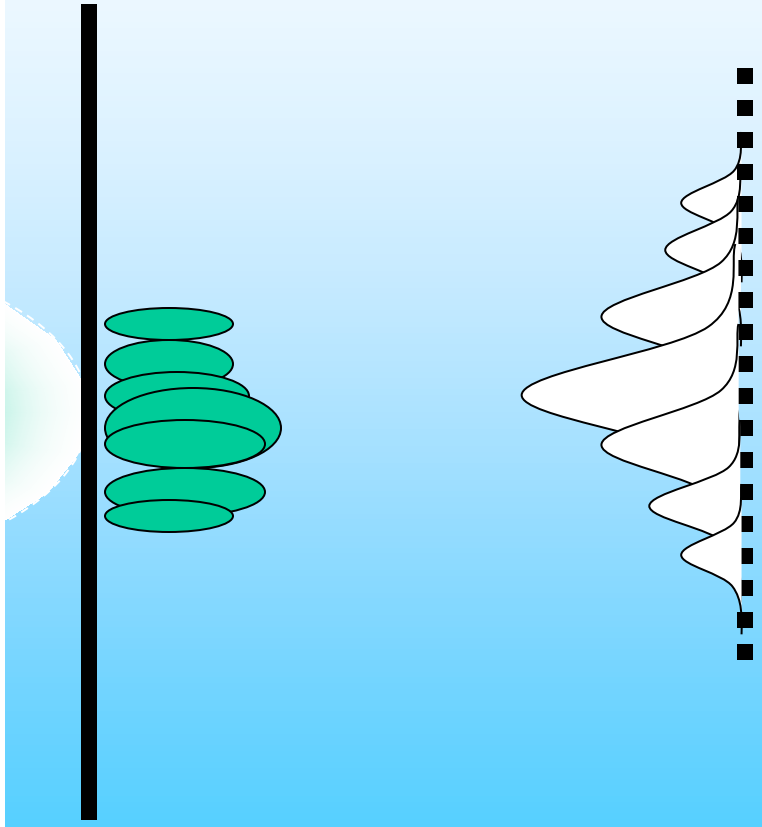

Emittance measurement by Slit + screen/harp

Low energy hadron particles which have a **penetration depth of a cm or less** can be stopped by a simple metallic plate. A small transversal slit of height h_{slit} selects a beamlet which shines on a screen or harp monitor in a drift distance d.

The width of the measured beamlet is defined by

- the **divergence of the beam x'** at the slit position x_n, on the distance d and
- on the **resolution of the system defined by the h_{slit}**- and
- the **resolution of the screen/harp device**.

The height of the signal depends on the bunch current I_0 and on the current distribution in the bunch (the beam profile). The slit is scanned across the beam profile and for each position x_n a beamlet distribution $I(x_n, x')$ is collected.

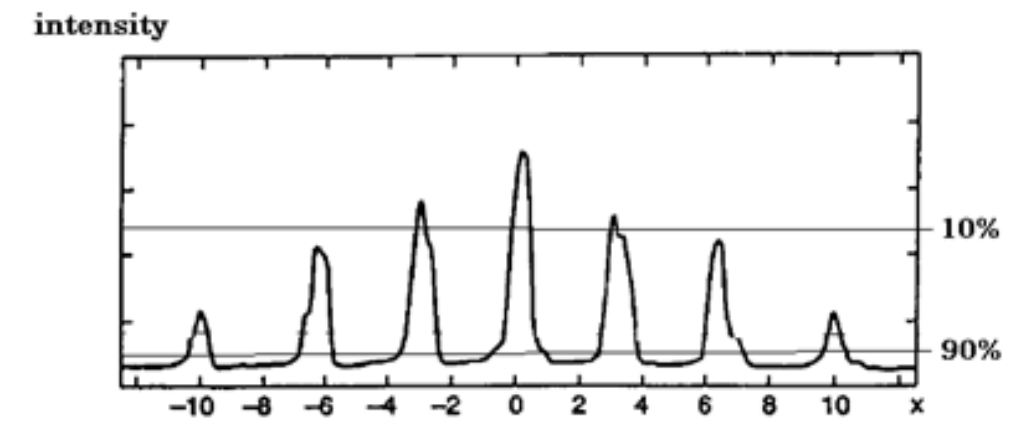

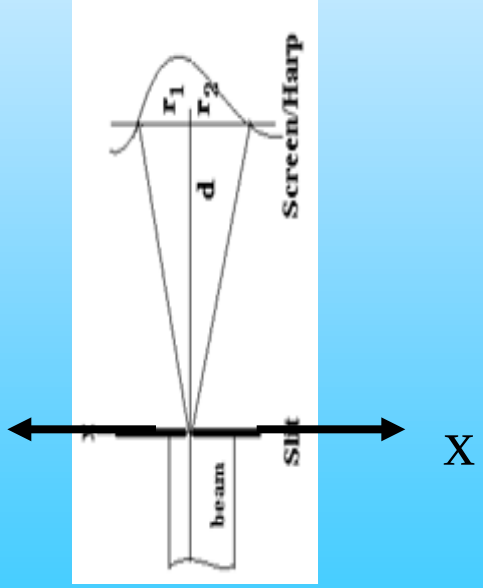

Emittance measurement by Slit + screen/harp

The radii $r_{1,2}/d = x_{1,2}'$ give the angular spread of the beam at the position x_n at **a defined amount of current** included in the emittance ellipse.
The emittance is:

$$\varepsilon_x(x,x') = 1/\pi \int dx\, dx' = 1/\pi \cdot A_x$$

The **rms** emittance of the incident beam is:

$$\varepsilon_{rms}(x,x') = \sqrt{\langle x^2 \rangle \langle x'^2 \rangle - \langle xx' \rangle^2}$$

$$\varepsilon_{rms}^2 \approx \frac{1}{N^2} \cdot \left[\sum_{j=1}^{p} n_j \left(x_{nj} - \bar{x} \right)^2 \right] \cdot \left[\sum_{j=1}^{p} \left(n_j \cdot \left(\frac{\sigma_j}{d} \right)^2 + n_j (\bar{x}'_j - \bar{x}')^2 \right) \right]$$

$$- \frac{1}{N^2} \left[\sum_{j=1}^{p} n_j x_{nj} \bar{x}'_j - N \bar{x} \bar{x}' \right]^2$$

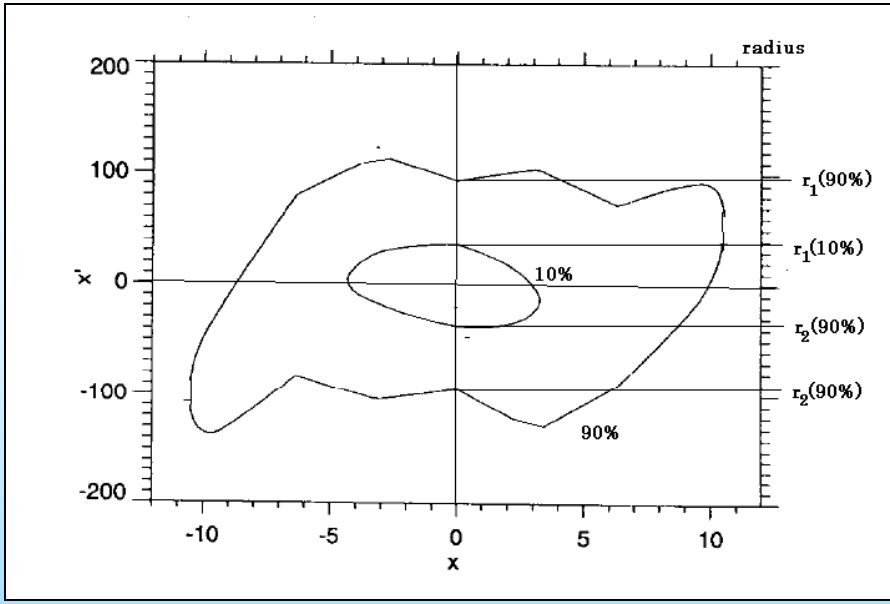

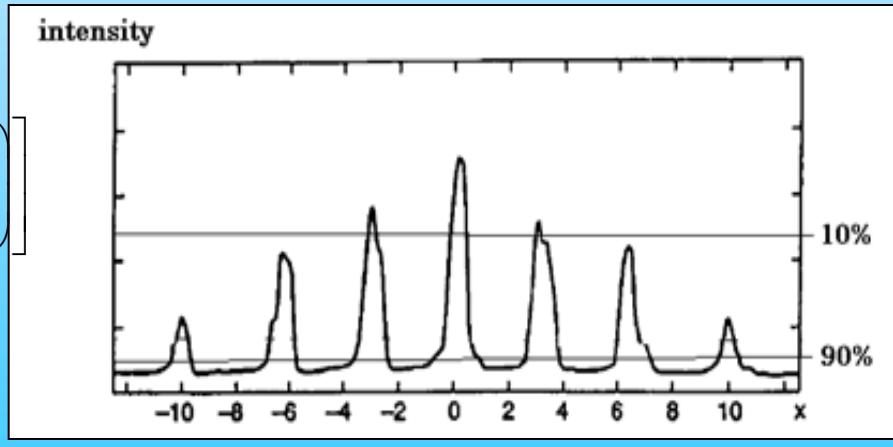

Calc. details see: M. Zhang, Emittance Formula for Slits and Pepper-pot Measurement, TM-1988, Fermilab, 1996.

Emittance measurement by Pepperpot/slits

What kind of emittance-picture do you expect from this picture at almost 100%?

Assume d=1 unit

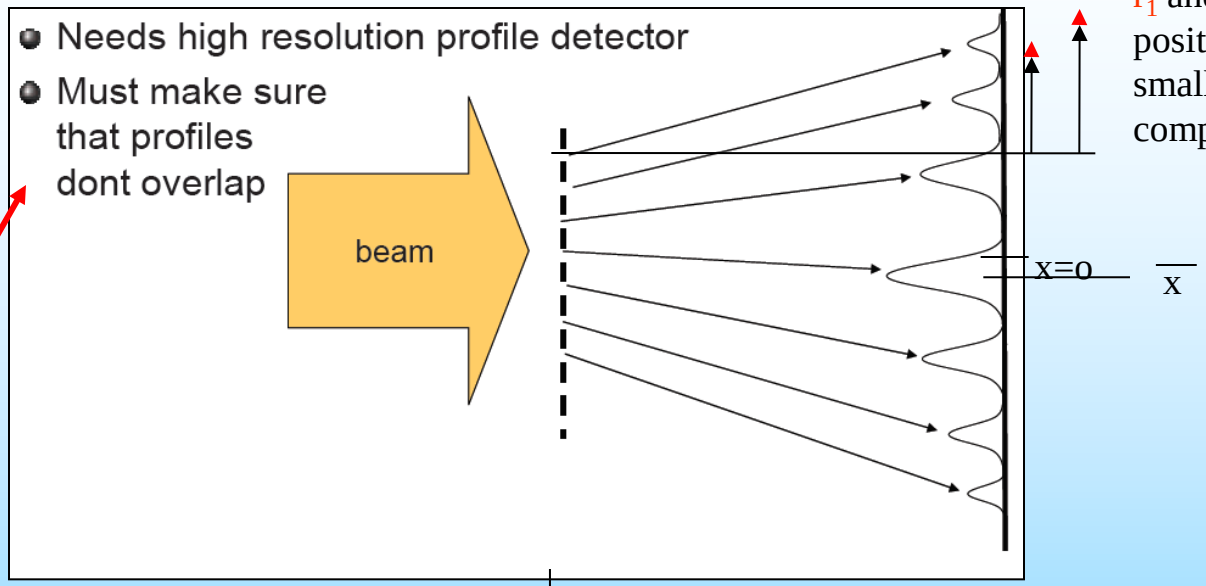

r_1 and r_2 both positive and small compare to x

=> very good resolution is required !

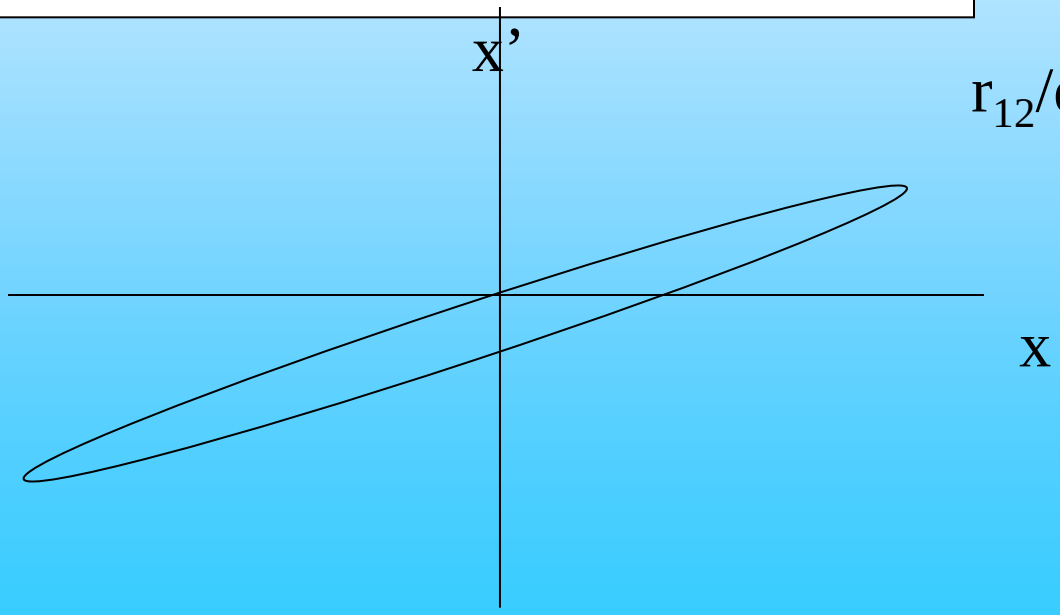

$r_{12}/d = x_{1,2}'$

Pepperpot/slits emittance measurement

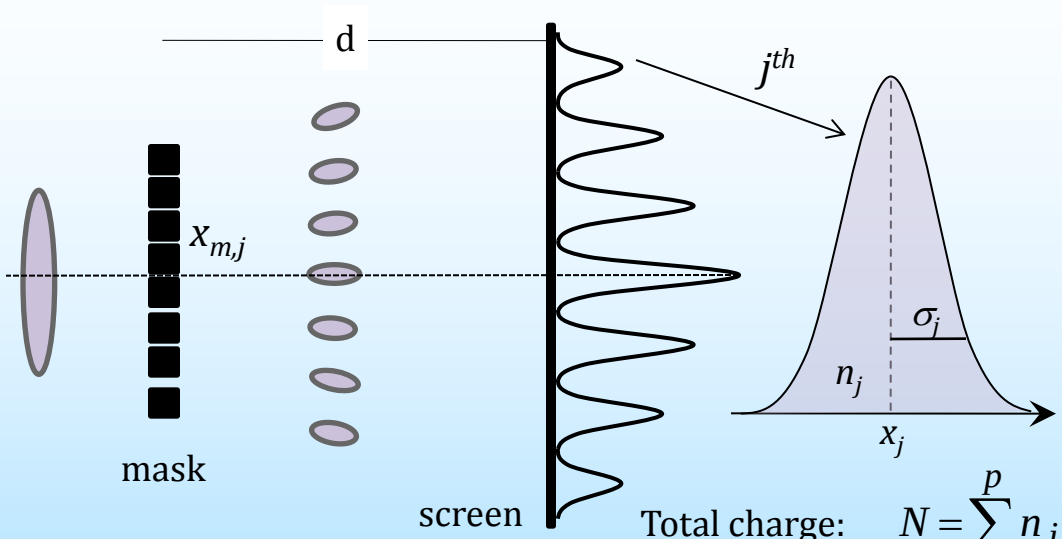

Total charge: $N = \sum_j^p n_j$

$$\varepsilon_{rms} = \sqrt{\langle x^2 \rangle \langle x'^2 \rangle - \langle xx' \rangle^2}$$

$$\langle x^2 \rangle = \frac{1}{N^2} \sum_{j=1}^{p} n_j (x_{mj} - \bar{x})^2$$

$$\langle x'^2 \rangle = \frac{1}{N^2} \sum_{j=1}^{p} n_j \left[\left(\frac{\sigma_j}{d} \right)^2 + (x_{mj} - \bar{x})^2 \right]$$

$$\langle xx' \rangle^2 = \frac{1}{N^2} \left[\sum_{j=1}^{p} n_j x_j \overline{x'_j} - N \bar{x} \bar{x}' \right]^2$$

In all beamlets:

Mean position:

$$\bar{x} = 1/N \sum_j^p n_j x_{m,j} = \langle x \rangle$$

Mean divergence:

$$\bar{x}' = 1/N \sum_j^p n_j \bar{x}'_j = \langle x' \rangle$$

In j^{th} beamlet:

Mean divergence:

$$\bar{x}'_j = 1/n_j \Sigma x'_{ij}$$

rms divergence:

$$\sigma_{j,x'} = \frac{\sigma_j}{d}$$

with

$$\sigma_j \equiv \sqrt{\frac{1}{n_j} \sum_{i=1}^{n_j} (X_{ji} - \bar{X}_j)^2},$$

which is the rms spot size of j-th beamlet on screen.

p = number of slits, $x_{m,j}$ = j-th slit position, N = all particles behind the slits
n_j = number of particles passing through slit (weight of spot intensity)

Emittance measurement by Pepperpot

The scanning of the whole beam size in both planes needs quite a lot of time with very stable beam conditions. To overcome the scanning procedure a plate with thin holes in defined distances (pepperpot) produces a lot of beamlets in the x, y plane..

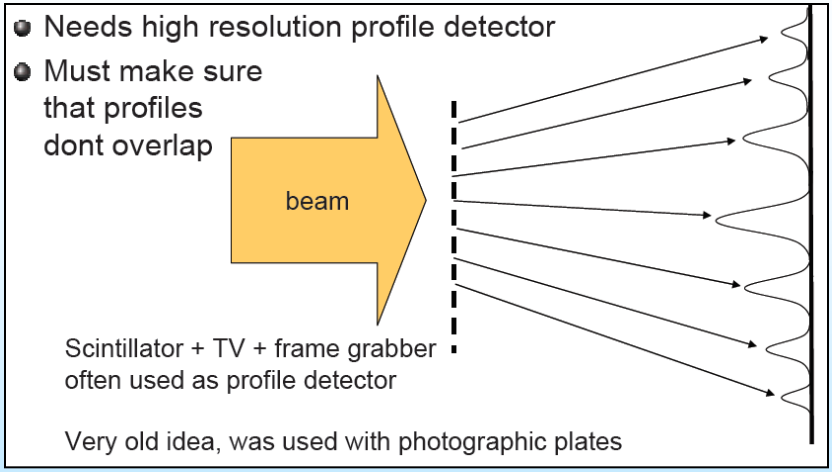

U. Raich CERN Accelerator School 2005

Advantages of pepper-pot method

- Single shot measurement
- Less prone to space charge effect
- Can obtain x and y emittance at one measurement
- Reduced heat load of the plate compare to slowly scanning slits.

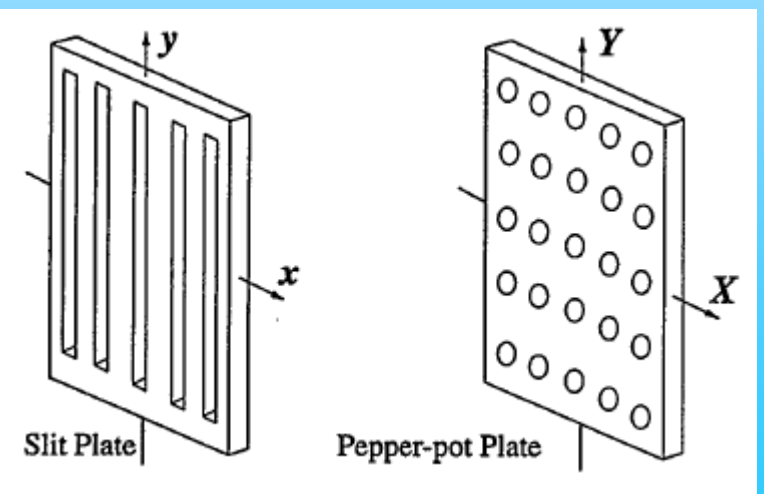

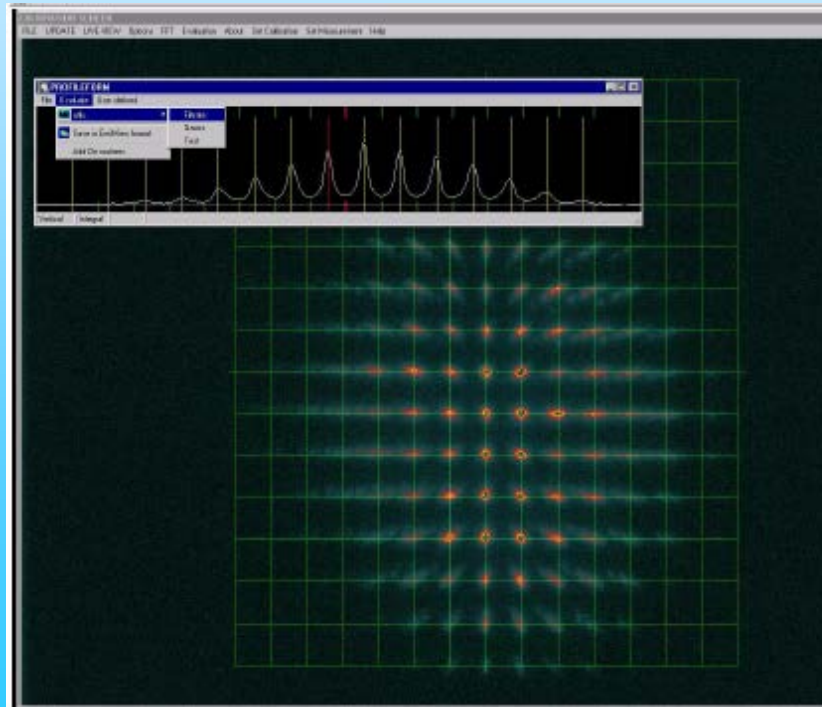

Photo P. Forck

The ultimate emittance measurement

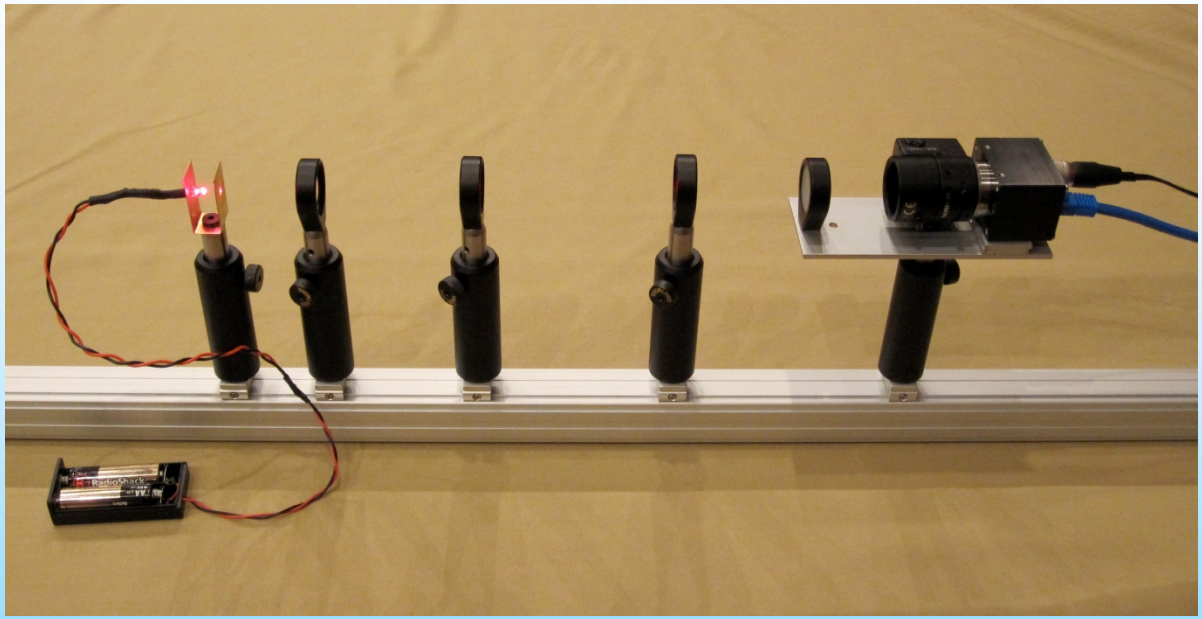

Optical bench with:

- Point light source
- Pepperpot plate
- Screen
- Lenses
- Data acquisition
- Evaluation programs

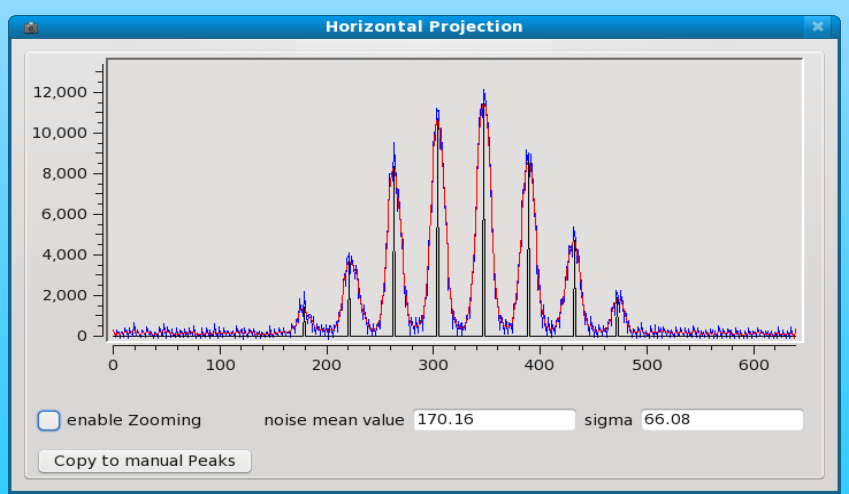

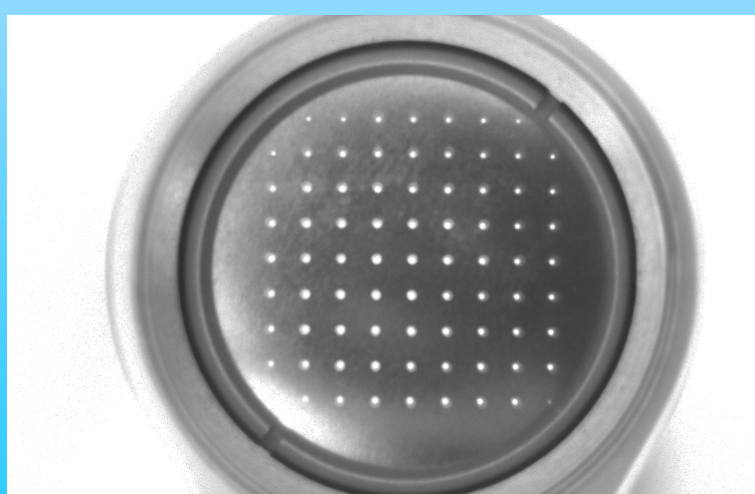

Emittance measurement by Slit + screen/harp

The procedures descript above neglect the finite **resolution** of the device.

- A **small h_{slit} and small step sizes** of the slit positioning improve the resolution.
- When using a grid as detector its resolution can be improved by **scanning the grid** as well.
- A **position of the device in a region with high x'** is most helpful for a good resolution.
- In high density beams care has to be taken that **space charge in a beamlet** might extend the angular spread of its on the way to the detector.

Comparisons (simulations 3 MeV protons) of **different geometries** (stainless steel) show that

- geometry (d) gives results similar to geometry (a),
- geometry (b) gives the best (smallest) results and
- geometry (c) gives the worse results, with about 30% of the particles that reach the SEM-grid being scattered.

But at (b) the aperture of the slit is smaller than its thickness
=> the measured phase-space distribution is flowed by an **angular cut** and the emittance is **underestimated**.

From: Design of a New Emittance Meter for LINAC4; B. Cheymol, et al. ; DIPAC2009

If β is known unambiguously as in a circular machine, then a single profile measurement determines the emittance ε by

$$\sigma_y^2 = \varepsilon\beta_y.$$

But it is not easy to be sure in a transfer line which β to use, or rather, whether the beam that has been measured is matched to the β-values used for the line. This problem can be resolved by using …

Three screen method:

If β is known unambiguously as in a circular machine, then a single profile measurement determines ε by

$$\sigma_y^2 = \varepsilon\beta_y.$$

But it is not easy to be sure in a transfer line which β to use, or rather, whether the beam that has been measured is matched to the β-values used for the line. This problem can be resolved by using **three monitors (see Fig. 1), i.e. the three width measurement determines the three unknown α, β and ε of the incoming beam.**

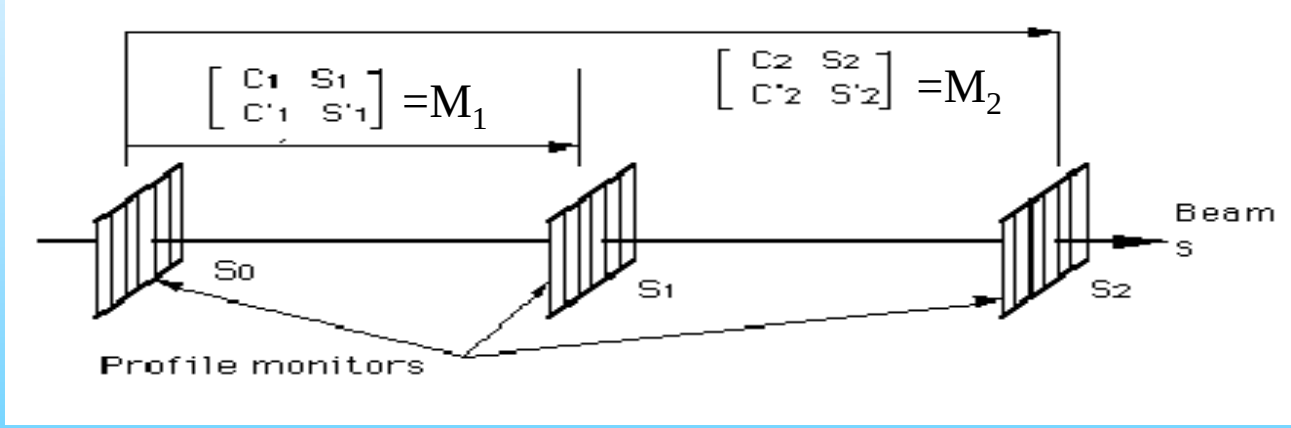

Introduction of σ-Matrix (see for example: K. Wille; Physik der Teilchenbeschleuniger, Teubner)

$$\sigma = \begin{pmatrix} \sigma_{11} & \sigma_{12} \\ \sigma_{21} & \sigma_{22} \end{pmatrix} = \begin{pmatrix} \sigma_y^2 & \sigma_{yy'} \\ \sigma_{yy'} & \sigma_{y'}^2 \end{pmatrix} = \varepsilon_{rms} \begin{pmatrix} \beta & -\alpha \\ -\alpha & \gamma \end{pmatrix} = \sigma\, matrix$$

$$\boxed{\varepsilon_{rms} = \sqrt{\det \sigma} = \sqrt{\sigma_{11}\sigma_{22} - \sigma_{12}^2}}$$

$\boxed{\bigcirc = \text{beam size}}$

$$(\beta\gamma - \alpha^2 = 1)$$

Beam width$_{rms}$ of measured profile = σ_y = $\sqrt{\sigma_{11}} = \sqrt{\beta(s)\cdot\varepsilon}$

Transformation of σ-Matrix through the elements of an accelerator:

$$\boxed{\sigma_{s1} = M \cdot \sigma_{s0} \cdot M^t}$$

$$M = \begin{pmatrix} M_{11} & M_{12} \\ M_{21} & M_{22} \end{pmatrix}; M^t = \begin{pmatrix} M_{11} & M_{21} \\ M_{12} & M_{22} \end{pmatrix}$$

L_1, L_2 = distances between screens or from Quadrupole to screen and Quadrupole field strength are given, therefore the transport matrix M is known.
Applying the transport matrix gives (now time for exercise):

<u>Exercise L2:</u> Assuming that the geometry between the measurement stations and the transport matrices M1,2 of the transport line are well defined (including magnetic elements), describe a way to get the emittance using the 3 screens and the σ-matrix.

Write down the equation how the beam width σ is transferred from s_0 to the next screen s_1.

$$\sigma_{s_1} = M \cdot \sigma_{s_0} \cdot M^t$$

$$= \begin{pmatrix} M_{11} & M_{12} \\ M_{21} & M_{22} \end{pmatrix} \cdot \begin{pmatrix} \sigma_{11} & \sigma_{12} \\ \sigma_{21} & \sigma_{22} \end{pmatrix}_{s_0} \cdot \begin{pmatrix} M_{11} & M_{21} \\ M_{12} & M_{22} \end{pmatrix} = \sigma^{measured} = \begin{pmatrix} \sigma_y^2 & \sigma_{yy'} \\ \sigma_{y'y} & \sigma_{y'}^2 \end{pmatrix}_{s_1}^{measured} = \varepsilon_{rms} \begin{pmatrix} \beta & -\alpha \\ -\alpha & \gamma \end{pmatrix}$$

$$= \begin{pmatrix} M_{11} & M_{12} \\ M_{21} & M_{22} \end{pmatrix} \cdot \begin{pmatrix} \sigma_{11}M_{11} + \sigma_{12}M_{12} & \sigma_{11}M_{21} + \sigma_{12}M_{22} \\ \sigma_{21}M_{11} + \sigma_{22}M_{12} & \sigma_{12}M_{21} + \sigma_{22}M_{22} \end{pmatrix}$$

$$= \begin{pmatrix} M_{11}(\sigma_{11}M_{11} + \sigma_{12}M_{12}) + M_{12}(\sigma_{21}M_{11} + \sigma_{22}M_{12}) & \cdots \\ \cdots & \cdots \end{pmatrix}$$

$$\underbrace{\sigma(s_1)_{11}^{new} = \sigma^2(s_1)_y^{new}}_{\text{new (transferred) beam width}} = M_{11}^2 \underbrace{\sigma(s_0)_{11}}_{\text{measured beam width}} + 2M_{11}\, M_{12}\, \sigma(s_0)_{12} + M_{12}^2\, \sigma(s_0)_{22} \quad (\sigma_{12} = \sigma_{21}) \qquad (1)$$

unknown

Solving $\sigma(s)_{11}$ $\sigma(s_0)_{12}$ and $\sigma(s_0)_{22}$ while Matrix elements are known: <u>Needs minimum of three different measurements, either three screens or three different Quadrupole settings with different field strength</u>.

$$\boxed{\varepsilon_{rms} = \sqrt{\det \sigma} = \sqrt{\sigma_{11}\sigma_{22} - \sigma_{12}^2}} \qquad (2)$$

<u>Exercise L3:</u> In a transport line for p = 7.5 GeV/c protons are two measurement stations. The first is located exactly in the waist of the beam and shows a beam width of σ_y = 3 mm, the second at a distance of s = 10 m shows a width of σ_y = 9 mm. Assuming no optical elements in this part, calculate the emittance and the normalized emittance of the beam.

<u>Exercise L3:</u> In a transport line for p = 7.5 GeV/c protons are two measurement stations. The first is located exactly in the waist of the beam and shows a beam width of σ_y = 3 mm, the second at a distance of s = 10 m shows a width of σ_y = 9 mm. Assuming no optical elements in this part, calculate the emittance and the normalized emittance of the beam.

No optical elements => M= $\begin{pmatrix} M_{11} & M_{12} \\ M_{21} & M_{22} \end{pmatrix} = \begin{pmatrix} 1 & s \\ 0 & 1 \end{pmatrix}$ (3)

Waist => α = $\alpha = \sigma_{12} = \sigma_{21} = 0$ $\left(= -\frac{1}{2} \cdot \frac{d\beta}{ds}\right)$ $\left(\varepsilon_{rms} = \sqrt{\sigma_{11}\sigma_{22} - \sigma_{12}^2} = \sqrt{\sigma_{11}\sigma_{22}}\right)$ (4)

Measured width at s = 0 => $\sigma_{11} = (3\text{ mm})^2 = \sigma_y^2(0)$ (5)

Calculate σ_{22} with width measured at s = 10 m and with (1 and α=0) =>

$(9\text{ mm})^2 = \sigma_y^2(10) = M_{11}^2\sigma_{11} + M_{12}^2\sigma_{22} = \sigma_{11} + s^2\sigma_{22}$ (σ_{11} and σ_{22} at s=0) (6)

=> ($\sigma_{11} = \sigma_y(10)$ = 9 mm and σ_{22} =?)

=> $$\sigma_{22} = \frac{\sigma_y^2(10) - \sigma_y^2(0)}{s^2} \quad (7)$$

With (4) and (7) = $$\varepsilon_{rms} = \sqrt{\sigma_{11}\sigma_{22}} = \sqrt{\sigma_y^2(0) \cdot \frac{\sigma_y^2(10) - \sigma_y^2(0)}{s^2}} = \frac{\sigma_y(0)}{s}\sqrt{\sigma_y^2(10) - \sigma_y^2(0)}$$

ε_{rms} = <u>$2.5 \cdot 10^{-6}\ \pi$ m rad</u> or with Momentum p = 7.5 GeV/c => relativistic $\gamma\beta \approx 7.5$

$\varepsilon^{normalized} = \varepsilon_{rms}\ \gamma\ \beta = 19 \cdot 10^{-6}\ \pi$ m rad = <u>19 π mm mrad</u>

Emittance measurements by quadrupole variation or 3 screens/harps methods

Profiles are measured by thin screens or harps.

=> small and almost negligible beam blowup due to the measurement itself so that the beam can transverse a few screens.

=> "one shot" measurement

=> scanning methods need a stable beam over the scanning time.

Three measurements give a unique solution but no error estimation.

=> more stations or by more quadrupole settings are recommended.

=> variation of the quadrupole settings allows a quadratic fit of the square of the measured beam size versus the quadrupole gradient together with an estimate of the errors in the measurement.

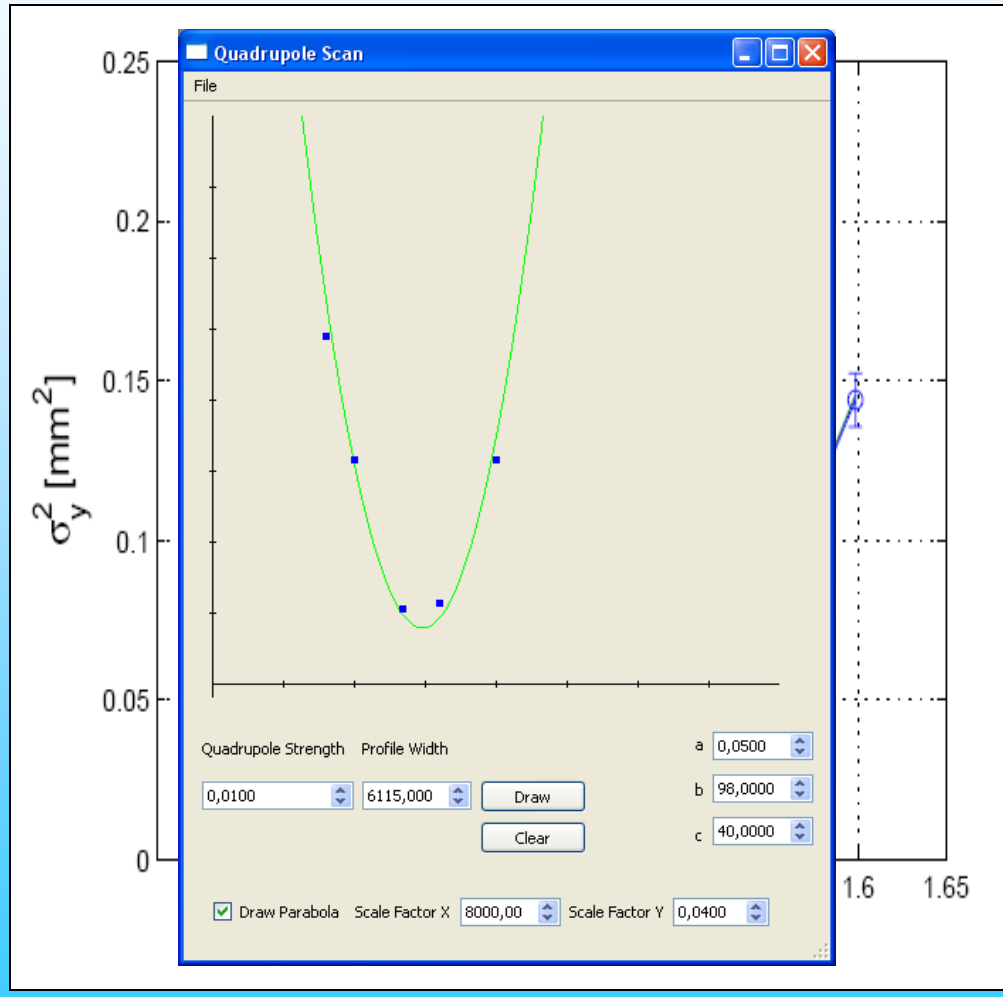

Beam Emittance Measurement for the New Full Energy Injector at ELETTRA; Giuseppe Penco et al, EPAC'08,

Screens will show often this kind of beam profiles, sometime not really Gaussian. Let's make an emittance measurement on a real beam with real pictures:

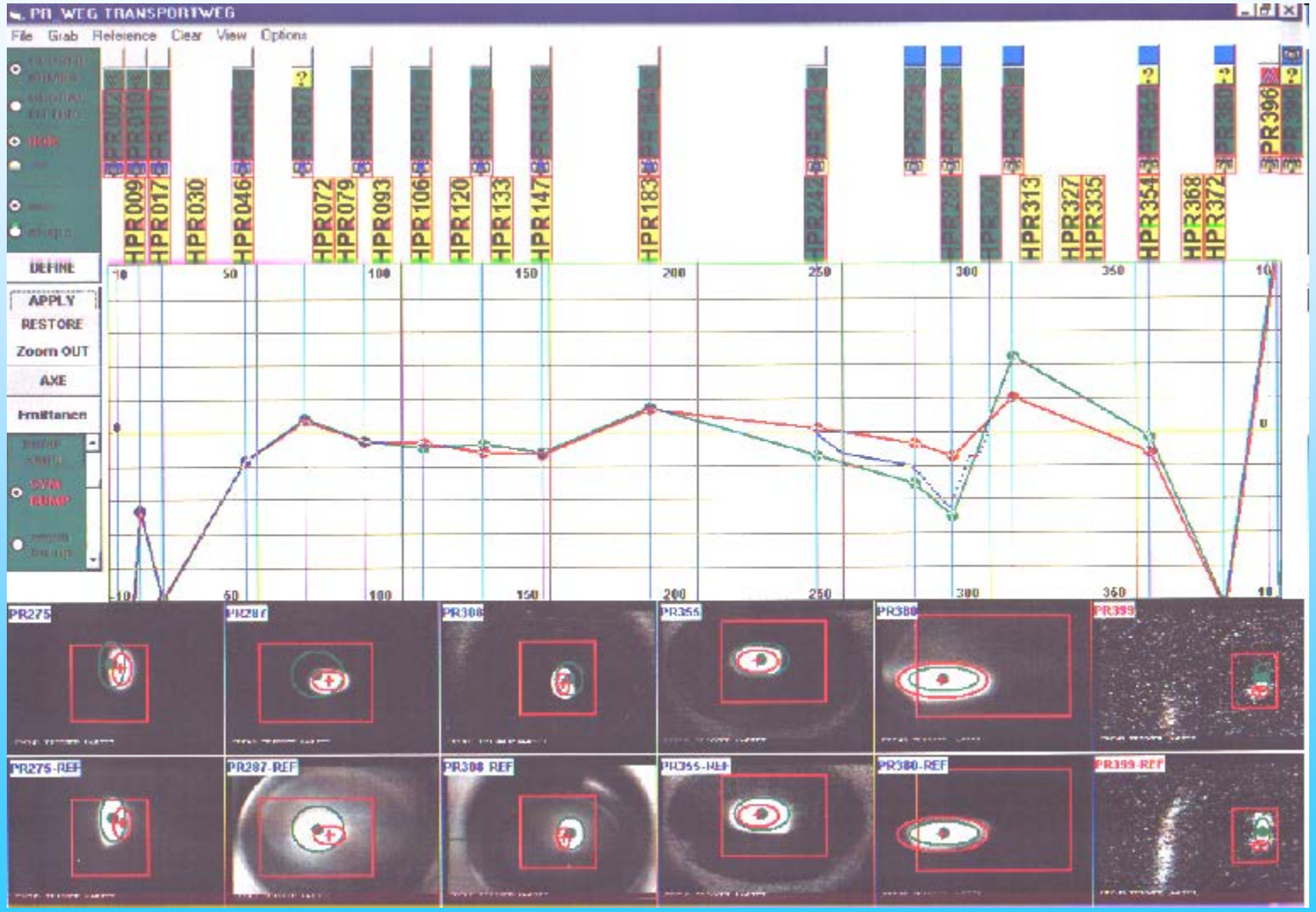

Exercise: Determine the horizontal emittance of a laser beam by using the 3 screen method:

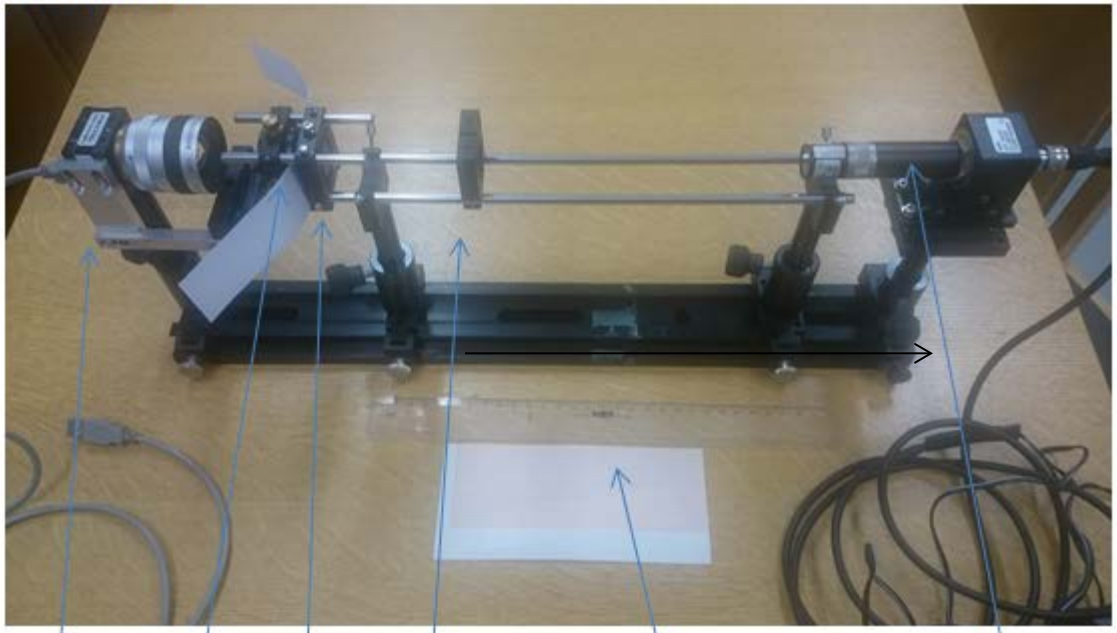

USB Camera, Screen, Filter, moveable Lens, Ruler and calibration screen, Laser

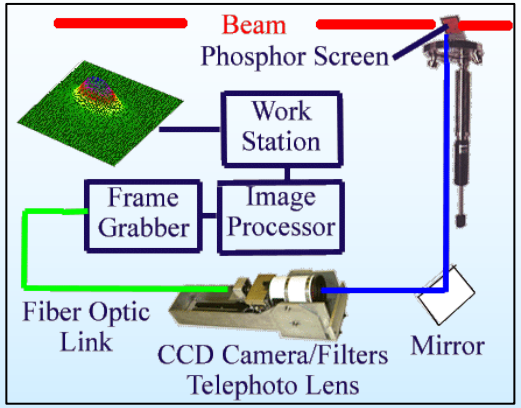

By moving the lens one can take pictures from the camera in the focus (not preferred due to limited resolution of the optic system) and on other positions. The distance to various screen positions can be measured by a simple ruler*. The camera is connected to a Computer where the readout software is installed. The pictures (.jpg) can be saved and can be loaded into a free software called “ImageJ” where a profile of an area can be displayed and the curser position and the value is displayed (8 bit). The σ of the profile have to be found for each screen (camera) position and the emittance have to be calculated.

* Move the lens to simulate different screen positions

Emittance measurements by quadrupole variation or 3 screens/harps methods

The standard methods descript above are valid under the assumption that:

- the dispersion along the section is zero,
- the transfer matrices are known,
- no coupling between the two planes is present and
- no space charge or other non-linear forces are present.

With dispersion the particle trajectory vector then includes the momentum spread = $(x, x', \Delta p/p)$ and the σ-matrix and the transport matrix M becomes 3x3 matrices. In this case at least four measurements are necessary to determine all σ-matrix elements to resolve the emittance.

End of emittance calculations

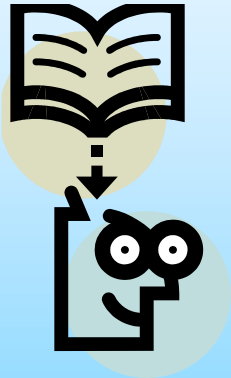

What's Halo?

… because of the beam distribution's phase-space rotations, the observed halo in 1D oscillates, so that halo at different locations along the beam line is observable in differing degrees. For example, at some locations the halo may project strongly along the spatial coordinate and only weakly along the momentum coordinate, while at others the reverse is true, and the halo can be hidden in the spatial projection. In most circumstances, the beam halo from simulation appears as an irreversible effect, when observed in the 2D phase-space distributions. Therefore, it is also important to search for another definition of halo in the 2D phase-space distributions….

…it became clear that even at this workshop (HALO 03) **a general definition of "Beam Halo" could not be given,** because of the **very different requirements** in different machines, and because of the **differing perspectives** of instrumentation specialists and accelerator physicists.

From the diagnostics point of view, one thing is certainly clear – by definition halo is low density and therefore difficult to measure…

- **Profile measurements are often questioned at the level of a few percent**, the difficulty is easily seen in making halo measurements already at the level of 10^{-4} and beyond.

What is Halo?

From the diagnostics point of view, one thing is certainly clear – by definition halo is low density and therefore difficult to measure…

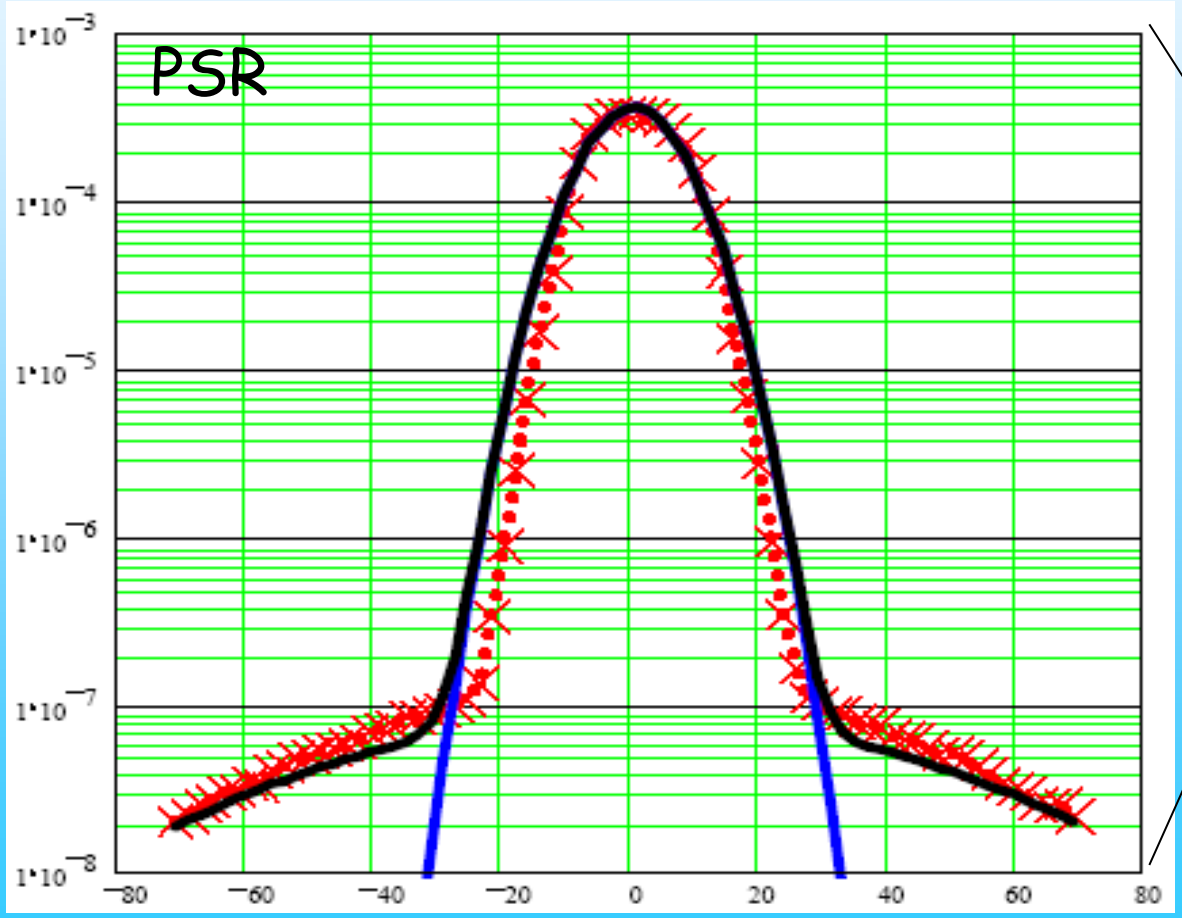

Halo measurements require **high dynamic range instruments** and methods

Dynamic range > 10

What is Halo?

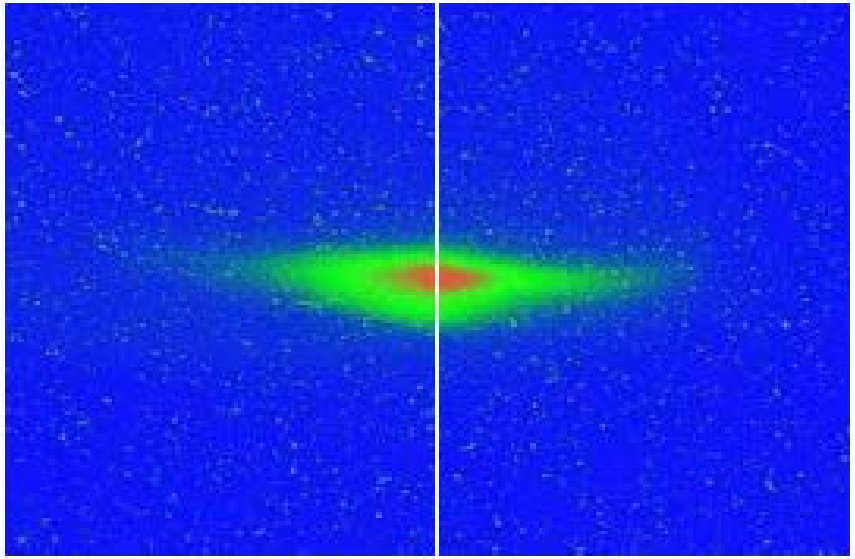

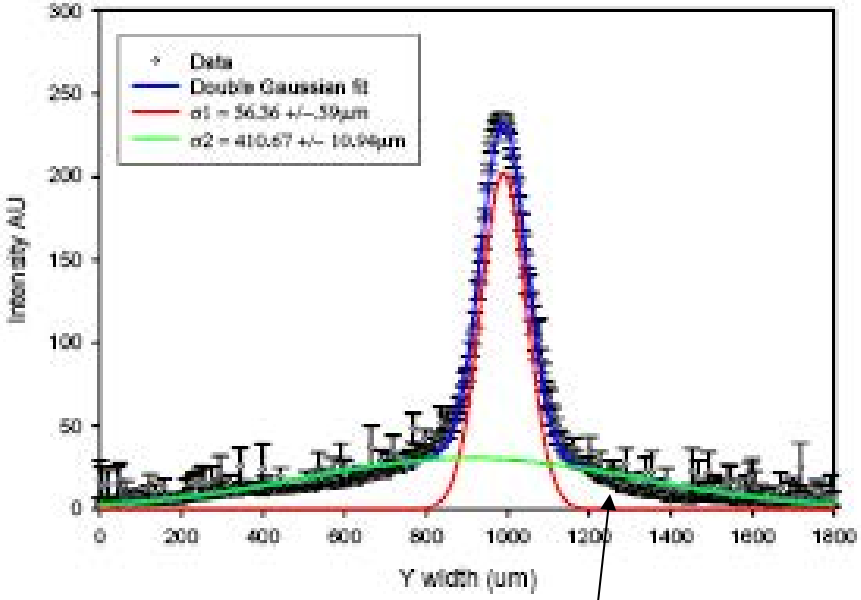

That's not a halo,
that's a tail!
Dynamic range <10^3

Wire Scanners at LEDA
(Proton LINAC, SEM readout)

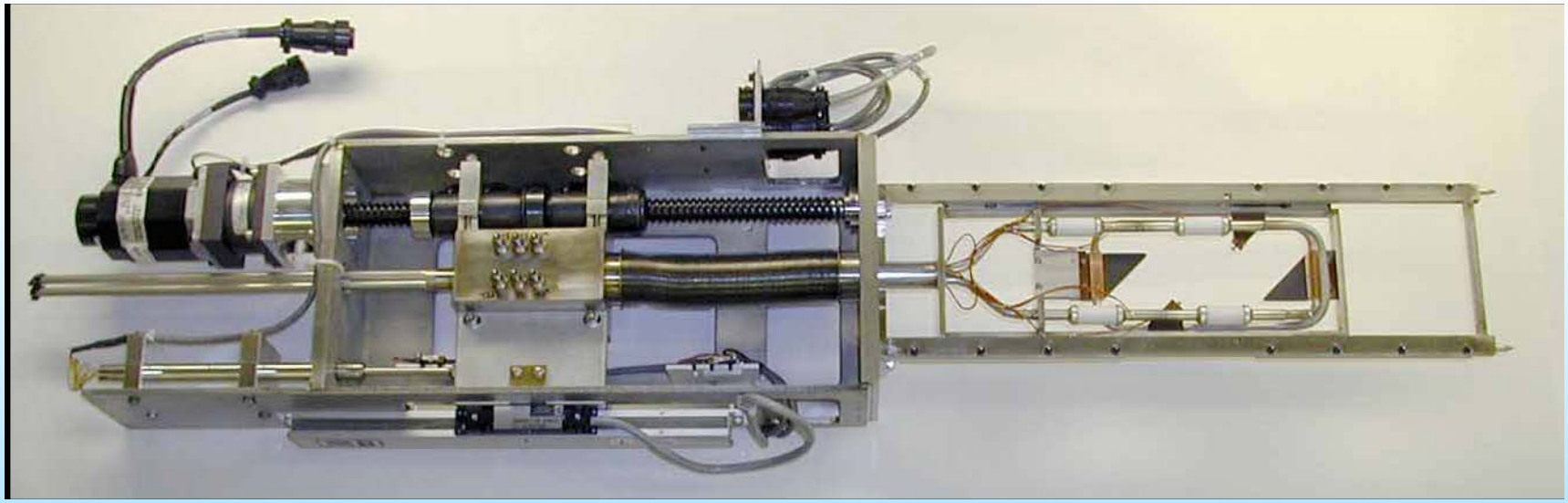

WS can move a 33-μm carbon mono filament and two halo scraper consisting of two graphite scraping devices (one for each side of the distribution).
The high-heat flux testing performed on the prototype scrapers revealed that the design can withstand the thermally induced fatigue loading. The peak heat flux that these scrapers have experienced in actual service is approximately 600 kW/cm^2

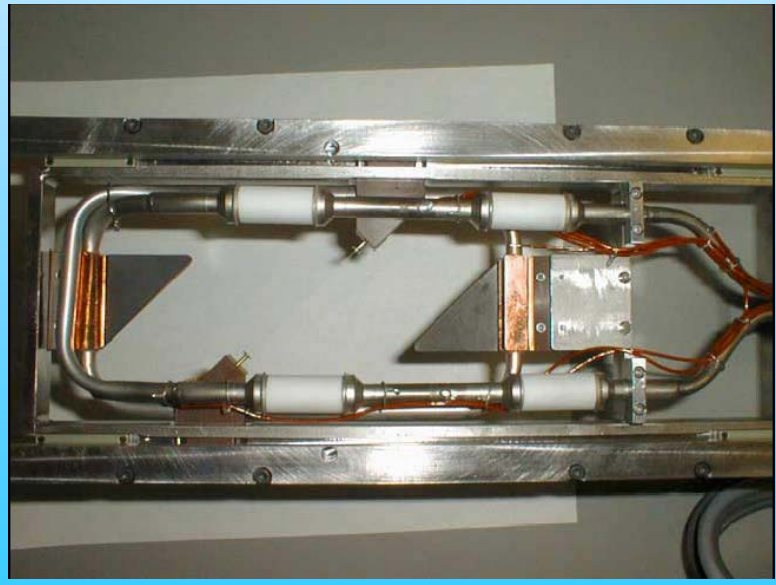

Y-axis wire scan

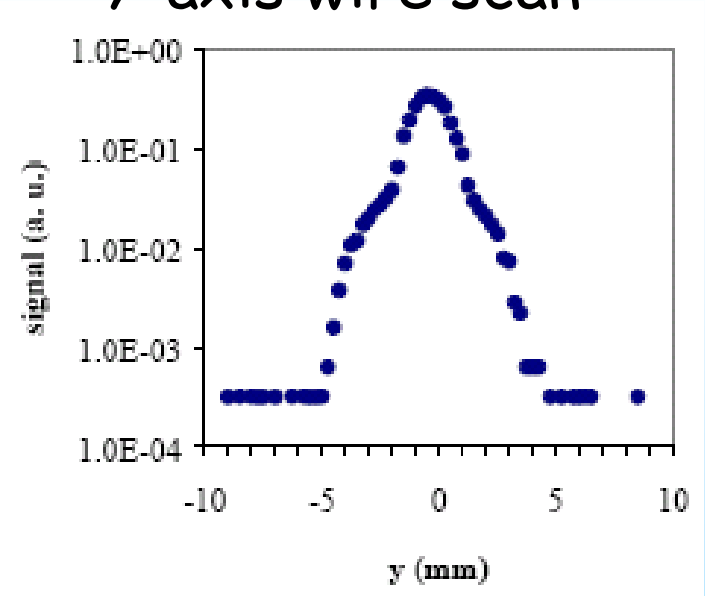

=>

Combined distribution in y.

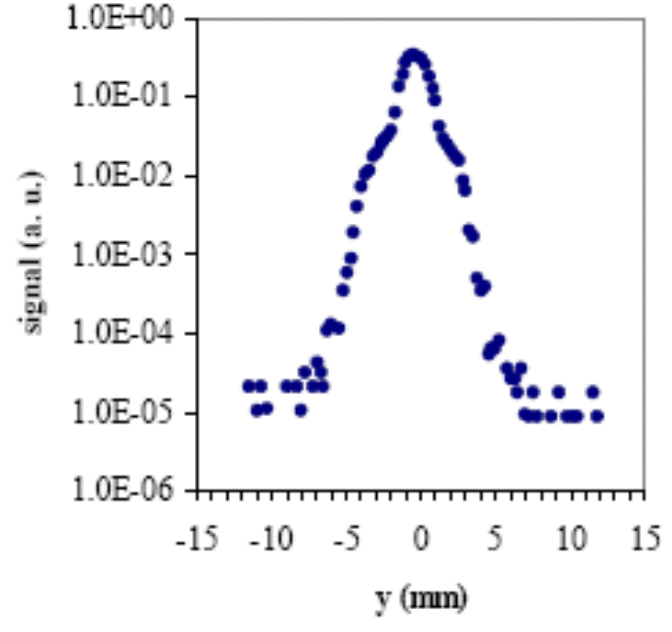

+

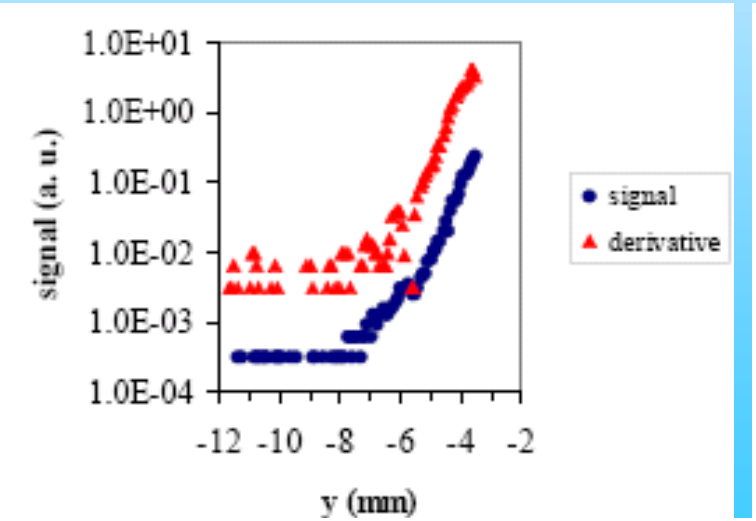

+

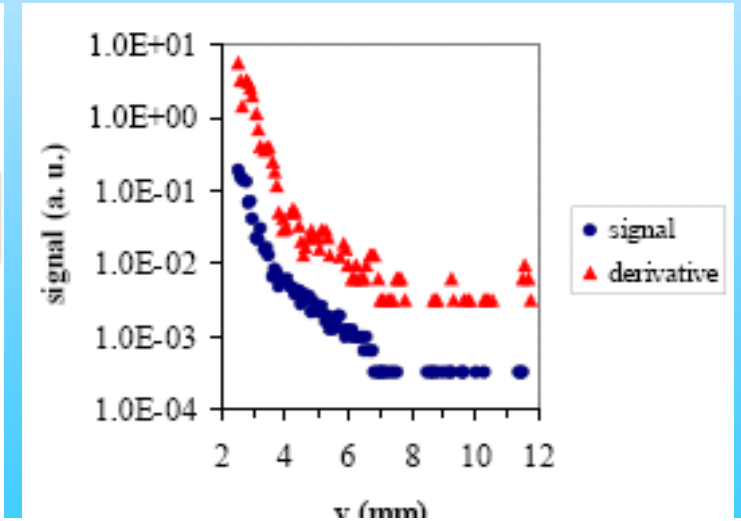

-Y and + Y scrape signal and derivative. The derivative has been multiplied by ten.

Scraping by collimators

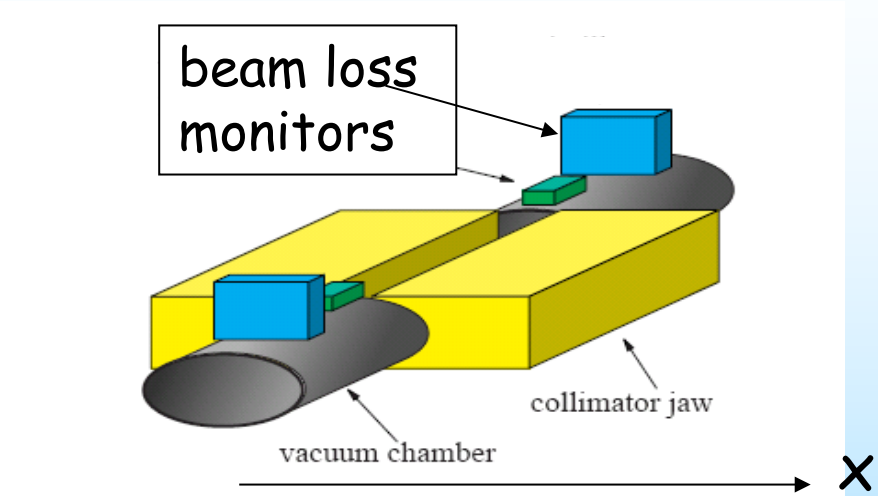

In a synchrotron one jaw will scrape both sides of the beam distribution (β-oszillation)
=> meas. symmetric halo
Such a tail scan yields information about particles which oscillate with an amplitude larger than the position of the collimator

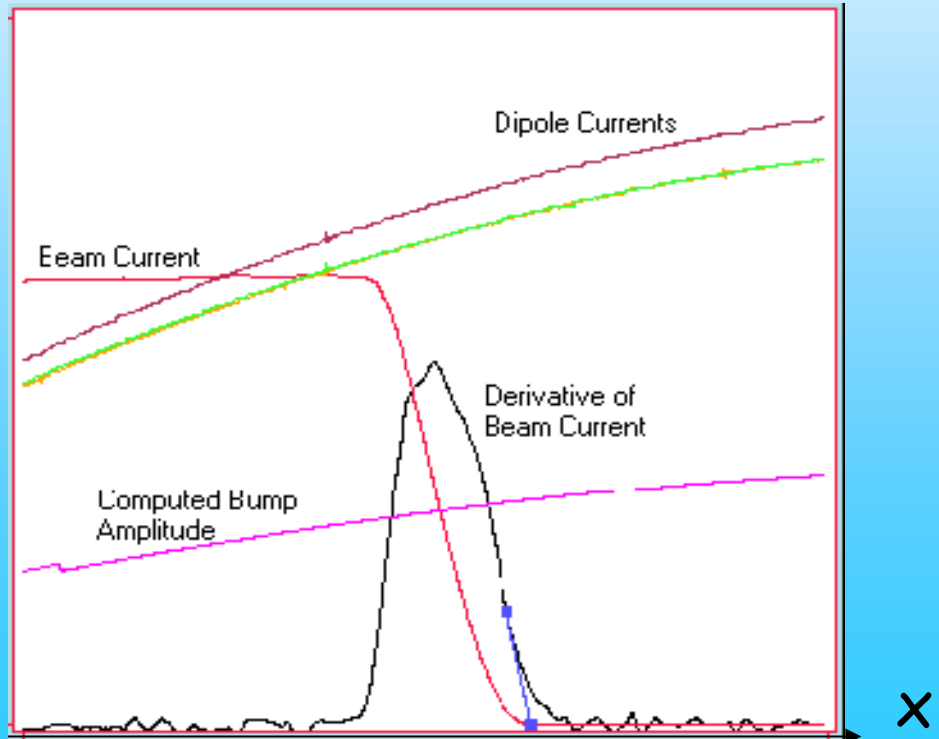

Scraping by collimators + BLM

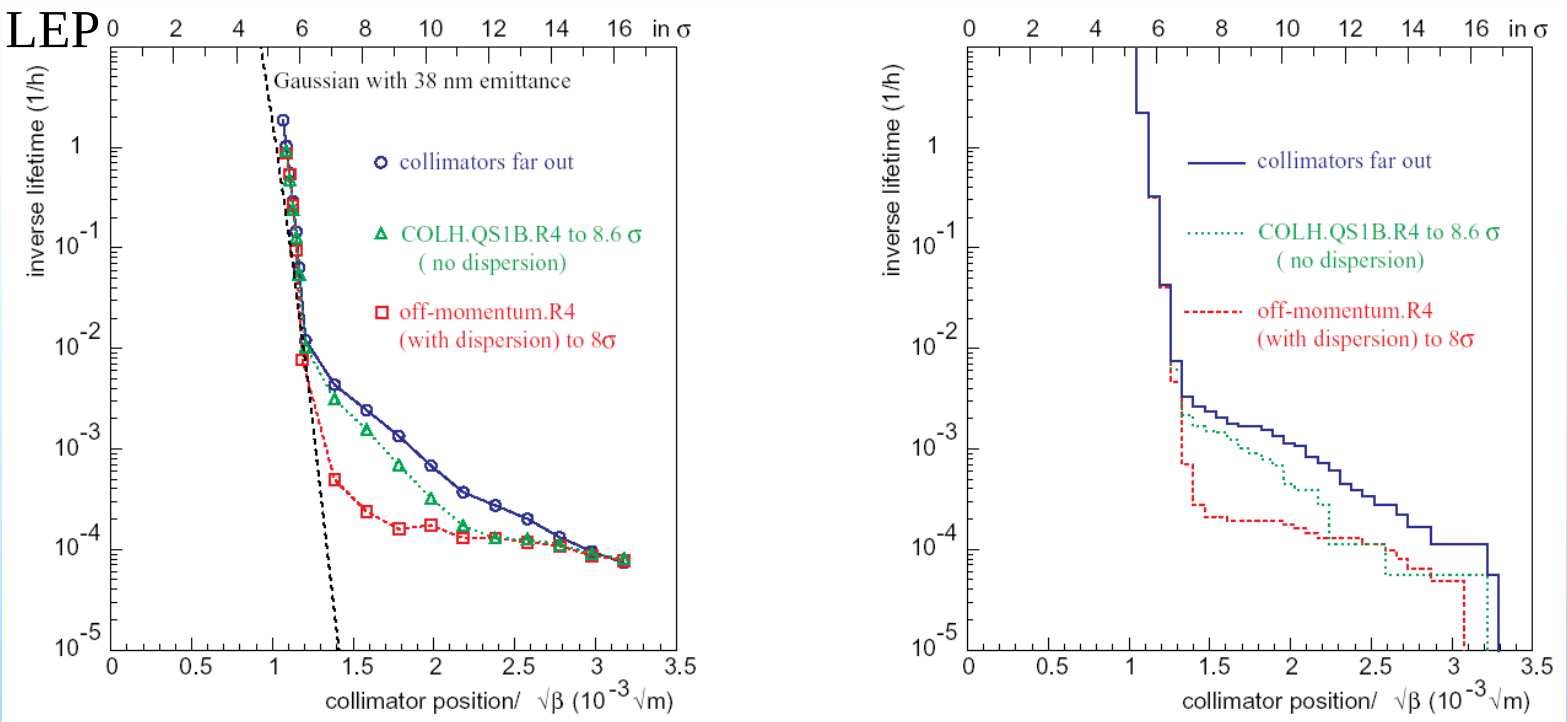

Measurement (left) and simulation (right) of the horizontal beam tails for a beam energy of 80.5 GeV and for different collimator settings at LEP. The simulation is the result of tracking particles after Compton scattering on thermal photons (black body radiation of vacuum chamber).

Measurements were performed by moving one jaw of a collimator closer to the beam in steps. Beam current and beam size measurements were recorded for each collimator setting. The collimators were moved closer until significant lifetime reductions were observed. Lifetimes calculated from beam currents for these points were used to calibrate the loss monitors. This allows to give loss rates directly in terms of equivalent lifetimes

End of Halo
More in CAS08
and CAS18 (Helsinki, coming soon)
Topical CAS in Beam Diagnostics
Dourdan, France
Proceedings: CERN-2009-005